Exact Equilibrium Solutions of the Magnetohydrodynamic Plasma Model

A thesis submitted to the
College of Graduate and Postdoctoral Studies
in partial fulfillment of the requirements
for the degree of Master of Science
in the Department of Mathematics
University of Saskatchewan
Saskatoon

By
Jason Meinrad Keller

Permission to Use

In presenting this thesis in partial fulfillment of the requirements for a Postgraduate degree from the University of Saskatchewan, I agree that the Libraries of this University may make it freely available for inspection. I further agree that permission for copying of this thesis in any manner, in whole or in part, for scholarly purposes may be granted by the professor or professors who supervised my thesis work or, in their absence, by the Head of the Department or the Dean of the College in which my thesis work was done. It is understood that any copying or publication or use of this thesis or parts thereof for financial gain shall not be allowed without my written permission. It is also understood that due recognition shall be given to me and to the University of Saskatchewan in any scholarly use which may be made of any material in my thesis.

Disclaimer

Reference in this thesis to any specific commercial products, process, or service by trade name, trademark, manufacturer, or otherwise, does not constitute or imply its endorsement, recommendation, or favoring by the University of Saskatchewan. The views and opinions of the author expressed herein do not state or reflect those of the University of Saskatchewan, and shall not be used for advertising or product endorsement purposes.

Requests for permission to copy or to make other uses of materials in this thesis in whole or part should be addressed to:

Head of the Department of Mathematics
University of Saskatchewan
142 Mclean Hall, 106 Wiggins Road
Saskatoon, Saskatchewan, S7N 5E6 Canada

OR

Dean
College of Graduate and Postdoctoral Studies
University of Saskatchewan
116 Thorvaldson Building, 110 Science Place
Saskatoon, Saskatchewan S7N 5C9 Canada

Abstract

The use of plasma descriptions in areas such as space sciences and thermonuclear fusion devices are of great importance. Of these descriptions, the most widely used are the fluid descriptions which view plasma as a continuum medium and out of these fluid descriptions, the idealized isotropic magnetohydrodynamics (MHD) system of equations is the most used and arguably the most important. Due to the complex non-linear structure of this system of equations, very few exact solutions are known, and of the know ones, even fewer have physically relevant behaviour. In most cases, solutions are sought for simpler forms of the MHD equations such as the time independent and static equilibrium simplifications. In this work, new exact solutions are derived for the incompressible axially and helically symmetric static and dynamic equilibrium MHD equations. The static equilibrium MHD equations with axial or helical symmetry reduce to a single partial differential equation (PDE). In the case of axial symmetry this is known as the Grad-Shafranov equation and in the case of helical symmetry this is the JFKO equation. New families of separated solutions are found for both of these PDEs and in both cases, the two separate families of solutions arise depending on the type of pressure profile. As most literature focuses on a pressure profile which is lower in the centre of the plasma and goes to a higher ambient pressure at the boundary (that is, the plasma configuration is supported by external pressure), such as those found in [11, 12] emphasis in this work is directed towards the other type of pressure profile where the pressure is higher inside the plasma domain and lower or vanishing outside. Such solutions are relevant to modelling plasma in a vacuum. Using a transformation described in [13, 14], the new static solutions are transformed into dynamic solutions which satisfy the incompressible equilibrium MHD equations. In the last chapter, a modern derivation of Hill's spherical vortex [30] is presented that employs the Galilean invariance and the axially symmetry reduction to the Grad-Shafranov equation. Along with this, a similar and more general MHD spherical vortex-type solution is derived. Stability analysis of the localized vortex-type solutions is considered.

Acknowledgements

I want to thank with the utmost respect, my supervisor Professor Shevyakov for his deep knowledge, continual support and encouragement as well as providing a fun and creative atmosphere for my research. I would also like to thank the mathematics department at the University of Saskatchewan for financial support and academic advice. I also thank NSERC and the government of Canada for financial support. I thank my girlfriend Rachel for her constant love, encouragement and patience as well as my parents for their love, support and financial help.

Contents

List of Tables

List of Figures

1 Introduction

1.1 Plasma in nature and in applications

With the addition of energy to a material, its state changes from solid to liquid and then to gas. If one continues to add energy to the gas, the atoms that constitute the gas begin to have their electrons stripped off creating a gas full of positive ions and negative electrons where, in the macroscopic view, the equal number of ions and electrons give a net neutral charge. This ionized gas is referred to as a *plasma*. The ratio of ionized atoms to neutral atoms in thermal equilibrium can be shown using the Saha equation [43]

$$\frac{n_i}{n_n} \approx 2.4 \times 10^{21} \frac{T^{3/2}}{n_i} e^{-U_i/kT}, \tag{1.1}$$

where n_i and n_n are the density of ionized and neutral atoms respectively, T is the gas temperature in degrees Kelvin, k is the Boltzmann's constant and U_i is the ionization energy of the gas [18]. For example, at room temperature ($T = 300°K$) ordinary air has an extremely low fractional ionization [18]:

$$\frac{n_i}{n_n} \approx 10^{-122}.$$

Once U_i is only a few times kT then this ratio grows quickly and the gas is considered to be in a plasma state. Increasing the temperature further can make the plasma become fully ionized. Not all ionized gases can be called a plasma. One definition from [18] describes plasma as a quasi-neutral gas of charged and neutral particles which exhibits *collective behaviour*.

The vast majority of matter in the observable universe is in a plasma state. There are many astrophysical examples as one leaves Earth's atmosphere. Even close to Earth we can observe plasma making up the Van Allen radiation belts, solar winds, and the Aurora Borealis in the ionosphere (seen in Figure 1.1) [18].

The study of plasma has many applications in modelling these and other astrophysical phenomena such as extragalactic jets [26], accretion discs [8], and magnetized jets in radio galaxies [17] as well as important industrial uses. Industrial applications include plasma surface engineering, jet propulsion systems, nuclear-fusion devices and even fluorescent tubes [29, 20]. One other interesting use of the mathematical models for plasma regards the modelling of so called *ball lightning* which has yet to be replicated correctly in the laboratory and is still considered an unexplained phenomenon. However, one solution to an ideal plasma model does give one possible explanation [33].

Figure 1.1: Image of the Aurora Borealis in the ionosphere.
Image taken from https://eos.org/research-spotlights/auroras-may-explain-an-anomaly-in-earths-ionosphere.

Of the industrial applications mentioned, confined thermonuclear fusion is one of the most important and sought after engineering challenges of the today's age. Most attempts at creating fusion devices that would give a net energy gain incorporate superheated plasma confined in a tokamak with strong magnets. Here the term tokamak is a Russian abbreviation for "toroidal chamber with magnetic coils". An image of one can be seen in Figure 1.2.

With megaprojects such as ITER (International Thermonuclear Experimental Reactor) planning on achieving first plasma in late 2025, and being crowned as the largest magnetic confinement plasma physics experiment ever, the drive to achieve fusion devices that can generate clean electrical energy is very high. Some of the nuclear reactions of interest between tritium (T), deuterium (D), lithium (L) and helium (He) include:

1. $\mathrm{T} + \mathrm{D} \rightarrow \mathrm{He}^4(3.52\ \mathrm{MeV}) + \mathrm{n}(14.06\ \mathrm{MeV})$
2. $\mathrm{D} + \mathrm{D} \rightarrow \mathrm{T}(1.01\ \mathrm{MeV}) + \mathrm{p}(3.03\ \mathrm{MeV})$
3. $\mathrm{D} + \mathrm{D} \rightarrow \mathrm{He}^3(0.82\ \mathrm{MeV}) + \mathrm{n}(2.45\ \mathrm{MeV})$
4. $\mathrm{D} + \mathrm{He}^3 \rightarrow \mathrm{He}^4(3.67\ \mathrm{MeV}) + \mathrm{p}(14.67\ \mathrm{MeV})$
5. $\mathrm{Li}^6 + \mathrm{n} \rightarrow \mathrm{T} + \mathrm{He}^4 + 4.8\ \mathrm{MeV}$

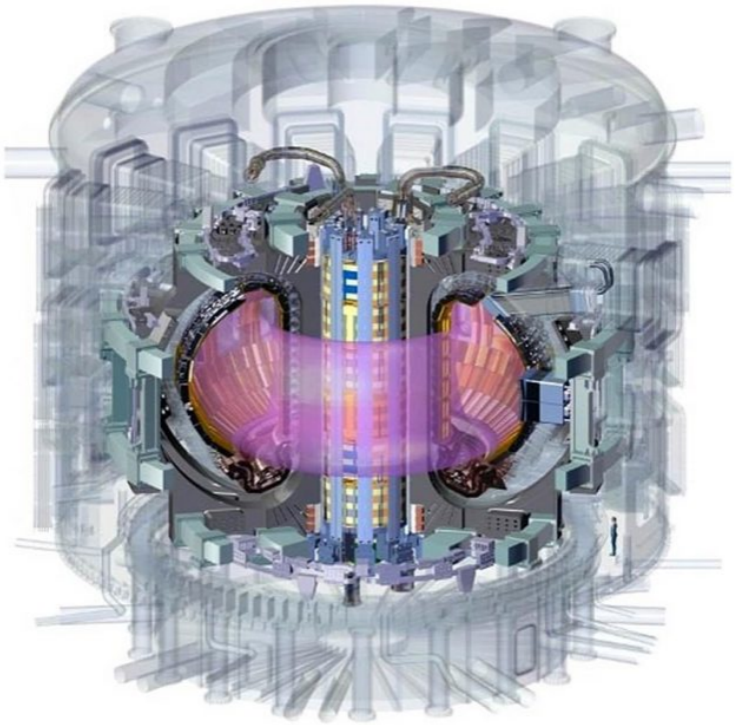

Figure 1.2: Side view of ITER's tokamak fusion reactor.
Image taken from https://scitechdaily.com/iter-global-fusion-energy-project-after-a-decade-of-design-and-fabrication-worlds-most-powerful-magnet-ready/.

6. $\mathrm{Li}^7 + \mathrm{n}(2.5\ \mathrm{MeV}) \rightarrow \mathrm{T} + \mathrm{He}^4 + \mathrm{n}$

The first type of reaction between deuterium and tritium will be used in the ITER megaproject. These applications, along with others left unmentioned, show just how important having a precise model of plasma is for both the space sciences and industry.

1.2 Mathematical models for plasma

There are many different ways of describing a plasma. Like any model, there are limitations and advantages for using each one. The most fundamental descriptions arise from kinetic theory considering each particle separately on its own or density functions in six dimensional phase space. Equations such as the Klimontovich equation, Boltzmann equation, and Vlasov equation appear in this context. The other main type of model uses a fluid descriptions which can be derived from the former using the moments of the distribution functions.

The most fundamental description of plasma utilizes the Klimontovich equation [39] which is written in terms of the density functional $N_s(\mathbf{x}, \mathbf{v}, t)$ given by

$$N_\alpha(\mathbf{x},\mathbf{v},t) = \sum_{i=1}^{N_0} \delta(\mathbf{x}-\mathbf{X}_i(t))\delta(\mathbf{v}-\mathbf{V}_i(t)). \tag{1.2}$$

where $\mathbf{X}_i$ and $\mathbf{V}_i$ are the position and velocity orbits in six dimensional phase space for each partical i of species α and $\delta(x)$ is the Dirac delta function. Taking the total time derivative of the density functional and setting it to zero gives the Klimontovich equation

$$\frac{\partial N_\alpha}{\partial t} + \mathbf{v}\cdot\nabla N_\alpha + \frac{q_\alpha}{m}\left(\mathbf{E}^m + \mathbf{v}\times\mathbf{B}^m\right)\cdot\nabla_{\mathbf{v}} N_\alpha = 0. \tag{1.3}$$

This equation, along with the Maxwell's equations gives an exact description of a plasma. Here $\mathbf{E}^m$ and $\mathbf{B}^m$ are the microscopic electric and magnetic fields produced selfconsistently by each point particle themselves, m_α is the mass of species α with charge q_α, and $\nabla_{\mathbf{v}}$ is the gradient in velocity space [39].

As there is little interest in the spikey function $N_\alpha(\mathbf{x},\mathbf{v},t)$ one can take the ensamble average of the equation with $f_\alpha(\mathbf{x},\mathbf{v},t)$ being the ensamble average of $N_\alpha(\mathbf{x},\mathbf{v},t)$ and $\mathbf{E}$ and $\mathbf{B}$ are the ensamble averages of $\mathbf{E}^m$ and $\mathbf{B}^m$. Performing this averaging along with the assumption that collisional effects are neglected one arrives at the *Vlasov equation*:

$$\frac{\partial f_\alpha}{\partial t} + \mathbf{v}\cdot\nabla f_\alpha + \frac{q_\alpha}{m}\left(\mathbf{E} + \mathbf{v}\times\mathbf{B}\right)\cdot\nabla_{\mathbf{v}} f_\alpha = 0. \tag{1.4}$$

The Vlasov equation along with the Maxwell's equations

$$\operatorname{div}\mathbf{E} = \frac{\rho}{\epsilon_0}, \tag{1.5a}$$

$$\operatorname{div}\mathbf{B} = 0, \tag{1.5b}$$

$$\operatorname{curl}\mathbf{E} = -\frac{\partial\mathbf{B}}{\partial t}, \tag{1.5c}$$

$$\operatorname{curl}\mathbf{B} = \mu_0\mathbf{J} + \frac{1}{c^2}\frac{\partial\mathbf{E}}{\partial t}, \tag{1.5d}$$

where $\mathbf{E}$ is the electric field, $\mathbf{B}$ is the magnetic induction field, ϵ_0 and μ_0 are the the electric permittivity and magnetic permeability of free space, q is the charge of the particle, ρ is the charge density, and $\mathbf{J}$ is the current density form the *Vlasov-Maxwell* system of equations. Here the electric charge density and the electric current are given by

$$\rho = \sum_\alpha \int q_\alpha f_\alpha d^3\mathbf{v} \tag{1.6}$$

and

$$\mathbf{J} = \sum_\alpha \int \mathbf{v} q_\alpha f_\alpha d^3\mathbf{v} \tag{1.7}$$

respectively.

With the assumption that the velocity distribution is Maxwellian, the zeroeth and first moments of the Vlasov equation lead to the standard *fluid description* of a plasma. Here the k^{th} moment is defined as a multiplication by $\mathbf{v}$ k times and then integrating over the entire velocity space. This fluid description drastically reduces the complexities in the kinetic description.

1. Zeroeth moment (conservation of mass)

$$\frac{\partial \rho}{\partial t} + \operatorname{div}(\rho \mathbf{V}) = 0. \tag{1.8}$$

2. First moment (conservation of momentum)

$$\rho \left(\frac{\partial \mathbf{V}}{\partial t} + (\mathbf{V} \cdot \operatorname{grad}) \mathbf{V} \right) = qn \left(\mathbf{E} + \mathbf{V} \times \mathbf{B} \right) - \operatorname{div} \boldsymbol{\mathcal{P}}. \tag{1.9}$$

Here $\rho = nm$ where m is the mass of the particle,

$$n = \int f d^3\mathbf{v} \tag{1.10}$$

is the number of particles per unit volume, $\boldsymbol{\mathcal{P}}$ is the pressure tensor given by

$$\boldsymbol{\mathcal{P}} = m \int (\mathbf{V} - \mathbf{v})(\mathbf{V} - \mathbf{v})^T f d^3\mathbf{v}. \tag{1.11}$$

and $\mathbf{V}$ is the average velocity in the stationary (Eulerian) frame of reference given by

$$\mathbf{V} = \frac{1}{n} \int \mathbf{v} f d^3\mathbf{v}. \tag{1.12}$$

Here the divergence of the pressure tensor can be written as

$$\operatorname{div} \boldsymbol{\mathcal{P}} = \frac{\partial \mathcal{P}_{ij}}{\partial x_i} \mathbf{e}_j, \quad i = 1, 2, 3 \tag{1.13}$$

However, in the case of an isotropic plasma, the pressure tensor's nonzero elements only appear in the diagonal and in this case, the pressure tensor $\boldsymbol{\mathcal{P}}$ is replaced with the scalar pressure, P, where $\boldsymbol{\mathcal{P}} = \operatorname{diag}(P, P, P)$ and the divergence in (1.9) becomes a gradient operation. In this work the scalar pressure will be used exclusively.

Along with the zeroeth and first moment, one can compute the second moment which is related to the conservation of energy but will not be needed in this work. The Maxwell's equations (1.5) along with (1.8), (1.9) and different simplifying assumptions form the starting point for several important fluid models. This includes the isotropic magnetohydrodynamic (MHD) system of equations which will be the main focus of this work.

In other physical context, different plasma descriptions can be used, including the following ones.

- **Gyrokinetic description**: the kinetic equations are averaged over fast circular motion of the gyroradius. Here a gyroradius is the radius of the circular motion of a charged particle in the presence of a uniform magnetic field, namely

$$r_g = \frac{mv_\perp}{|q|B}, \tag{1.14}$$

where m is the mass of the particle, $v_\perp$ is the perpendicular velocity with respect to the magnetic field, q as before is the electric charge of the particle and B is the magnetic field magnitude [19]. This model assumes a strongly magnetized plasma, the spatial scale is on the order of the gyroradius and frequencies considerably lower than the cyclotron frequencies ($\omega = qB/m$). Appropriate sources are [16, 38, 32, 31].

- **Hybrid kinetic/fluid description**: in this description some components are modelled with a fluid description and some others kinetically in order to reduce the heavy computational demands of a fully kinetic description while retaining some kinetic information of one or several components. For example, a very common approach is to apply a fully kinetic treatment only of the ions and describe the electrons with a simpler fluid model. This method has been utilized for over 45 years in the computational physics community. Further information is available in [21, 49].

- **Quantum plasma description**: Most plasmas are associated with charged particles that behave classically. However, if the density is increased and temperature decreased sufficiently, the plasma particles, mostly electrons, become quantum degenerate as the extension of their wave functions are on the order of the distance between particles [15]. In quantum plasma their are additional forces that arise that need to be accounted for. These include things such as quantum statistical pressure, and angular momentum spin [44, 36].

1.3 The MHD system of equations and MHD waves

One can consider the isotropic MHD model for an ideal plasma as an extension of the Euler fluid equations

$$\frac{\partial \mathbf{V}}{\partial t} + (\mathbf{V}\cdot\nabla)\mathbf{V} = -\frac{1}{\rho}\operatorname{grad} P, \tag{1.15a}$$

$$\operatorname{div}\mathbf{V} = 0, \tag{1.15b}$$

with an extra forcing term coming from the electrodynamic Lorentz force. For a quasi-neutral plasma with roughly an equal amount of ions and electrons, this force can be written as $\mathbf{f} = \mathbf{J}\times\mathbf{B}$, where $\mathbf{J} = \frac{1}{\mu}\operatorname{curl}\mathbf{B}$ is the electric current density and μ is the magnetic permeability of the plasma. This isotropic model of plasma is suitable when the mean free path of plasma particles is much less than the typical length scale of the problem. The plasma is also considered ideal with infinite conductivity and negligible viscosity. Both of these approximations are valid for large magnetic and kinetic Reynolds numbers [20]. Here the magnetic

Reynolds number is given by $\mathcal{R}_m = VL/\eta$ and the kinetic Reynolds number $\mathcal{R}_k = VL/\nu$ where V is the typical velocity scale, L is the typical length scale and η and ν are the magnetic diffusivity and kinematic viscosity respectively. Following these assumptions, the ideal isotropic MHD model takes on the form

$$\frac{\partial \rho}{\partial t} + \operatorname{div} \rho \mathbf{V} = 0, \tag{1.16a}$$

$$\rho \frac{\partial \mathbf{V}}{\partial t} = \rho \mathbf{V} \times \operatorname{curl} \mathbf{V} + \mathbf{J} \times \mathbf{B} - \operatorname{grad} P - \rho \operatorname{grad} \frac{\mathbf{V}^2}{2}, \tag{1.16b}$$

$$\frac{\partial \mathbf{B}}{\partial t} = \operatorname{curl}(\mathbf{V} \times \mathbf{B}), \tag{1.16c}$$

$$\operatorname{div} \mathbf{B} = 0. \tag{1.16d}$$

In (1.16) ρ is the plasma density, $\mathbf{V}$ is the plasma velocity, P is the scalar pressure (while models of anisotropic plasmas utilize tensor valued pressure) and $\mathbf{B}$ is the magnetic induction vector. Even in the idealized MHD equations the rich mathematical structure gives rise to many different instabilities and waves. This system of equations (1.16) needs to be closed with an appropriate equation of state. For example, it is common to study certain types of plasma waves using a compressible MHD framework with an adiabatic equation of state

$$\left(\frac{\partial}{\partial t} + \mathbf{V} \cdot \operatorname{grad} \right) \left(\frac{P}{\rho^\Gamma} \right) = 0, \tag{1.17}$$

where Γ is the ratio of specific heats, which for a monatomic ideal gas has the value of $5/3$.

The equations (1.16), (1.17) can be linearised using first order perturbations with the assumption that the equilibrium value of the plasma current and velocity are both zero, namely

$$\rho = \rho_0 + \epsilon \tilde{\rho}, \tag{1.18a}$$

$$P = P_0 + \epsilon \tilde{P}, \tag{1.18b}$$

$$\mathbf{B} = \mathbf{B}_0 + \epsilon \tilde{\mathbf{B}}, \tag{1.18c}$$

$$\mathbf{V} = \epsilon \tilde{\mathbf{B}}, \tag{1.18d}$$

$$\mathbf{J} = \epsilon \tilde{\mathbf{J}}. \tag{1.18e}$$

Upon substitution of the perturbations into (1.16) and (1.17), discarding higher order terms of ϵ and dropping the tildes, one obtains the linear system

$$\frac{\partial \rho}{\partial t} + \rho_0 \operatorname{div} \mathbf{V} = 0, \tag{1.19a}$$

$$\rho_0 \frac{\partial \mathbf{V}}{\partial t} = \mathbf{J} \times \mathbf{B_0} - \operatorname{grad} P, \tag{1.19b}$$

$$\frac{\partial \mathbf{B}}{\partial t} = \operatorname{curl}(\mathbf{V} \times \mathbf{B_0}), \tag{1.19c}$$

$$\operatorname{div} \mathbf{B} = 0, \quad \mathbf{J} = \frac{1}{\mu} \operatorname{curl} \mathbf{B}, \tag{1.19d}$$

$$\frac{\partial}{\partial t} \left(\frac{P}{P_0} - \frac{\Gamma \rho}{\rho_0} \right) = 0. \tag{1.19e}$$

Following the method described in [27] and searching for harmonic wave-like solutions in which perturbations behave like $e^{i(\mathbf{k}\cdot\mathbf{x} - \omega t)}$, relations for ρ, P and $\mathbf{B}$ can be found from the first, third and last equation of (1.19). These are given by

$$\rho = \rho_0 \frac{\mathbf{k} \cdot \mathbf{V}}{\omega}, \tag{1.20a}$$

$$P = \Gamma P_0 \frac{\mathbf{k} \cdot \mathbf{V}}{\omega}, \tag{1.20b}$$

$$\mathbf{B} = \frac{\mathbf{k} \times \mathbf{B_0} \times \mathbf{V}}{\omega}. \tag{1.20c}$$

Upon substituting these expressions into the second equation of (1.19), assuming without loss of generality that $\mathbf{B_0}$ is directed along the z axis and $\mathbf{k}$ lies in the xz plane one can write the following matrix equation [27]

$$\begin{bmatrix} \omega^2 - k^2 v_a^2 - k^2 v_s^2 \sin^2\theta & 0 & -k^2 v_s^2 \sin\theta\cos\theta \\ 0 & \omega^2 - k^2 v_a^2 \cos^2\theta & 0 \\ -k^2 v_s^2 \sin\theta\cos\theta & 0 & \omega^2 - k^2 v_s^2 \cos^2\theta \end{bmatrix} \begin{bmatrix} V_x \\ V_y \\ V_z \end{bmatrix} = \begin{bmatrix} 0 \\ 0 \\ 0 \end{bmatrix}, \tag{1.21}$$

where θ is the angle between $\mathbf{k}$ and $\mathbf{B}$,

$$v_s = \sqrt{\frac{\Gamma P_0}{\rho_0}} \tag{1.22}$$

is the standard acoustic wave speed, and

$$v_a = \frac{B_0}{\sqrt{\mu \rho_0}} \tag{1.23}$$

is called the *Alfvén speed*.

In order to solve (1.21) for non-trivial $\mathbf{V}$, the determinant of the matrix in (1.21) must vanish. This gives three roots for ω corresponding to three distinct dispersion relations

1.
$$\omega = k v_a \cos\theta, \tag{1.24}$$

2.
$$\omega = k\frac{1}{\sqrt{2}}\sqrt{v_a^2 + v_s^2 - \sqrt{(v_a^2+v_s^2)^2 - 4v_a^2 v_s^2\cos^2\theta}}, \tag{1.25}$$

3.
$$\omega = k\frac{1}{\sqrt{2}}\sqrt{v_a^2 + v_s^2 + \sqrt{(v_a^2+v_s^2)^2 - 4v_a^2 v_s^2\cos^2\theta}}. \tag{1.26}$$

The first dispersion relation is for *shear-Alfvén waves*. This is named after Hannes Alfvén who showed the existence of these transverse waves in 1942, this is discussed further in [1]. From (1.21), it is clear that $\mathbf{V} = (0, V_y, 0)$, so the motion is perpendicular to the magnetic field.

The second and third dispersion relations are referred to as the slow and fast *magnetosonic waves* respectively with $\mathbf{V} = (V_x, 0, V_z)$. Magnetosonic waves are purely longitudinal waves driven by thermal pressure, magnetic pressure and magnetic tension. For more information about waves in plasma, appropriate sources are [46, 27, 45, 2].

1.4 Incompressible MHD model and related models

For the majority of this work the ideal isotropic incompressible MHD model will be the starting point. Incompressible models are commonly used in a variety of labs and physical applications. This system is given by

$$\frac{\partial \rho}{\partial t} + \operatorname{div}\,\rho\mathbf{V} = 0, \tag{1.27a}$$

$$\rho\frac{\partial \mathbf{V}}{\partial t} = \rho\mathbf{V}\times\operatorname{curl}\mathbf{V} + \mathbf{J}\times\mathbf{B} - \operatorname{grad}P - \rho\operatorname{grad}\frac{\mathbf{V}^2}{2}, \tag{1.27b}$$

$$\frac{\partial \mathbf{B}}{\partial t} = \operatorname{curl}(\mathbf{V}\times\mathbf{B}), \tag{1.27c}$$

$$\operatorname{div}\mathbf{B} = 0, \quad \operatorname{div}\mathbf{V} = 0. \tag{1.27d}$$

One can see that if the magnetic field is set to zero, the above system becomes the incompressible Euler fluid equations (1.15).

Another important system of interest is the incompressible *equilibrium* (time independent) MHD system

$$\operatorname{div} \rho \mathbf{V} = 0, \tag{1.28a}$$

$$\rho \mathbf{V} \times \operatorname{curl} \mathbf{V} + \mathbf{J} \times \mathbf{B} - \operatorname{grad} P - \rho \operatorname{grad} \frac{\mathbf{V}^2}{2} = 0, \tag{1.28b}$$

$$\operatorname{curl} (\mathbf{V} \times \mathbf{B}) = 0, \tag{1.28c}$$

$$\operatorname{div} \mathbf{B} = 0, \tag{1.28d}$$

$$\operatorname{div} \mathbf{V} = 0. \tag{1.28e}$$

An immediate consequence of equation (1.28a) and equation (1.28e) is

$$(\operatorname{grad} \rho) \cdot \mathbf{V} = 0, \tag{1.29}$$

which implies that the plasma density does not change along streamlines. The streamlines of a time independent vector field, $\mathbf{A}$, are defined by the parametric equation

$$\frac{d\mathbf{r}}{ds} = \mathbf{A}(\mathbf{r}(s)). \tag{1.30}$$

For these curves $\mathbf{A}$ is tangent to the curve at every point.

A further reduction of (1.27), (1.28) is the static equilibrium MHD system ($\mathbf{V} = 0$) given by

$$\operatorname{div} \mathbf{B} = 0, \tag{1.31a}$$

$$\operatorname{curl} \mathbf{B} \times \mathbf{B} = \mu \operatorname{grad} P. \tag{1.31b}$$

Exact solutions of the system (1.31) are studied in Chapter 2 below.

1.5 Equilibrium field line topology

An important property of equilibrium and static equilibrium MHD models given by (1.31) and (1.28) is their magnetic field line topology. Some important applications of the topological properties of the field lines can be found in [14, 20]. Specifically, in most cases, the plasma streamlines (field lines of $\mathbf{V}$), and magnetic field lines (field lines of $\mathbf{B}$), are tangent to *magnetic surfaces* spanning the plasma domain. An example of the magnetic field lines lying on a magnetic surface can be seen in Figure 1.3. At every point of the magnetic surface, $\mathbf{V}$ and $\mathbf{B}$ are defined uniquely. It then follows that lines cannot intersect.

For MHD equilibrium (1.28), the following cases can arise.

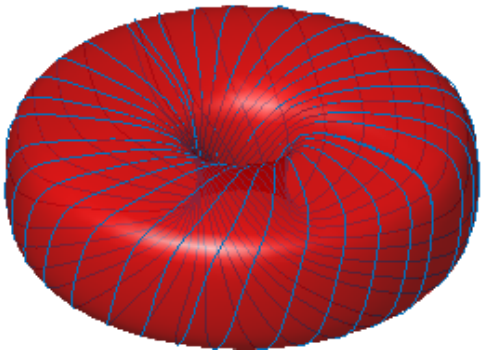

Figure 1.3: Field lines tangent to *magnetic surfaces*.

- If $\mathbf{V}$ and $\mathbf{B}$ are non-collinear, it follows from equation (1.28c) by the *Poincaré lemma* that locally (in a simply connected domain) there exists a function $\alpha = \alpha(\mathbf{x})$ such that $\mathbf{V} \times \mathbf{B} = \operatorname{grad} \alpha$, [48] and thus, $\alpha = \text{const}$ defines the magnetic surfaces to which both $\mathbf{V}$ and $\mathbf{B}$ are tangent.

- In the case when $\mathbf{V}$ and $\mathbf{B}$ are collinear, (i.e. $\mathbf{V} = f(\mathbf{x})\mathbf{B}$), which, from the solenoidality of $\mathbf{V}$ and $\mathbf{B}$ one has $\operatorname{grad} f(\mathbf{x}) \cdot \mathbf{V} = 0$, both $f(\mathbf{x})$ and $\rho(\mathbf{x})$, from equation (1.29), are constant on plasma streamlines and magnetic field lines. (i.e. $\mathbf{V} = f(\mathbf{x})\mathbf{B}$), which, from the solenoidality of $\mathbf{V}$ and $\mathbf{B}$ one has $\operatorname{grad} f(\mathbf{x}) \cdot \mathbf{V} = 0$, so both $f(\mathbf{x})$ and $\rho(\mathbf{x})$, from equation (1.29), are constant on plasma streamlines and magnetic field lines.

For static equilibrium (1.31), the following cases can arise.

- If $\mathbf{J} \sim \operatorname{curl} \mathbf{B}$ and $\mathbf{B}$ are non-collinear, then the pressure P will be non-constant, and lines of constant pressure will enumerate the magnetic surfaces that both $\mathbf{B}$ and $\mathbf{J}$ are tangent to.

- For $\operatorname{curl} \mathbf{B}$ and $\mathbf{B}$ collinear (i.e. $\operatorname{curl} \mathbf{B} = \alpha(\mathbf{x})\mathbf{B}$) both $\operatorname{curl} \mathbf{B}$ and $\mathbf{B}$ are tangent to magnetic surfaces which are enumerated by constant levels of $\alpha(\mathbf{x})$.

One can conclude that all magnetic field lines and plasma streamlines, except for *Beltrami flows* ($\alpha(\mathbf{x}) = \text{const}$), lie on 2D magnetic surfaces. Bounded magnetic surfaces are topologically equivalent to tori [35, 20].

1.6 Some approaches to the solution of MHD equations

Due to the highly non-linear form of the MHD equations, very few closed-form solutions are available in literature. For the ones available, significant simplifications are made. For the incompressible MHD equations when $\mathbf{B} = 0$, this system (1.27) reduces to the incompressible Euler equations (1.15). One simple solution that shows up is the Arnold-Beltrami-Childress (ABC) flow given in Cartesian coordinates by

$$\mathbf{V}(x,y,z) = (A\sin z + C\cos y)\mathbf{e}_x + (B\sin x + A\cos z)\mathbf{e}_y + (C\sin y + B\cos x)\mathbf{e}_z. \tag{1.32}$$

As static MHD (1.31) and the incompressible, time independent Euler equations (1.15) are equivalent up to notation (which will be further discussed in Chapter 3), the ABC flow solution (1.32) is also a solution to the static MHD equation (1.31). Even this simple looking solution has very complicated behaviour. In [50], chaotic and resonant streamlines are studied in the ABC flow and analytical criteria for the existence of these streamlines are obtained.

Many solutions available in literature are to the static equilibrium MHD equations ($\mathbf{V} = 0$). This assumption greatly reduces the difficulty in finding solutions. One interesting boundary value problem solution to the static equilibrium MHD equations (1.31) is shown in [37] where Coulomb wave functions are used. These special functions also make an appearance in the next chapter.

The static equilibrium MHD equations (1.31) are still quite complicated nonlinear PDEs in three spatial dimensions. A common technique of further simplification through the reduction of the number of independent variables, valid in many practical situations, is *symmetry reduction*.

1.6.1 Symmetry reductions of static equilibrium MHD equations

Several orthogonal coordinates systems are used in the following work: Cartesian coordinates (x, y, z), cylindrical coordinates (r, ϕ, z), and helical coordinates (r, η, ξ). In each case any vector field, $\mathbf{A}$ can be expressed by

$$\mathbf{A} = A^x\mathbf{e}_x + A^y\mathbf{e}_y + A^z\mathbf{e}_z = A^r\mathbf{e}_r + A^\phi\mathbf{e}_\phi + A^z\mathbf{e}_z = A^r\mathbf{e}_r + A^\eta\mathbf{e}_\eta + A^\xi\mathbf{e}_\xi. \tag{1.33}$$

Here, the helical coordinates can be defined from cylindrical coordinates as

$$r = r, \quad \eta = \phi - \gamma z/r^2, \quad \xi = z - \gamma\varphi, \tag{1.34}$$

where γ is some constant parameter which is related to the tightness of the helices. In helical coordinates, the equations $\xi = \text{const}$ and $\eta = \text{const}$ define two families of helices tangent to every cylinder $r = \text{const}$. Note that helical curvilinear coordinates (r, ξ, η) are not orthogonal. This coordinate system can be visualized as shown in Figure 1.4 which is taken from [23].

In nature and applications, several types of stable plasma equilibrium configurations are observed to have approximate axial or helical symmetry. These include axially and helically symmetric astrophysical jets and even helical plasma thrusters [5]. These observed symmetries act as the motivation to seek symmetric solutions to (1.31). By using the coordinate systems described above, we can impose the desired invariance to further simplify the system (1.31). These include $\partial/\partial\phi = 0$ for axial symmetry and $\partial/\partial\eta = 0$ for helical symmetry.

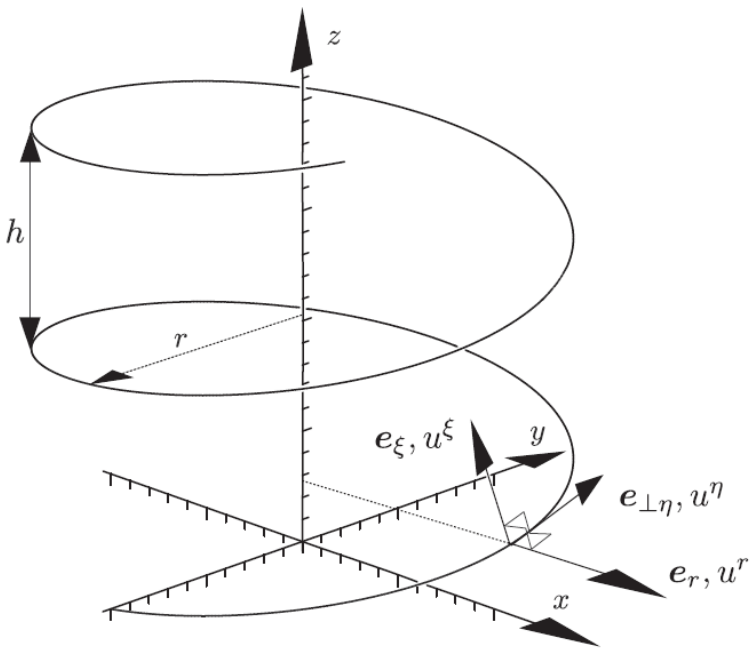

Figure 1.4: Image of the helix $\xi = \text{const}$ for $\gamma = h/2\pi$, where h is the z-step over one helical turn. The helical basis vectors can be seen. This image has been taken from [23].

1.6.2 Axially symmetric static equilibrium reduction

After imposing axial symmetry on (1.31), this system of PDEs can be reduced to a single PDE after introducing a potential flux function $\psi(\mathbf{x})$. Below we present a brief derivation of a single PDE on $\psi(x)$ that is equivalent to the four static MHD equations in the case of axial symmetry. This describes the Grad-Shafranov equation but also serves as a derivation of the Bragg-Hawthorne equation in equilibrium fluid dynamics when $\mathbf{B}$ is set to $\mathbf{V}$ and P is set to H. Starting with (1.31) given by

$$\left(\frac{\partial B^x}{\partial z} - \frac{\partial B^z}{\partial x}\right) B^z - \left(\frac{\partial B^y}{\partial x} - \frac{\partial B^x}{\partial y}\right) B^y = \frac{\partial P}{\partial x},$$
$$\left(\frac{\partial B^y}{\partial x} - \frac{\partial B^x}{\partial y}\right) B^x - \left(\frac{\partial B^z}{\partial y} - \frac{\partial B^y}{\partial z}\right) B^y = \frac{\partial P}{\partial y},$$
$$\left(\frac{\partial B^z}{\partial y} - \frac{\partial B^y}{\partial z}\right) B^y - \left(\frac{\partial B^x}{\partial z} - \frac{\partial B^y}{\partial x}\right) B^x = \frac{\partial P}{\partial z},$$
$$\frac{\partial B^x}{\partial x} + \frac{\partial B^y}{\partial y} + \frac{\partial B^z}{\partial z} = 0.$$

This system is now converted into cylindrical coordinates (r, ϕ, z) using the transformations

$$x = r\cos\phi, \quad y = r\sin\phi, \quad z = z,$$

with the differentials written as

$$\frac{d}{dx} = \cos\phi \frac{\partial}{\partial r} - \frac{\sin\phi}{r}\frac{\partial}{\partial \phi},$$

$$\frac{d}{dy} = \sin\phi \frac{\partial}{\partial r} + \frac{\cos\phi}{r} \frac{\partial}{\partial \phi}.$$

The projections of B^r and B^ϕ are related to B^x and B^y in the notation of 1.33 by

$$B^x = B^r \cos\phi - B^\phi \sin\phi,$$

$$B^y = B^r \sin\phi + B^\phi \cos\phi.$$

After simplifying and imposing axial invariance ($\partial/\partial\phi$) the following reduced system of PDEs is obtained

$$rB^z(B^r_z - B^z_r) - B^\phi(rB^\phi)_r = rP_r, \tag{1.36a}$$

$$B^z(rB^\phi)_z + B^r(rB^\phi)_r = 0, \tag{1.36b}$$

$$B^r(B^z_r - B^r_z) - B^\phi B^\phi_z = P_z, \tag{1.36c}$$

$$(rB^z)_z + (rB^r)_r = 0, \tag{1.36d}$$

where the superscripts describe the vector components of $\mathbf{B}$ and the subscripts represent the partial differentiation. A potential *flux function* is now introduced based on the vanishing divergence expression (1.36d),

$$-\psi_r = rB^z, \quad \psi_z = rB^r. \tag{1.37}$$

The above is now substituted into the second equation of (1.36) giving

$$\{\psi, rB^\phi\} = 0,$$

where $\{...\}$ denotes the Poisson bracket. The vanishing Poisson bracket in r and z between ψ and rB^ϕ implies a functional relationship between the two, which can be written as

$$rB^\phi = I(\psi), \tag{1.38}$$

where I is arbitrary. Multiplying the first equation of (1.36) by ψ_z/r and subtracting the third equation from (1.36) multiplied by ψ_r gives another vanishing Poisson bracket

$$\{P, \psi\} = 0,$$

in r and z between P and ψ, which leads to the following functional relationship:

$$P = P(\psi). \tag{1.39}$$

Using the obtained relationships, (1.37), (1.38), (1.39) from above and substituting these into the first (or third) equation of (1.36) one arrives at a single PDE for the unknown flux function $\psi(r, z)$. This is known as the *Grad-Shafranov equation*.

$$\frac{\partial^2\psi}{\partial r^2} + \frac{\partial^2\psi}{\partial z^2} - \frac{1}{r}\frac{\partial\psi}{\partial r} + I(\psi)I'(\psi) = -\mu r^2 P'(\psi), \tag{1.40}$$

Here primes denote derivatives with respect to ψ and the magnetic field components are given by

$$\mathbf{B} = \frac{\psi_z}{r}\mathbf{e}_r + \frac{I(\psi)}{r}\mathbf{e}_\phi + \frac{-\psi_r}{r}\mathbf{e}_z. \tag{1.41}$$

In the fluid dynamics setting, the PDE (1.40) arises for axially symmetric incompressible fluid flows, and is commonly referred to as the *Bragg-Hawthorne equation*.

$$\frac{\partial^2\psi}{\partial r^2} + \frac{\partial^2\psi}{\partial z^2} - \frac{1}{r}\frac{\partial\psi}{\partial r} + F(\psi)F'(\psi) = -r^2 H'(\psi). \tag{1.42}$$

In this case, $\psi(r, z)$ is the scalar *stream function* and the components of the velocity are given by

$$\mathbf{V} = \frac{\psi_z}{r}\mathbf{e}_r + \frac{F(\psi)}{r}\mathbf{e}_\phi + \frac{-\psi_r}{r}\mathbf{e}_z,$$

and

$$H = H(\psi), \quad F = F(\psi), \tag{1.43}$$

are arbitrary functions where

$$H = -\left(\frac{P}{\rho} + \frac{1}{2}\mathbf{V}^2\right) \tag{1.44}$$

is known as the Bernoulli function.

One important fluid parameter is known as the vorticity denoted by $\boldsymbol{\omega}$ and computed from $\mathbf{v}$ by $\boldsymbol{\omega} \equiv \operatorname{curl}\mathbf{v}$. This is analogous to the current density in MHD. In the case of axial symmetry and utilitzing the Bragg-Hawthorne equation, $\boldsymbol{\omega}$ can be written as:

$$\boldsymbol{\omega} = \left(-F'(\psi)\frac{\psi_z}{r}\right)\mathbf{e}_r + \left(r^2 H'(\psi) - F(\psi)F'(\psi)\right)\mathbf{e}_\phi + \left(F'(\psi)\frac{\psi_r}{r}\right)\mathbf{e}_z. \tag{1.45}$$

In the special case when $\boldsymbol{\omega} = 0$ one has *potential flow*, as $\operatorname{curl}\mathbf{v} = 0$ implies, by the Poincaré lemma, the local existence of the potential φ such that $\mathbf{v} = \operatorname{grad}\varphi$. Potential flow theory is a powerful way to model simpler settings such as motion of shallow water waves and flows around aerofoils [4]. In the case of an incompressible flow, φ must satisfy the Laplace equation $\nabla^2\varphi = 0$. potential flows in two dimensions reduces to a very simple model that can be analyzed with *conformal maps* utilizing complex analysis. More information on potential flow and conformal maps can be found in [4, 7].

There have been some important exact solutions obtained from equation (1.40) for different choices of $P(\psi)$ and $I(\psi)$. In [11] the solutions to the Grad-Shafranov equation modeling astrophysical jets and solar prominences were derived.. For astrophysical jets, the following solution to equation (1.40) was found

$$\Psi(r,z) = e^{-\beta r^2}\left(a_N L_N^*(2\beta r^2) + \sum_{n=1}^{N-1} a_n \sin(\omega_n z + b_n) L_n^*(2\beta r^2)\right). \tag{1.46}$$

Here L_n^* are anti-derivatives of the Laguerre polynomials. In this case, the free functions were chosen to be

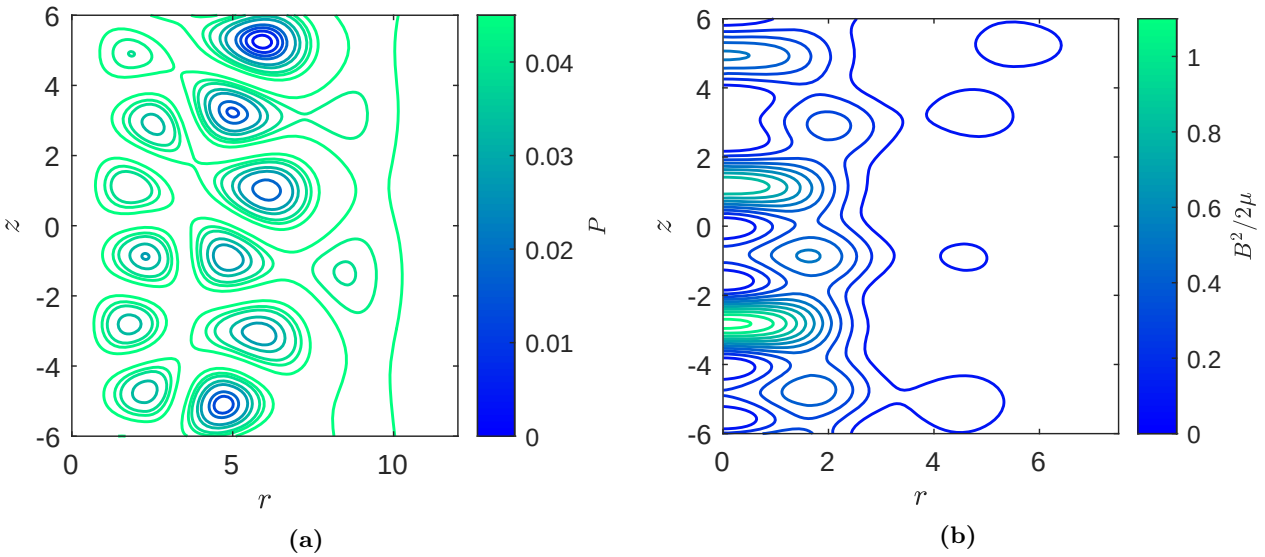

Figure 1.5: A cross-section of magnetic surfaces $P = \text{const}$ for a sample axially symmetric plasma equilibrium solution given by (1.46) is seen on the left, for $N = 3$, $\beta = 0.1$, $\alpha^2 = 24\beta$. The picture is quasi-periodic in z. The colour-bar shows the values of the dimensionless pressure $P = P_0 - 2\beta^2\psi^2/\mu$. Here $P_0 = 0.05$. On the right one can see lines of constant magnetic energy density $|\mathbf{B}|^2/2\mu$ where the magnetic field components are given by 2.10. This comes from a axially symmetric plasma equilibrium solution given by (1.46), for $N = 3$, $\beta = 0.1$ and $\alpha^2 = 24\beta$.

$$I(\psi) = \alpha\psi, \quad P(\psi) = p_0 - 2\beta^2\psi^2/\mu, \tag{1.47}$$

where α, p_0 and β are real constants and μ is the magnetic permeability. Level curves of the pressure P for the above solution are shown in Figure 1.5a along with the magnetic energy density seen in Figure 1.5b. If one takes the pressure contour and rotates it about the z axis the *magnetic surfaces* to which both the magnetic field $\mathbf{B}$ and the current density $\mathbf{J}$ are tangent can be seen. This image is shown Figure 1.6.

1.6.3 Helically symmetric static equilibrium reduction

Similarly to the axial reduction, after converting the static equilibrium MHD equations (1.31) to helical coordinates given by (1.34) and imposing helical symmetry $\partial/\partial\eta = 0$, this system of PDEs can be reduced to a single PDE after introducing a potential flux function $\psi(\mathbf{x})$ and following a similar derivation as the one above. This PDE in the two helical coordinates (r,ξ) is known as the Johnson-Frieman-Kulsrud-Oberman (JFKO) equation.

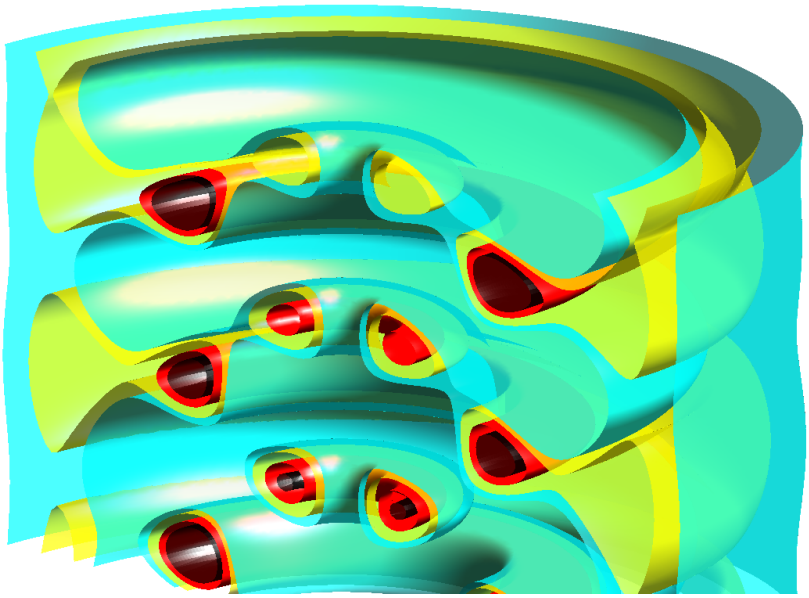

Figure 1.6: Axially symmetric magnetic surfaces $P = \text{const}$ given by equation (1.46), for $N = 3$, $\beta = 0.1$, $\alpha^2 = 24\beta$ takes the form of nested tori and wavy cylinders. This figure is created by the rotation of 1.5a about the z axis.

$$\frac{\psi_{\xi\xi}}{r^2} + \frac{1}{r}\frac{\partial}{\partial r}\left(\frac{r}{r^2+\gamma^2}\psi_r\right) + \frac{I(\psi)I'(\psi)}{r^2+\gamma^2} + \frac{2\gamma I(\psi)}{(r^2+\gamma^2)^2} = -\mu P'(\psi). \tag{1.48}$$

Here subscripts denote partial derivatives and primes denote regular derivatives with respect to the given variable. Again, $P(\psi)$ and $I(\psi)$ are arbitrary functions of ψ. Here γ is a constant parameter arising from the helical coordinate system $r = r$, $\eta = \phi - \gamma z/r^2$ and $\xi = z - \gamma\phi$. The magnetic field $\mathbf{B}$ written in cylindrical coordinates has the following form

$$\mathbf{B} = \frac{\psi_\xi}{r}\mathbf{e}_r + \frac{rI(\psi) + r\psi_r}{r^2+\gamma^2}\mathbf{e}_\phi + \frac{\gamma I(\psi) - r\psi_r}{r^2+\gamma^2}\mathbf{e}_z. \tag{1.49}$$

There have been some exact physical solutions to equation (1.48) such as an interesting example which is presented in [12]. These solutions describe helically symmetric astrophysical jets with the exact solutions written as

$$\Psi_{Nmn}(r,\xi) = e^{-\beta r^2}\left(a_N B_{0N}(2\beta r^2) + r^m B_{mn}(2\beta r^2)(a_{mn}\cos(m\xi/\gamma) + b_{mn}\sin(m\xi/\gamma))\right). \tag{1.50}$$

Here B_{mn} are related to the Laguerre polynomials by the following.

$$B_{mn}(x) = \frac{d^m}{dx^m}L_{m+n} - k_{mn}(x)\frac{d^{m+1}}{dx^{m+1}}L_{m+n}(x), \tag{1.51}$$

where $k_{mn} = (m + 2\beta\gamma^2 - \alpha\gamma)/(4n\beta\gamma^2)$. In equation (1.50) N,m and n are arbitrary non-negative integers which all satisfy the inequality $2N > 2n + m$ [12]. Here the free functions are given by

$$I(\psi) = \alpha\psi, \quad P(\psi) = p_0 - 2\beta^2\psi^2\mu.$$

An example of a helically invariant solution is shown in Figure 1.7a along with the corresponding magnetic energy density in Figure 1.7b. Solutions of both the Grad-Shafranov equation and the JFKO equation will be discussed in further detail in Chapter 2. Some interesting related work in fluid dynamics regarding helical flows and their conservation laws can be found [34, 24].

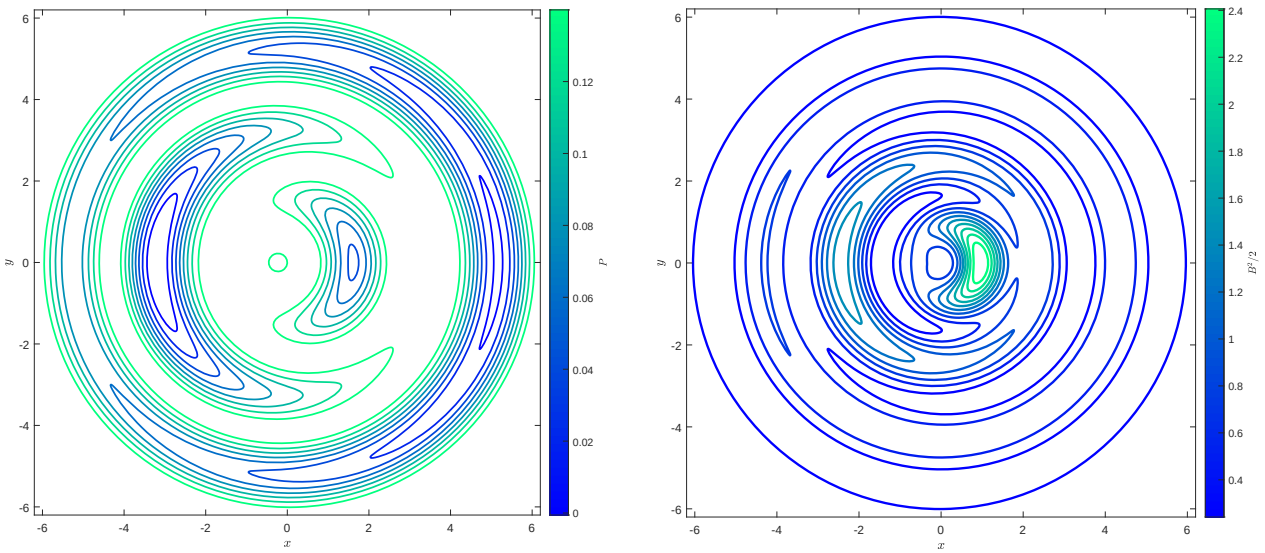

(a) **(b)**

Figure 1.7: Helically symmetric magnetic surfaces $P = \text{const}$ can be seen in 2.12a. $\Psi(r, \xi)$ is given by 1.50 with $N = 4$, $n = 0$, $m = 1$, $\kappa = 0.2$, $\gamma = 1$, $a_N = a_n = 1$ and $b_n = 0$. The corresponding magnetic energy density can be seen in 1.7b.

1.7 Infinite symmetries of MHD equilibrium equations

Looking back at the equilibrium MHD equations (1.28), and letting $\mathbf{V}$, $\mathbf{B}$, P and ρ being a solution to equation (1.28) in which the density ρ is constant on both magnetic field lines and streamlines, there exists an infinite family of solutions $\mathbf{V}_1$, $\mathbf{B}_1$, P_1 and ρ_1 as discussed in [14], which can be computed from the original solution as follows

$$\mathbf{B}_1 = b(\psi)\mathbf{B} + c(\psi)\sqrt{\mu\rho}\mathbf{V}, \tag{1.52a}$$

$$\mathbf{V}_1 = \frac{c(\psi)}{a(\psi)\sqrt{\mu\rho}}\mathbf{B} + \frac{b(\psi)}{a(\psi)}\mathbf{V}, \tag{1.52b}$$

$$P_1 = CP + \frac{C\mathbf{B}^2 - \mathbf{B}_1^2}{2\mu}, \tag{1.52c}$$

$$\rho_1 = a^2(\psi)\rho; \tag{1.52d}$$

here $a = a(\psi)$, $b = \underline{(}\psi)$, $c = c(\psi)$ are arbitrary functions constant on both magnetic fields lines and streamlines, with the only restriction, $b^2(\psi) - c^2(\psi) = C = \text{const}$. The transformation (1.52) is such as to preserve the magnetic surfaces of the initial plasma configuration $(\mathbf{V}, \mathbf{B}, P, \rho)$.

For the static equilibrium case ($\mathbf{V} = 0$) this transformation simplifies to

$$\mathbf{B}_1 = \sqrt{C + c^2(\psi)}\mathbf{B}, \quad \mathbf{V}_1 = \frac{c(\psi)}{a(\psi)\sqrt{\mu\rho}}\mathbf{B}, \tag{1.53a}$$

$$P_1 = CP + -\frac{c^2(\psi)\mathbf{B}^2}{2\mu}, \tag{1.53b}$$

$$\rho_1 = a^2(\psi)\rho. \tag{1.53c}$$

Written this way, it can be seen that it allows the construction of infinitely many solutions parameterized by two arbitrary functions from any given starting solution of the MHD equilibrium system

$$F_1(\psi) = c(\psi), \quad F_2(\psi) = a(\psi)\sqrt{\rho(\psi)}. \tag{1.54}$$

Therefore the transformations (1.53) can then be written as

$$\mathbf{B}_1 = \sqrt{C + F_2^2(\psi)}\mathbf{B}, \quad \mathbf{V}_1 = \frac{F_2(\psi)}{F_1(\psi)\sqrt{\mu}}\mathbf{B}, \tag{1.55a}$$

$$P_1 = CP - \frac{F_2^2(\psi)\mathbf{B}^2}{2\mu}, \tag{1.55b}$$

$$\rho_1 = F_2^2(\psi), \tag{1.55c}$$

and used to transform the exact axially and helically symmetric static equilibrium solutions into new solutions with $\mathbf{V_1} \neq 0$.

It should be noted that while the original and transformed solutions may or may not be stable solutions of (1.27), Vladimirov in [47] showed that no new instability would arise from the transformations given by (1.52). In other words, if one can show that the static equilibrium solutions are stable then these transformed solutions will also be stable. These transformations will be used in Chapter 2 to convert new exact static equilibrium solutions that we derive into non-zero velocity solutions which satisfy dynamic MHD equilibrium equations (1.28).

2 Exact solutions to axially and helilcally symmetric MHD static equilibrium equations

2.1 Introduction

In this chapter, new exact physical solutions to the equilibrium MHD equations (1.28) for both axial and helical reductions are presented. These solutions are obtained by first deriving new axial and helical solutions to the static equilibrium MHD equations (1.31) and then utilizing the Bogoyavlenskij transformation discussed in the previous chapter for ($\mathbf{V} \neq 0$), are given by 1.53 in order to transform them into dynamic solutions which solve (1.28). The conditions that a solution to (1.28) must satisfy in order to be considered physical are discussed along with the boundary conditions of *truncated* solutions which have a restricted domain outside of which have vanishing magnetic fields and pressure. Starting with the static equilibrium MHD equations (1.31) in the axial case, solutions to the Grad-Shafranov equation (1.40) for the highest power series expansion of both free functions, $I(\psi)$ and $P(\psi)$, such that the Grad-Shafranov equation is separable are considered. This corresponds to $I(\psi)$ being linear in ψ and $P(\psi)$ being quadratic in ψ. After separation of variables, two separate families of solutions arise depending on the sign of the ψ^2 coefficient in the pressure. In the first family when the coefficient is negative, the separated solutions are written in terms of Whittaker functions. A proposition is proven that shows these solutions do not need to be truncated to be physical if and only if the first parameter of the Whittaker functions are integers. In this case, these solutions are related to previously discussed solutions given by (1.46) which are found in [11]. In the second family when the coefficient is negative, the separated solution is written in terms of Coulomb wave functions. All of the solutions of this type must be truncated to be physical due to the Coulomb wave functions oscillatory nature. Similar to the axial case, the helical symmetric solutions of (1.31) split into two families of solutions to the JFKO equation (1.48) again depending on the sign of the ψ^2 coefficient in the pressure. Both of the families are expressed in terms of the confluent Heun function. The first family behaves similar to the Whittaker solution and has to be truncated to be physical except for the special case when the confluent Heun function produces polynomials. This case is related to (1.50) and found in [12]. The second family which is also written in terms of the confluent Heun function only with complex parameters has oscillatory nature similar to the Coulomb wave functions and needs to be truncated to be a physical solution. In the last part of this chapter, an axial and helical solution are transformed into solutions to (1.28) utilizing the Bogoyavlenskij transformations (1.53).

2.2 Physical solutions to MHD equilibria

For solutions to the equilibrium MHD equations given by

$$\operatorname{div} \rho \mathbf{V} = 0, \tag{2.1a}$$

$$\rho \mathbf{V} \times \operatorname{curl} \mathbf{V} + \mathbf{J} \times \mathbf{B} - \operatorname{grad} P - \rho \operatorname{grad} \frac{\mathbf{V}^2}{2} = 0, \tag{2.1b}$$

$$\operatorname{curl} (\mathbf{V} \times \mathbf{B}) = 0, \tag{2.1c}$$

$$\operatorname{div} \mathbf{B} = 0, \tag{2.1d}$$

$$\operatorname{div} \mathbf{V} = 0, \tag{2.1e}$$

and the static equilibrium equations given by

$$\operatorname{div} \mathbf{B} = 0, \tag{2.2a}$$

$$\operatorname{curl} \mathbf{B} \times \mathbf{B} = \mu \operatorname{grad} P, \tag{2.2b}$$

to be physically relevant, the following conditions may be expected to hold.

1. The regularity, continuity and sufficient smoothness of the dependent variables $\mathbf{B}, \mathbf{V}, P, \rho$.
2. In the case of a localized plasma configuration in unbounded 3D space, $P = 0$ outside $\mathcal{U}$, or $P \leq P_0 = \text{const} > 0$ with $P \to P_0$ when $|\mathbf{x}| \to \infty$.
3. Finite total kinetic and magnetic energy: $\displaystyle\int_{\mathcal{U}} \left(\frac{|\mathbf{B}(\mathbf{x})|^2}{2\mu} + \rho \frac{|\mathbf{V}(\mathbf{x})|^2}{2} \right) d\mathbf{x} < +\infty$.

Here $\mathcal{U}$ is either the whole plasma domain or, for a plasma configuration stretched along, say, the z-axis, a slice $x, y \in \mathbb{R}$, $z_1 \leq z \leq z_2$.

For a plasma in a domain $\mathcal{U}$ bounded by $\partial\mathcal{U}$ which is referred to as the *current sheet* and $\mathbf{B}, \mathbf{V}, P \to 0$ on $\partial\mathcal{U}$, the tangential boundary of the magnetic field can be derived as follows.

By integrating the Maxwell's equation

$$\operatorname{curl} \mathbf{H} = \mathbf{J} \tag{2.3}$$

where $\mathbf{H} = \mathbf{B}/\mu$, over a small rectangle $\mathcal{S}$ with height h and length l where the boundary of $\mathcal{S}$ is the curve $\mathcal{C}$ such that the bottom and top of $\mathcal{C}$ are parallel to the surface dividing the two magnetic fields given by $\mathbf{H}_1$ inside the plasma and $\mathbf{H}_2$ outside the plasma

$$\iint_{\mathcal{S}} \operatorname{curl} \mathbf{H} \cdot \mathbf{n} \, d\Sigma = \iint_{\mathcal{S}} \mathbf{J} \cdot \mathbf{n} \, d\Sigma \tag{2.4}$$

applying Stokes theorem, and taking the limit of the height of the rectangle to zero (so that the integration is happening over the boundary of the surface)

$$\lim_{h\to 0}\left(\oint_{\mathcal{C}} \mathbf{H}\cdot d\mathbf{r} = \iint_{\mathcal{S}} \mathbf{J}\cdot\mathbf{n}d\Sigma\right) \tag{2.5}$$

one arrives at

$$(\mathbf{H}_1^{\parallel} - \mathbf{H}_2^{\parallel})l = \mathbf{I}_{encl}\times\mathbf{n} \tag{2.6}$$

where I_{encl} is the total enclosed free current. Now defining $K = I_{encl}/l$ this gives

$$(\mathbf{H}_1^{\parallel} - \mathbf{H}_2^{\parallel}) = \mathbf{K}\times\mathbf{n}. \tag{2.7}$$

In our particular case where the outside magnetic field is being set to zero and the magnetic field inside is entirely in the tangential direction, the following boundary condition is obtained

$$\mathbf{H}_1 = \mathbf{K}_{encl}\times\mathbf{n} \tag{2.8}$$

where $\mathbf{n}$ is the outward facing normal and $\mathbf{K}$ is referred to as the *surface current density* and has SI units of A/m.

In the following sections, if a solution requires truncation at some chosen boundary, $\partial\mathcal{U}$, to satisfy the two physical constraints, then the solution is referred to as a *truncated* solution, which is still a valid solution inside a domain with a boundary, where the surface current defined by (2.8) is introduced on the boundary surface. However, if the solution satisfies the physical constraints in the whole space, then it will be referred to as a *global* solution.

First off, solutions to the static equilibrium problem (1.31) will be found with the help of the Grad-Shafranov equation in the axially symmetric case and the JFKO equation in the helically symmetric case. Using these new solutions and the Bogoyavlinskij transformations given by (1.55), solutions to the dynamic equilibrium problem (1.28) will be constructed.

2.3 Axially symmetric static MHD equilibria

Starting with the Grad-Shafronov equation

$$\frac{\partial^2\psi}{\partial r^2} + \frac{\partial^2\psi}{\partial z^2} - \frac{1}{r}\frac{\partial\psi}{\partial r} + I(\psi)I'(\psi) = -\mu r^2 P'(\psi), \tag{2.9}$$

where the primes denote derivatives with respect to ψ and the magnetic field components are given by

$$\mathbf{B} = \frac{\psi_z}{r}\mathbf{e}_r + \frac{I(\psi)}{r}\mathbf{e}_\phi + \frac{-\psi_r}{r}\mathbf{e}_z, \tag{2.10}$$

there are certain choices of the arbitrary functions P and I in equation (1.40) for which the Grad-Shafranov equation becomes linear.

Choosing the pressure to be quadratic and the arbitrary function related to the poloidal current to be linear,

$$P(\psi) = P_0 + \frac{1}{2\mu} a\psi^2, \quad I(\psi) = \alpha\psi, \tag{2.11}$$

the Grad-Shafranov equation becomes a linear homogeneous second order PDE

$$\frac{\partial^2\psi}{\partial r^2} - \frac{1}{r}\frac{\partial\psi}{\partial r} + \frac{\partial^2\psi}{\partial z^2} + (\alpha^2 + ar^2)\psi = 0. \tag{2.12}$$

Several interesting solutions to equation (2.12) have been found through the method of separation of variables. One of these examples was discussed in Chapter 1 regarding axially symmetric astrophysical jets with the exact solution given by (1.46).

The linear homogeneous PDE equation (2.12) admits separated solutions $\psi(r, z) = R(r)Z(z)$, satisfying

$$R'' - \frac{1}{r}R' + (\alpha^2 + ar^2 + \lambda)R = 0, \tag{2.13a}$$

$$Z'' = \lambda Z, \tag{2.13b}$$

where λ is an arbitrary separation constant.

Depending on the value of a in the pressure term, one obtains two different families of solutions. The two families of solutions correspond to two different types of pressure profiles. For $a < 0$, $P \leq P_1 = \text{const} > 0$ with $P \to P_1$ when $|\mathbf{x}| \to \infty$. For the case when $a > 0$, $P > 0$ inside of $\mathcal{U}$ and $P = 0$ outside of $\mathcal{U}$.

2.3.1 First family of new axially symmetric solutions

The first family of solutions arises when $a = -q^2 < 0$. This gives the following formula for the pressure

$$P(\psi) = P_0 - \frac{1}{2\mu} q^2\psi^2. \tag{2.14}$$

This corresponds to a pressure profile which is bounded above by some P_0 where $P \to P_0$ when $|\mathbf{x}| \to \infty$. This model is more appropriate with plasmas confined to atmosphere or in some ambient medium.

When the separation constant is a negative value, $\lambda = -k^2, k > 0$, the solution is more akin to model a plasma jet stretched along the z-axis. Now the solution to (2.13b) is simply

$$Z = C_1 \sin(kz) + C_2 \sin(kz). \tag{2.15}$$

In order to solve (2.13a) the substitution $x = qr^2$ can be used to transform this equation into a more familiar form, namely

$$R'' + \left(-\frac{1}{4} + \frac{\alpha^2 - k^2}{4qx}\right) R = 0. \tag{2.16}$$

This equation is now related to the following Whittaker ODE[1]

$$y''(s) + \left(-\frac{1}{4} + \frac{\delta}{s} + \frac{1/4 - \nu^2}{s^2}\right) y(s) = 0 \tag{2.17}$$

with the general solution

$$y(s) = C_1 W_M(\delta, \nu, s) + C_2 W_W(\delta, \nu, s).$$

This gives the following general solution to equation (2.16) as

$$R(r) = C_1 W_M(\delta, \nu, qr^2) + C_2 W_W(\delta, \nu, qr^2). \tag{2.18}$$

Here

$$\delta = \frac{\alpha^2 - k^2}{4q}, \tag{2.19}$$

and $\nu = 1/2$. This gives the separated solution of ψ as the product of (2.18) and (2.15).

$$\psi_k(r, z) = \left(C_1 W_M\left(\delta, \frac{1}{2}, qr^2\right) + C_2 W_W\left(\delta, \frac{1}{2}, qr^2\right)\right)(C_3 \sin kz + C_4 \cos kz), \tag{2.20}$$

where C_1, C_2, C_3 and C_4 are all arbitrary constants. It should be noted that due to the linearity of equation (2.12), any linear combination of equation (2.20) is also a solution to equation (2.12). This can be written in general as

$$\Psi(r, z) = \int_{-\infty}^{\infty} \psi_k(r, z)\, dk, \tag{2.21}$$

where $C_i = C_i(k)$, $i = 1, 2, 3, 4$ are arbitrary distributions. It should be noted that for the following C_i,

$$C_1(k) = \sum_{n=1}^{N-1} \tilde{a_n} \Delta\left(k - \sqrt{\alpha^2 - 4qn}\right), \quad C_2(k) = 0, \quad C_3(k) = a_n \cos b_n, \quad C_4(k) = a_n \sin b_n, \tag{2.22}$$

where $\Delta(\mathbf{x})$ denotes the Dirac delta function, equation (2.21) will have a similar form to Bogoyavlenskij's solutions given by equation (1.46). This solution corresponds to the special case of the linear combintations of (2.20) when $\delta \in \mathbb{N}$. In this case, both Whittaker functions become linearly dependent. The following proposition holds.

Proposition 1. *For a pressure type of the form given by (2.14), the separated solution (2.20) is a global solution if and only if* $\delta \in \mathbb{N}$.

The proof of this proposition is found in Appendix A.

Examples of the first family of axially symmetric solutions

Two different examples are considered for the first solution family. The first example utilizes the separated solution (2.20) for a case when $\delta \notin \mathbb{N}$.

[1]The hypergeometric equation for different parameters values gives rise to the Whittaker, Coulomb wave, Legendre and Bessel ODEs found in this work.

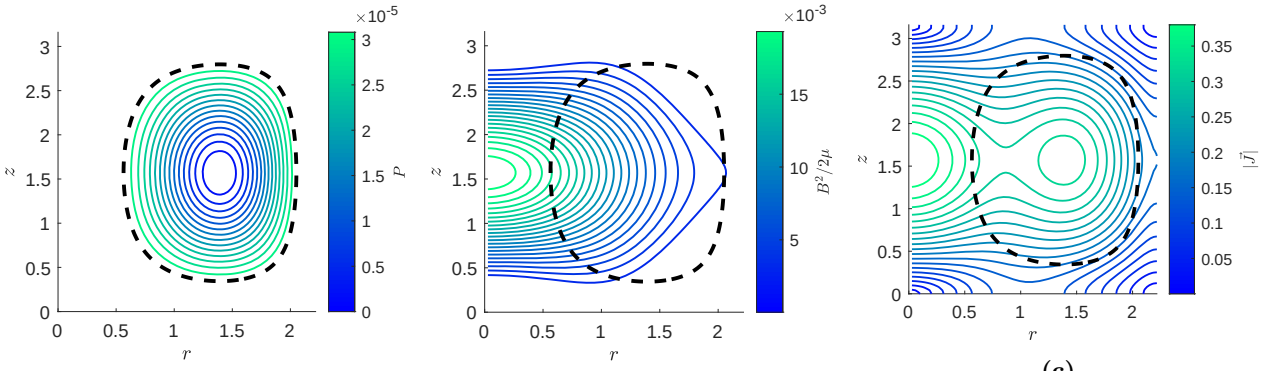

Figure 2.1: In Figure 2.1a, a cross-section of magnetic surfaces $P = \text{const}$ for an axially symmetric plasma equilibrium solution belonging to Family 1 with ψ given by (2.20), for $C_1 = 1$, $C_2 = 0$, $C_3 = 1$, $C_4 = 0$, $\mu = 1$, $q = 0.1$, $\alpha = 2$, $k = 1$ and truncated at the surface $P_0 = 3.3 \times 10^{-5}$ (shown with the black dashed line) can be seen. The color-bar shows the values of the dimensionless pressure $P = P_0 - q^2\psi^2/2$. chosen such that $P > 0$ inside of the chosen domain. The corresponding magnetic energy density, $|\mathbf{B}|^2/2\mu$, can be seen in 2.1b along with the magnitude of the current density in Figure 2.1c.

It should be noted that in order to achieve finite magnetic energy this solution must be *truncated* as, though not obvious from the plots, $\psi \to -\infty$ as $r \to \infty$. It should also be noted that the contours of Figure 2.1a and Figure 2.1b do not coincide as clearly the magnetic field components given by (2.10) are not functions of ψ. The dotted bold line in all three figures mark the boundary of the plasma domain. Along with this, the value of α was swept through three separate values to show how the solution changes. Here $\alpha_i = 2 + 0.1i, i = 1, 2, 3$ corresponds to the black, red and cyan coloured solutions respectively. These can be seen in Figure 2.4.

The second example that is shown is a linear combination of the special case of (2.20) when $\delta \in \mathbb{N}$. By Proposition 1 and the linearity of (2.12), this is a global solution. This is the same type of solution as those discussed in [11] with the solution's formula written by (1.46), only this time expressed as a linear combination of Whittaker functions, specifically with the requirement that $\alpha^2 = 4qN$.

$$\Psi(r,z) = \sum_{n=1}^{N} W_W\left(n, \frac{1}{2}, qr^2\right)\left(a_n \sin\sqrt{4q(N-n)}z + b_n \cos\sqrt{4q(N-n)}z\right). \tag{2.23}$$

A cross-section of the magnetic surfaces can be see in Figure 2.3a along with a contour of the magnetic energy density seen in 2.3b. It can be seen with this example that the magnetic energy is concentrated about the center of the plasma.

2.3.2 The second family of axially symmetric solutions

This second family of solutions arises when $a = q^2 > 0$. This corresponds to plasmas residing in vacuum in which the pressure, $P = 0$ outside of $\mathcal{V}$ with $P > 0$ inside the domain. Starting from the separated equations given by (2.13) with $a = q^2$, the same plasma jet ansatz for $Z(z)$ given by equation (2.15) can be used. After

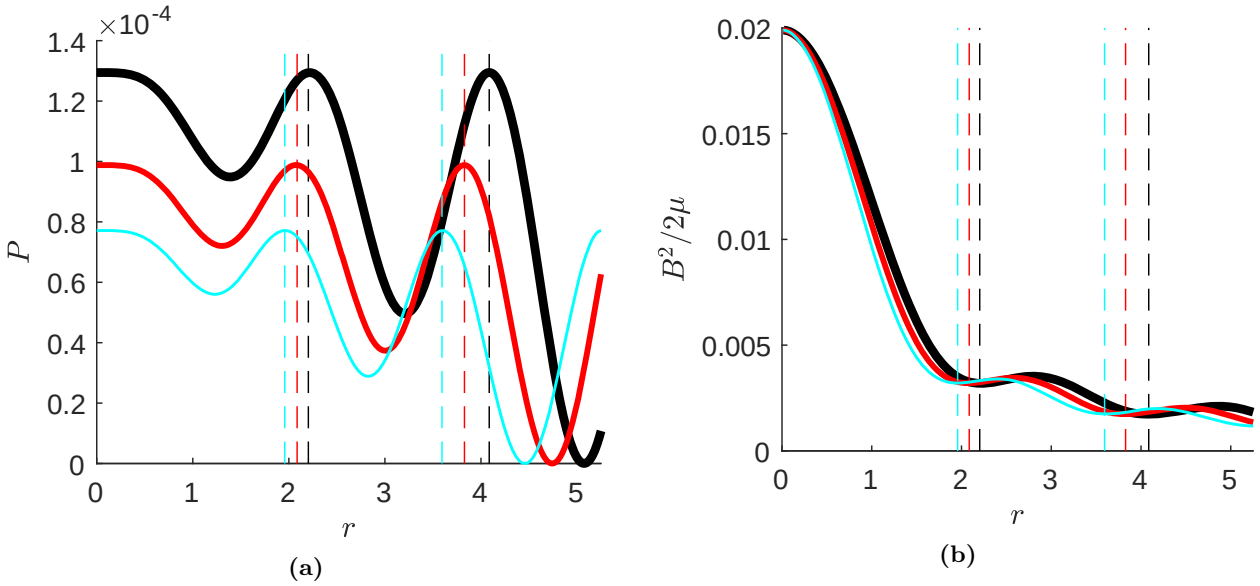

Figure 2.2: A pressure plot of the solution from Figure 2.1 for $z = 1.5$ and $\alpha_i = 2 + 0.1i, i = 1, 2, 3$ corresponding to the black, red and cyan plots can be seen in Figure 2.2a. The different magnetic energy densities for $z = 1.5$ can be seen in Figure 2.2b. The vertical dashed lines for each colour correspond to truncation surfaces that give physical solutions.

transforming the radial problem from (2.13) with $x = iqr^2$, where i is the imaginary unit, the following ODE related to the Whittaker ODE equation (2.17) is obtained:

$$R'' + \left(-\frac{1}{4} + \frac{k^2 - \alpha^2}{4qx}i\right) R = 0. \tag{2.24}$$

Therefore, by utilizing the general solution to the Whittaker ODE equation (2.17), the radial solution can be written in terms of Whittaker functions of a complex argument and parameter:

$$R(r) = C_1 W_M\left(-i\delta, \frac{1}{2}, iqr^2\right) + C_2 W_W\left(-i\delta, \frac{1}{2}, iqr^2\right), \tag{2.25}$$

where δ is specified in (2.19).

A relationship exists between Whittaker functions and the Coulomb wave functions:

$$W_M\left(-i\delta, \frac{1}{2}, iqr^2\right) = \frac{2\,i\,\mathcal{C}_F(0, -\delta, qr^2/2)}{|\Gamma(1 - i\delta)|e^{\frac{\pi}{2} - \delta}}. \tag{2.26}$$

Where $\Gamma(n)$ is the gamma function. This gives the motivation to transform the radial problem given in (2.13) into a related version of the Coulomb wave ODE using $x = qr^2/2$,

$$R'' + \left(1 + 2\frac{\alpha^2 - k^2}{4qx}\right) R = 0. \tag{2.27}$$

which is related to the Coulomb wave ODE

$$y''(s) + \left(1 - \frac{2\sigma}{s} - \frac{L(L+1)}{s^2}\right) y(s) = 0, \tag{2.28}$$

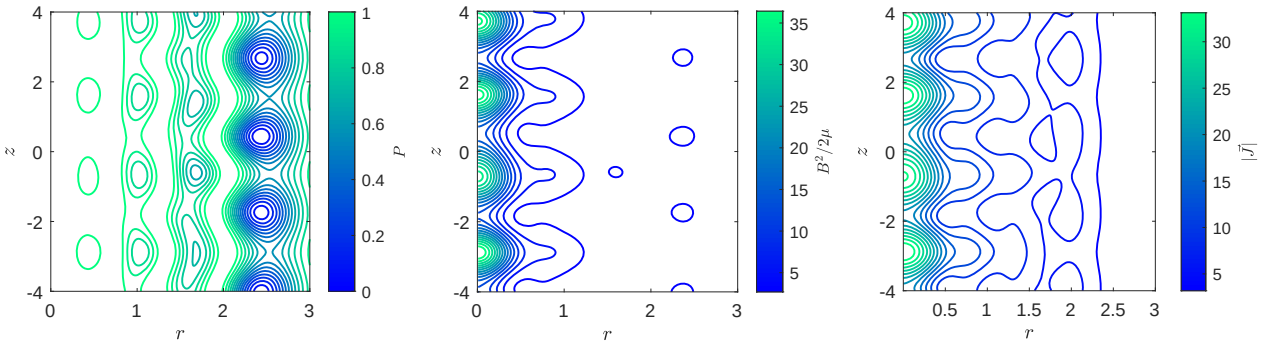

Figure 2.3: In Figure 2.3a, a cross-section of magnetic surfaces $P = \text{const}$ for an axially symmetric plasma equilibrium solution belonging to Family 1 for the case when $\delta \in \mathbb{N}$ with $\Psi(r, z)$ given by (2.23). Here $N = 4$, $a_n = 0.0002, .02, .05, .04$, $b_n = 0.0002, .01, .015, .05$, $\mu = 1$, $q = 2$, $\alpha = 4\sqrt{2}$. The color-bar shows the values of the dimensionless pressure $P = P_0 - q^2\psi^2/2\mu$ in Figure 2.3a. The corresponding magnetic energy density, $|\mathbf{B}|^2/2\mu$, can be seen in 2.3b along with the magnitude of the current density in Figure 2.3c.

with the general solution $y(s) = C_1\,\mathcal{C}_F(L, \sigma, s) + C_2\,\mathcal{C}_G(L, \sigma, s)$. By comparing (2.27) with (2.28) and substituting back $x = qr^2/2$, one arrives at

$$R(r) = C_1\,\mathcal{C}_F\left(0, -\delta, \frac{q}{2}r^2\right) + C_2\,\mathcal{C}_G\left(0, -\delta, \frac{q}{2}r^2\right). \tag{2.29}$$

The second family of solutions to equation (2.12) corresponding to plasma confined in a vacuum is:

$$\psi_k(r, z) = \left(C_1\,\mathcal{C}_F\left(0, -\delta, \frac{q}{2}r^2\right) + C_2\,\mathcal{C}_G\left(0, -\delta, \frac{q}{2}r^2\right)\right)(C_3 \sin kz + C_4 \cos kz), \tag{2.30}$$

where δ is the same as the first family, given by equation (2.19). Again, any linear combination of the above separated solution is also a solution which can be written as

$$\Psi(r, z) = \int_{-\infty}^{\infty} \psi_k(r, z)\, dk, \tag{2.31}$$

assuming $C_i = C_i(k)$, $i = 1, 2, 3, 4$. It should be noted that (2.30) can never satisfy all of the physical constraints, as both $\mathcal{C}_F$ and $\mathcal{C}_G$ oscillate and contain infinite zeros at infinity, therefore finite magnetic energy cannot be realized [11]. As resources for computing Coulomb wave functions are quite hard to find, a computation guide for these functions is found in appendix B. For the separated solution (2.30), after choosing some $P_0 = \text{const}$ to be the boundary of the plasma domain *truncated* solutions can indeed be considered as physical.

Examples of the second family of axial solutions

Utilizing equation (2.30), the contours of the pressure profile which give the magnetic surfaces can be seen in Figure 2.5.

However, this solution, as mentioned before, has infinitely many zeroes and grows unbounded as $r \to \infty$, thus by (2.8) it will not have finite magnetic energy. A corresponding truncated solution can be seen in Figure 2.6.

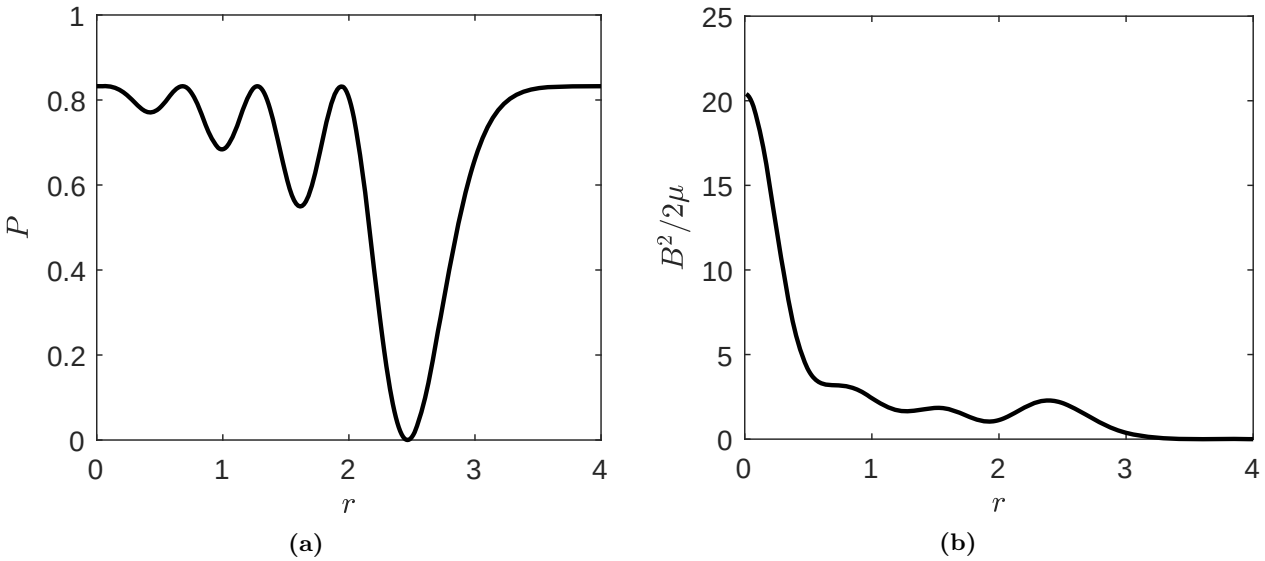

(a) **(b)**

Figure 2.4: A pressure plot of the solution from Figure 2.1 for $z = 0$ can be seen in 2.4a. The magnetic energy densities can be seen in Figure 2.2b. Here we can see that the majority of the magnetic energy is focused around the center of the plasma.

One should note the positive pressure profile inside of the chosen domain. The magnetic energy density inside of the domain is seen in Figure 2.7b. A 3D magnetic surface generated by rotating Figure 2.6a about the z axis can then be seen in Figure 2.8.

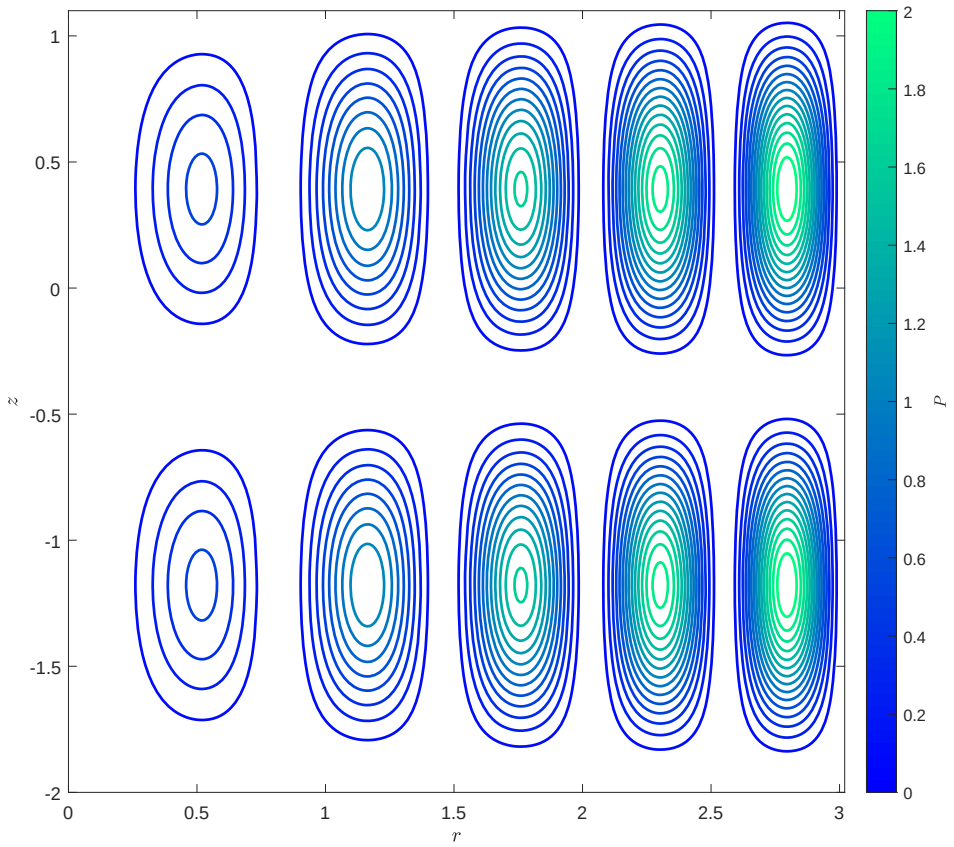

Figure 2.5: A cross-section of magnetic surfaces $\psi, P = \text{const}$ for a sample axially symmetric plasma equilibrium solution belonging to a Family 2, equation (2.30), with $C_1 = 1$, $C_2 = 0$, $C_3 = 1$, $C_4 = 1$, $k = 2$, $\alpha = 5$, and $q = \sqrt{3}$. The picture is periodic in r. The colorbar shows the values of the dimensionless pressure $P = P_0 + q^2 \frac{\psi^2}{2}$

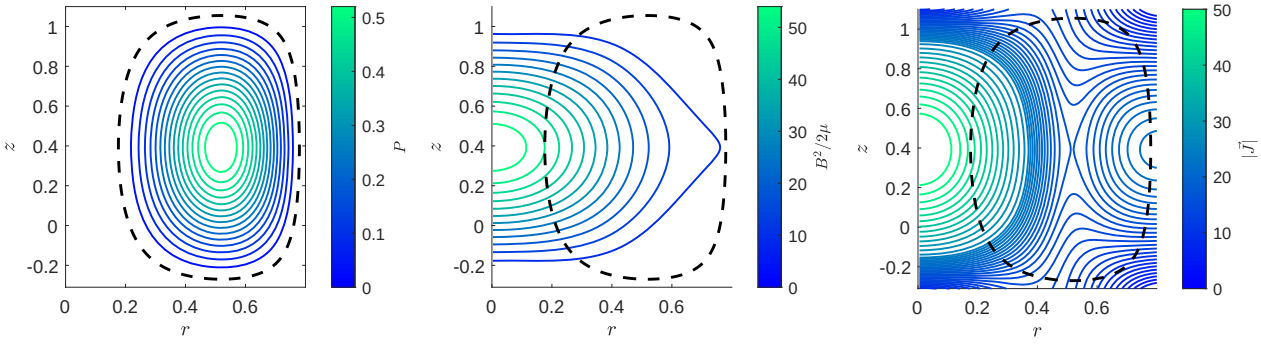

(a) **(b)** **(c)**

Figure 2.6: A cross-section of magnetic surfaces $\psi, P = \text{const}$ for a sample axially symmetric plasma equilibrium solution belonging to a Family 2, equation (2.30), with $C_1 = 1$, $C_2 = 0$, $C_3 = 1$, $C_4 = 1$, $k = 2$, $\alpha = 5$, and $q = \sqrt{3}$. The picture is periodic in r. The colorbar shows the values of the dimensionless pressure $P = P_0 + q^2 \frac{\psi^2}{2}$. The truncated boundary is shown boldface which coincides with the current sheet marking the boundary of the plasma.Lines of constant

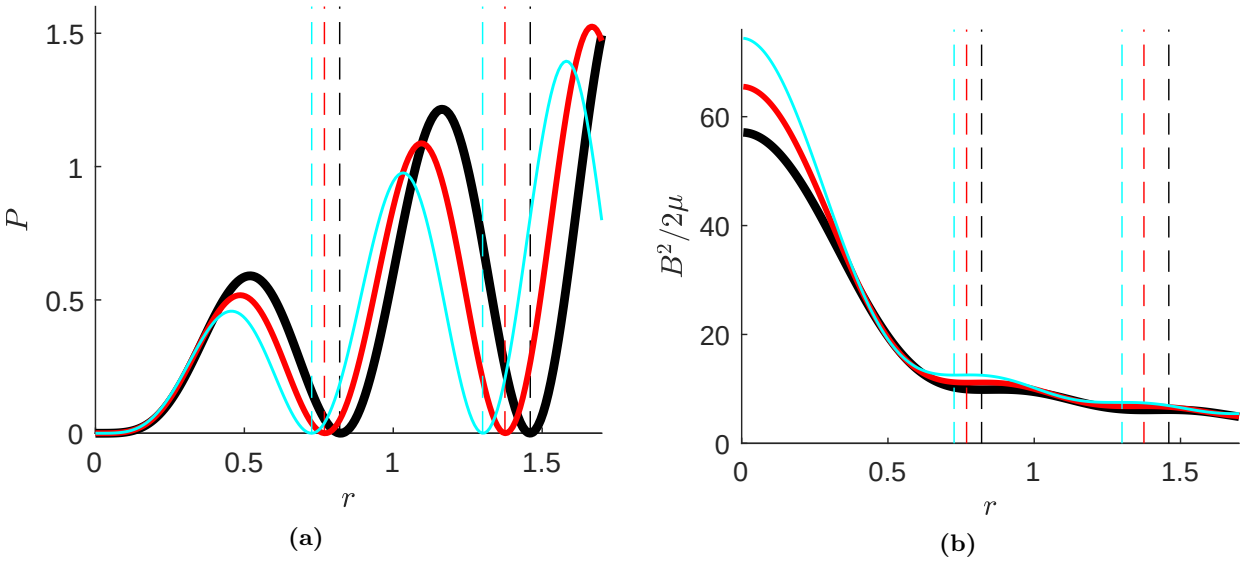

Figure 2.7: A pressure plot of the solution from Figure 2.6 for $z = 0.4$ and $\alpha_i = 4.7 + 0.3i, i = 1, 2, 3$ corresponding to the black, red and cyan plots can be seen in Figure 2.7a. The different magnetic energy densities for $z = 0.4$ can be seen in Figure 2.7b. The vertical dashed lines for each colour correspond to truncation surfaces that give physical solutions.

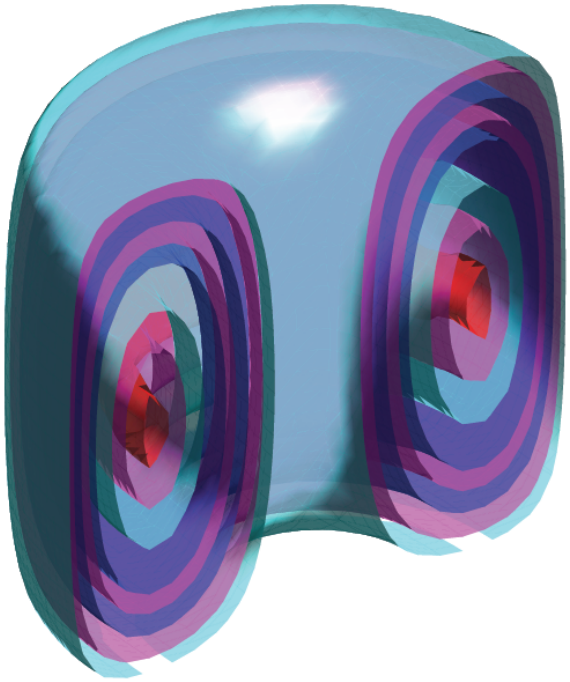

Figure 2.8: Axially symmetric magnetic surfaces $P = \text{const}$ for Family 2, equation (2.30), with $C_1 = 1$, $C_2 = 0$, $C_3 = 1$, $C_4 = 1$, $k = 2$, $\alpha = 5$, and $q = \sqrt{3}$ shown in 3D by rotating Figure 2.6a about the z axis.

2.4 Helically symmetric plasma equilibria and exact solutions

Now starting with the JFKO equation

$$\frac{\Psi_{\xi\xi}}{r^2}+\frac{1}{r}\frac{\partial}{\partial r}\left(\frac{r}{r^2+\gamma^2}\Psi_r\right)+\frac{I(\Psi)I'(\Psi)}{r^2+\gamma^2}+\frac{2\gamma I(\Psi)}{(r^2+\gamma^2)^2}=-\mu P'(\Psi), \tag{2.32}$$

for certain choices of the arbitrary functions P and I, (2.32) becomes a linear homogeneous PDE in which a separated solution can be looked for. Again, choosing the pressure P to be quadratic and the arbitrary function I to be linear:

$$P(\psi)=P_0+\frac{1}{2\mu}\sigma\psi^2,\quad I(\psi)=\alpha\psi, \tag{2.33}$$

the JFKO equation becomes a linear homogeneous second order PDE

$$\frac{1}{r^2}\frac{\partial^2\psi}{\partial\xi^2}+\frac{1}{r}\frac{\partial}{\partial r}\Big(\frac{r}{r^2+\gamma^2}\frac{\partial\psi}{\partial r}\Big)+\frac{\alpha^2\psi}{r^2+\gamma^2}+\frac{2\gamma\alpha\psi}{(r^2+\gamma^2)^2}+\sigma\psi=0, \tag{2.34}$$

which admits separated solutions $\psi(r,u)=R(r)\Xi(\xi)$, satisfying

$$\Xi''=\lambda\Xi, \tag{2.35a}$$

$$r\Big(\frac{r}{r^2+\gamma^2}R'\Big)'+\Big(\frac{\alpha^2r^2}{r^2+\gamma^2}+\frac{2\gamma\alpha r^2}{(r^2+\gamma^2)^2}+\sigma r^2\Big)R=-\lambda R. \tag{2.35b}$$

Here the separation constant, λ is taken to be negative $\lambda=-\omega^2$ which, as with the axial case, corresponds to a model of a plasma jet stretched along the z axis. Therefore, Ξ will have solutions in terms of sine and cosine. Depending on the value of σ in the pressure term of (2.33), one again obtains two different families of solutions. The two families of solutions correspond to two different types of pressure profiles. For $\sigma<0$, $P\leq P_1=\text{const}>0$ with $P\to P_1$ when $|\mathbf{x}|\to\infty$. For the case when $\sigma>0$, $P>0$ inside of the plasma domain $\mathcal{V}$ and $P=0$ outside of $\mathcal{V}$ similar to the axial cases discussed previously.

2.4.1 The first family of helically symmetric solutions

The first family of solutions arises when $\sigma=-\kappa^2<0$. This corresponds to a pressure profile which is bounded above by some P_1 where $P\to P_1$ when $|\mathbf{x}|\to\infty$. This model is more appropriate for plasmas residing in atmosphere. Upon the substitution of this pressure form and $\lambda=-\omega^2$ the following two equations arise

$$r\Big(\frac{r}{r^2+\gamma^2}R'\Big)'+\Big(\frac{\alpha^2r^2}{r^2+\gamma^2}+\frac{2\gamma\alpha r^2}{(r^2+\gamma^2)^2}-\kappa^2r^2\Big)R=\omega^2R, \tag{2.36}$$

$$\Xi''=-\omega^2\Xi.$$

Where the second equation has the general solution

$$\Xi(\xi)=C_1\sin(\omega\xi)+C_2\cos(\omega\xi). \tag{2.37}$$

The solution to equation (2.36) can be written in terms of the confluent Heun function [41] as:

$$R(r)=e^{-\kappa r^2/2}\Big(C_1r^b\mathcal{H}_C(a,b,-2,c,d,-r^2/\gamma^2)+C_2r^{-b}\mathcal{H}_C(a,-b,-2,c,d,-r^2/\gamma^2)\Big). \tag{2.38}$$

Here

$$a = \kappa\gamma^2, \tag{2.39a}$$

$$b = \gamma\omega, \tag{2.39b}$$

$$c = \frac{\gamma^2(\gamma^2\kappa^2 - \alpha^2 + \omega^2)}{4}, \tag{2.39c}$$

$$d = 1 - \frac{\kappa^2\gamma^4}{4} + \frac{\alpha^2 - \omega^2}{4}\gamma^2 + \frac{\alpha\gamma}{2}, \tag{2.39d}$$

where the confluent Heun function $\mathcal{H}_C(a, b, -2, c, d, x)$ satisfies the following confluent Heun ODE:

$$y'' - \frac{(-x^2a + (-b + a)x + b + 1)}{x(x-1)}y' - \frac{((-ba - 2c)x + (b+1)a + b - 2d + 2)}{2x(x-1)}y = 0. \tag{2.40}$$

Therefore, a separated solution for this first family can then be written as

$$\begin{aligned}\psi_\omega(r,\xi) = e^{-\kappa r^2/2}\left(C_1 r^b \mathcal{H}_C(a, b, -2, c, d, -r^2/\gamma^2) + C_2 r^{-b}\mathcal{H}_C(a, -b, -2, c, d, -r^2/\gamma^2)\right)\times \\ \times(C_3\sin(\omega\xi) + C_4\cos(\omega\xi)).\end{aligned} \tag{2.41}$$

Some important remarks about (2.41) and the confluent Heun function should be made here:

1. For the examples shown, C_2 will be set to zero, as a negative second parameter in the confluent Heun function appears to not be computable by the utilized method.

2. There exists necessary and sufficient conditions for the confluent Heun function to produce polynomials which are discussed thoroughly in [42]. These solutions correspond with helical solutions discussed in [12]. A necessary condition for the emergence of these polynomials is $c = -a(n + (b/2))$ where n is some positive integer which specifies the degree of this polynomial. The needed sufficient condition for the polynomials of this function come from choosing a finite number of characteristic values for d. These characteristic values are chosen such to be the roots of the coefficient of the $(n+1)$ degree of the series expansion. Further details on the conditions for these polynomials can be found in [41].

with the first remark, a more useful separated solution can be written as

$$\psi_\omega(r,\xi) = e^{-\kappa r^2/2} r^b \mathcal{H}_C(a, b, -2, c, d, -r^2/\gamma^2)(C_1\sin(\omega\xi) + C_2\cos(\omega\xi)). \tag{2.42}$$

As the above solution satisfies the linear equation (2.34) a general linear combination for different values of ω can be considered giving

$$\Psi(r,\xi) = \int_{-\infty}^{\infty} \psi_\omega(r,\xi)\, d\omega, \tag{2.43}$$

assuming $C_i = C_i(\omega)$, $i = 1, 2$ are arbitrary distributions.

2.4.2 Examples of the first family of new helical solutions

Two examples of the first family of solutions will be shown. The first is a look at a single separated solution given by (2.42). Here the parameters in (2.42) are chosen such to not produce polynomials from the confluent Heun part of the solution. Here the first part of the solution is shown before it starts to grow unboundedly similar to the Whittaker functions when $\delta \neq \mathbb{N}$. The magnetic surface cross-sections for this solution can be seen in Figure 2.9.

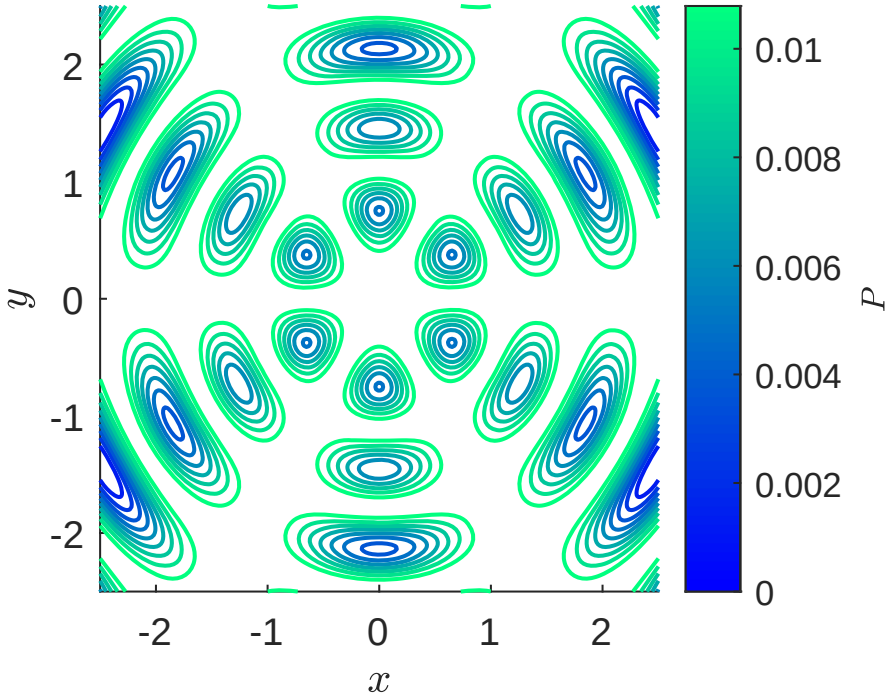

Figure 2.9: Helically symmetric magnetic surfaces $P = \text{const}$ for Family 1 where $c \neq -a(n + (b/2))$. Here $\psi(r, \xi)$ is given by (2.42) with $\alpha = 5.9$, $\kappa = 1$, $\gamma = 1$, $\omega = 3$, $C_1 = 1$ and $C_2 = 0$.

While globally the above solution is non-physical, it can be truncated to give solutions which satisfy the physical constraints. The physical solution with the pressure profile, magnetic energy density and the magnitude of the current density can be seen in Figure 2.10. As expected with the magnetic energy density, the higher concentration is seen in the center of each of the inner 6 sections.

An interesting linear combination of a non-physical solution can be seen in Figure 2.11.

The second example from this family of solutions is for the case when the confluent Heun function does produce polynomials. This is a special case when $\Psi(r, \xi)$ from (2.43) can be written as

$$\Psi_{Nmn}(r, \xi) = e^{-\kappa r^2/2} \left(a_N B_{0N}(\kappa r^2) + r^m B_{mn}(\kappa r^2)(a_{mn} \cos(m\xi/\gamma) + b_{mn} \sin(m\xi/\gamma)) \right). \tag{2.44}$$

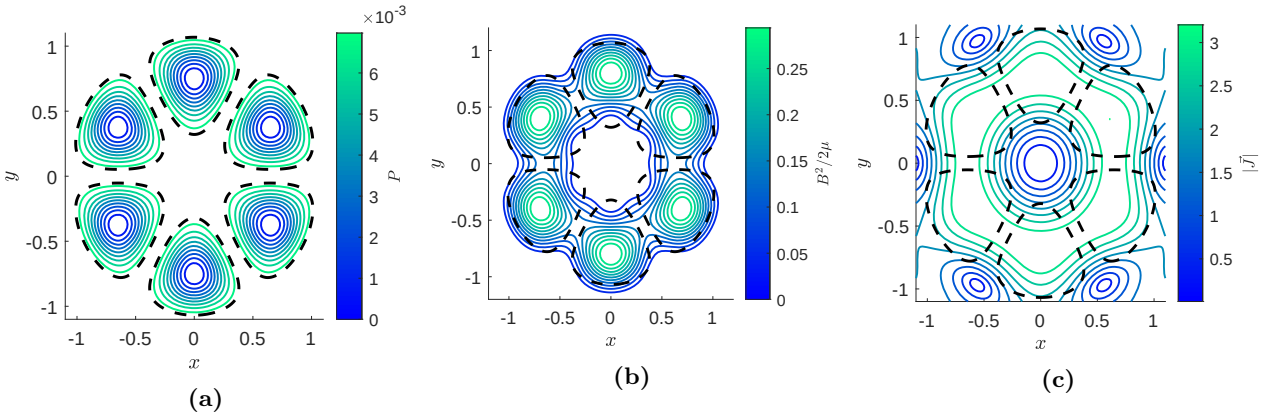

Figure 2.10: A truncated helically symmetric physical solution based off of the solution given in Figure 2.9. The pressure contour, magnetic energy density and current density magnitude can be seen from left to right.

Here B_{mn} are related to the Laguerre polynomials according to

$$B_{mn}(x) = \frac{d^m}{dx^m} L_{m+n} - k_{mn} x \frac{d^{m+1}}{dx^{m+1}} L_{m+n}(x), \tag{2.45}$$

where $k_{mn} = (m + \kappa\gamma^2 - \alpha\gamma)/(2n\kappa\gamma^2)$ and $L_(x)$ are the pth order Laguerre polynomials. In equation (2.44) N,m,n are arbitrary non-negative integers which all satisfy the inequality $2N > 2n + m$. This solution is derived in [12], where in the original paper the solution is written in terms of β where $\kappa = 2\beta$. The pressure profile and the magnetic energy density can be seen in 2.12.

With a lifting and rotating motion along and about the z axis, the three dimensional magnetic surfaces for which both the magnetic field $\mathbf{B}$ and the current density $\mathbf{J} \sim \operatorname{curl} \mathbf{B}$ are tangent can be seen in Figure 2.13.

2.4.3 The second family of new helically symmetric solutions

The second family arises when $\sigma = \kappa^2 > 0$ in equation (2.34). This corresponds to a positive pressure profile, $P > 0$, inside of $\mathcal{V}$ and $P = 0$ outside. This pressure profile is suitable for plasma in vacuum. After substituting this form of pressure into equation (2.24), the following ODE similar to (2.36) arises

$$r\Big(\frac{r}{r^2+\gamma^2}R'\Big)' + \Big(\frac{\alpha^2 r^2}{r^2+\gamma^2} + \frac{2\gamma\alpha r^2}{(r^2+\gamma^2)^2} - \kappa^2 r^2\Big)R = \omega^2 R. \tag{2.46}$$

The solution to (2.46) can again be written in terms of the confluent Heun function, $\mathcal{H}_C$, this time multiplied by a complex exponential and having complex parameters in the confluent Heun function.

$$R(r) = C_1 r^b e^{(-\frac{i}{2}\kappa r^2)} H_C\left(ia, b, -2, c, d, \frac{-r^2}{\gamma^2}\right) + C_2 r^b e^{(-\frac{i}{2}\kappa r^2)} H_C\left(ia, -b, -2, c, d, \frac{-r^2}{\gamma^2}\right), \tag{2.47}$$

where a, b, c, and d are given by (2.39). Following the 2nd remark about the confluent Heun function, the second solution is discarded by setting $C_2 = 0$ in (2.47). It should be noted, as it is not obvious, that the first solution of equation (2.47) is a real valued function for real a, b, c, d and r. Therefore, a separated solution

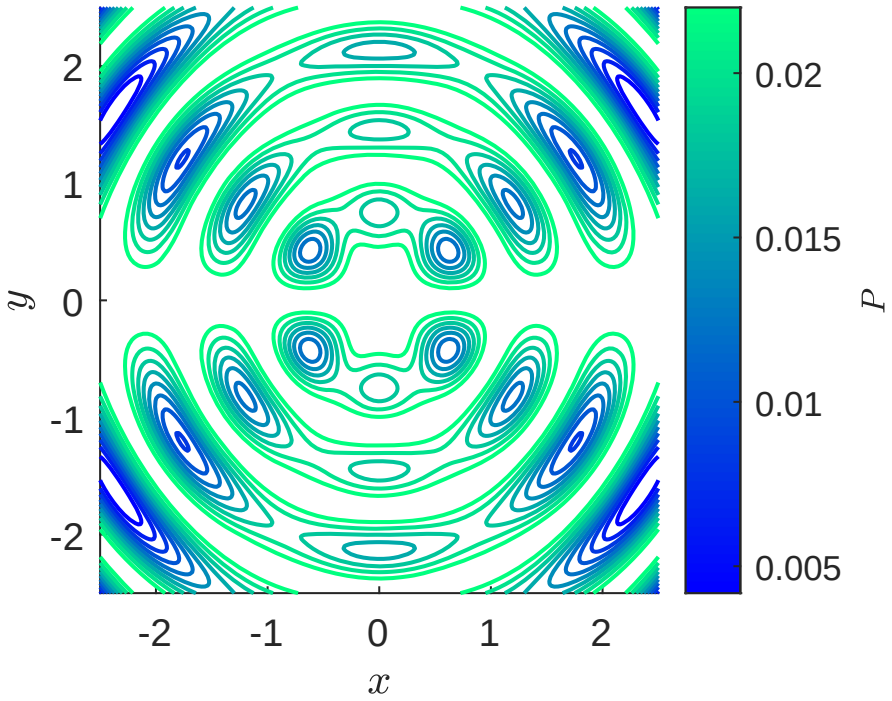

Figure 2.11: Pressure profile for a linear combination of ψ for Family 1 where $c \neq -a(n + (b/2))$. Here $\Psi(r, \xi) = \psi_1(r, \xi) + \psi_2(r, \xi)$ where $\psi_1(r, \xi)$ is given in Figure 2.9 and $\psi_2(r, \xi))$ is given by (2.42) with $\alpha = 5.9$, $\kappa = 1$, $\gamma = 1$, $\omega = 2$, $C_1 = 1$ and $C_2 = 0$. Here the solution is non-physical as it grows unbounded unless one restricts the plasma domain to within one helical cylinder or so.

to (2.34) corresponding to helically symmetric plasma in vacuum is

$$\psi_\omega(r, \xi) = e^{-i\kappa r^2/2} r^b \mathcal{H}_C \left(ia, b, -2, c, d, \frac{-r^2}{\gamma^2} \right) (C_1 \sin(\omega\xi) + C_2 \cos(\omega\xi)) \,. \tag{2.48}$$

Now a general solution can be written as discrete or, more generally, continuous linear combinations of the separated solutions (2.48):

$$\Psi(r, \xi) = \int_{-\infty}^{\infty} \psi_\omega(r, \xi) \, d\omega, \tag{2.49}$$

where $C_1 = C_1(\omega)$, $C_2 = C_2(\omega)$ are arbitrary weighting distributions. The radial part, $R(r)$, in the separated solution (2.48) for most choices of κ, α and ω behaves periodically, similarity to the Coulomb wave functions from before. Due to this, (2.48) must be truncated at some chosen magnetic surface $P = P_0$ outside of which P and $\mathbf{B}$ are set to zero.

2.4.4 An example of second family of helical solutions

Using equation (2.48) and choosing the following values for ω, C_1, C_2, κ, γ and α the following oscillating contours of the pressure $P(\psi) = \kappa^2\psi^2/2$ can be seen in Figure 2.14.

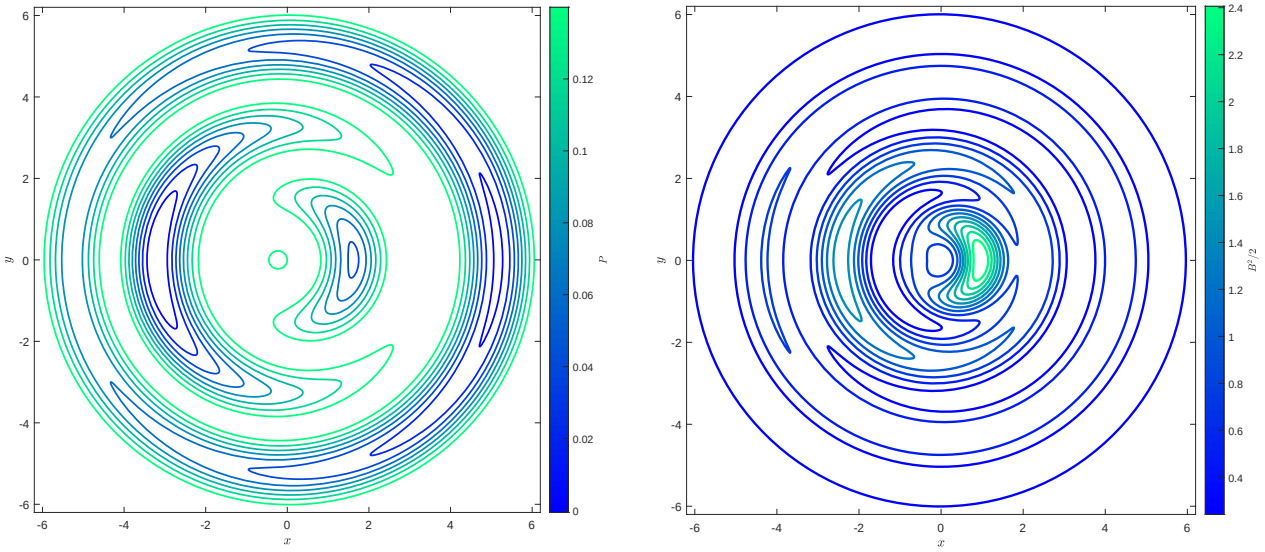

(a) **(b)**

Figure 2.12: Helically symmetric magnetic surfaces $P = \text{const}$ can be seen in 2.12a. This is a special case of Family 1 where the confluent Heun functions produce polynomials. $\Psi(r, \xi)$ is given by 2.44 with $N = 4$, $n = 0$, $m = 1$, $\kappa = 0.2$, $\gamma = 1$ $a_N = a_n = 1$ and $b_n = 0$. The corresponding magnetic energy density can be seen in 2.12b.

It appears that for the type of pressure configuration suitable for a plasma residing in vacuum the solutions for both axial and helical symmetry have oscillatory nature in the radial variable.

After truncating this solution at some chosen boundary $P(\psi) = 0$, the pressure contour can be seen in Figure 2.15a with the corresponding magnetic energy density seen in Figure 2.15b. For this example, two of the magnetic surfaces are shown in 3D with magnetic field lines shown twisting up the helical surfaces. This is shown in Figure 2.16.

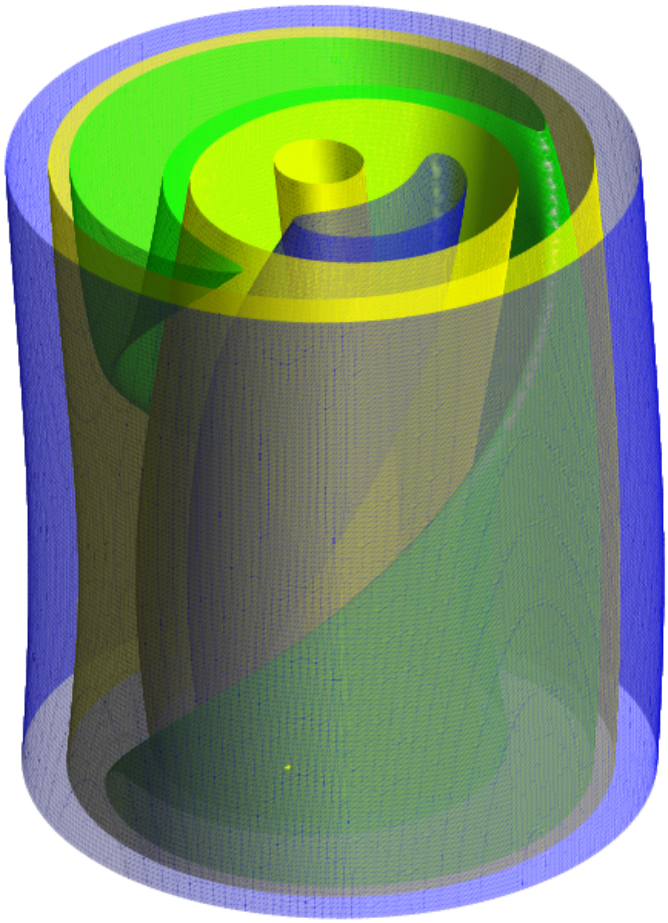

Figure 2.13: Helically symmetric magnetic surfaces $P = \text{const}$. This is a special case of Family 1 where the confluent Heun functions produce polynomials. $\Psi(r, \xi)$ is given by (2.44) with $N = 4$, $n = 0$, $m = 1$, $\kappa = 0.2$, $\gamma = 1$ $a_N = a_n = 1$ and $b_n = 0$. These surfaces are shown in 3D by a helical transformation of Figure 2.12a.

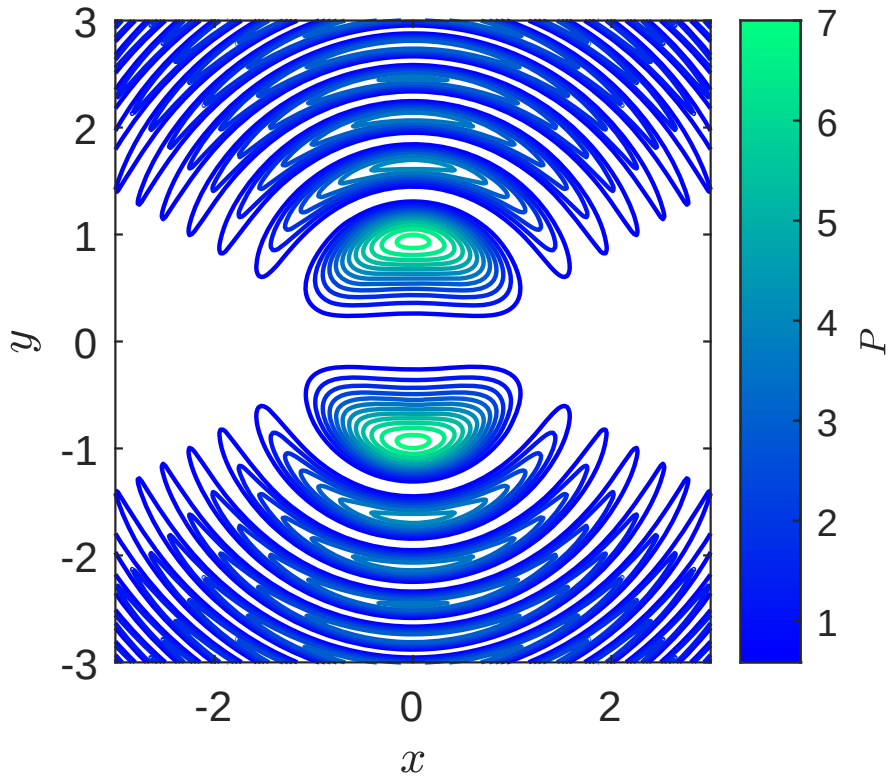

Figure 2.14: A cross-section of magnetic surfaces $P = \text{const}$ for a non-physical oscillating helically symmetric plasma equilibrium solution belonging to Family 2 given by (2.48), with $C_1 = 1$, $C_2 = 0$, $\alpha = 3$, $\kappa = 4$, $\gamma = 1$ and $\omega = 1$. The colour-bar shows the values of the dimensionless pressure $P = \kappa^2\psi^2/2$.

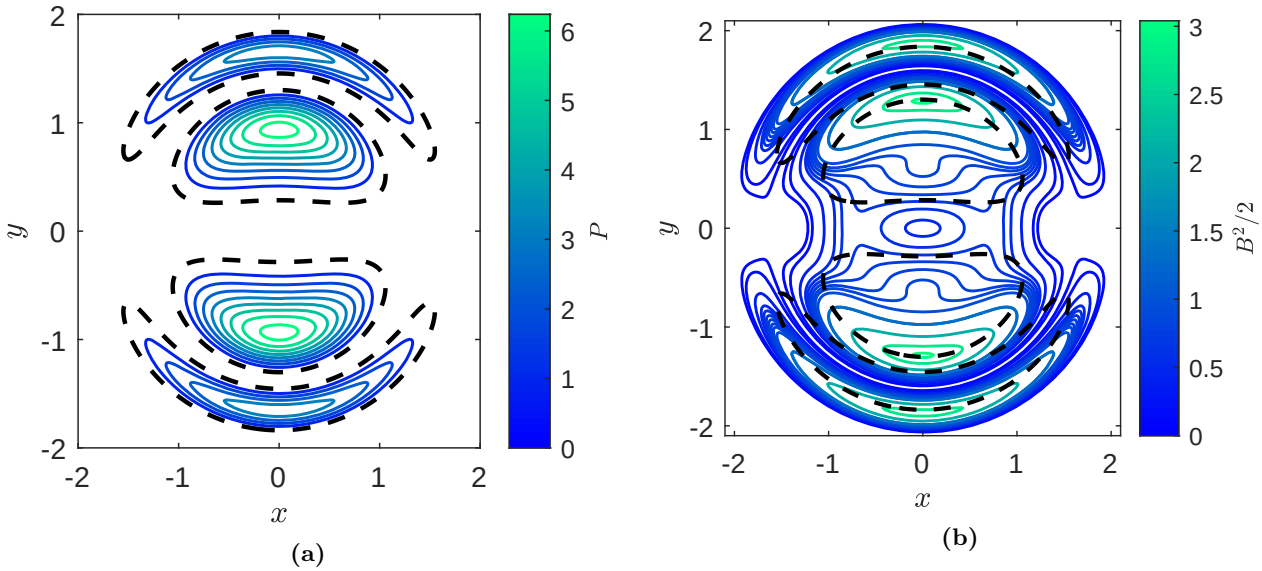

Figure 2.15: Truncated helically symmetric magnetic surfaces $P = \text{const}$ can be seen in 2.15a. This belongs to family 2 where $\Psi(r, \xi)$ is given by (2.48) with$C_1 = 1$, $C_2 = 0$, $\alpha = 3$, $\kappa = 4$, $\gamma = 1$ and $\omega = 1$. The corresponding magnetic energy density can be seen in 2.15b.

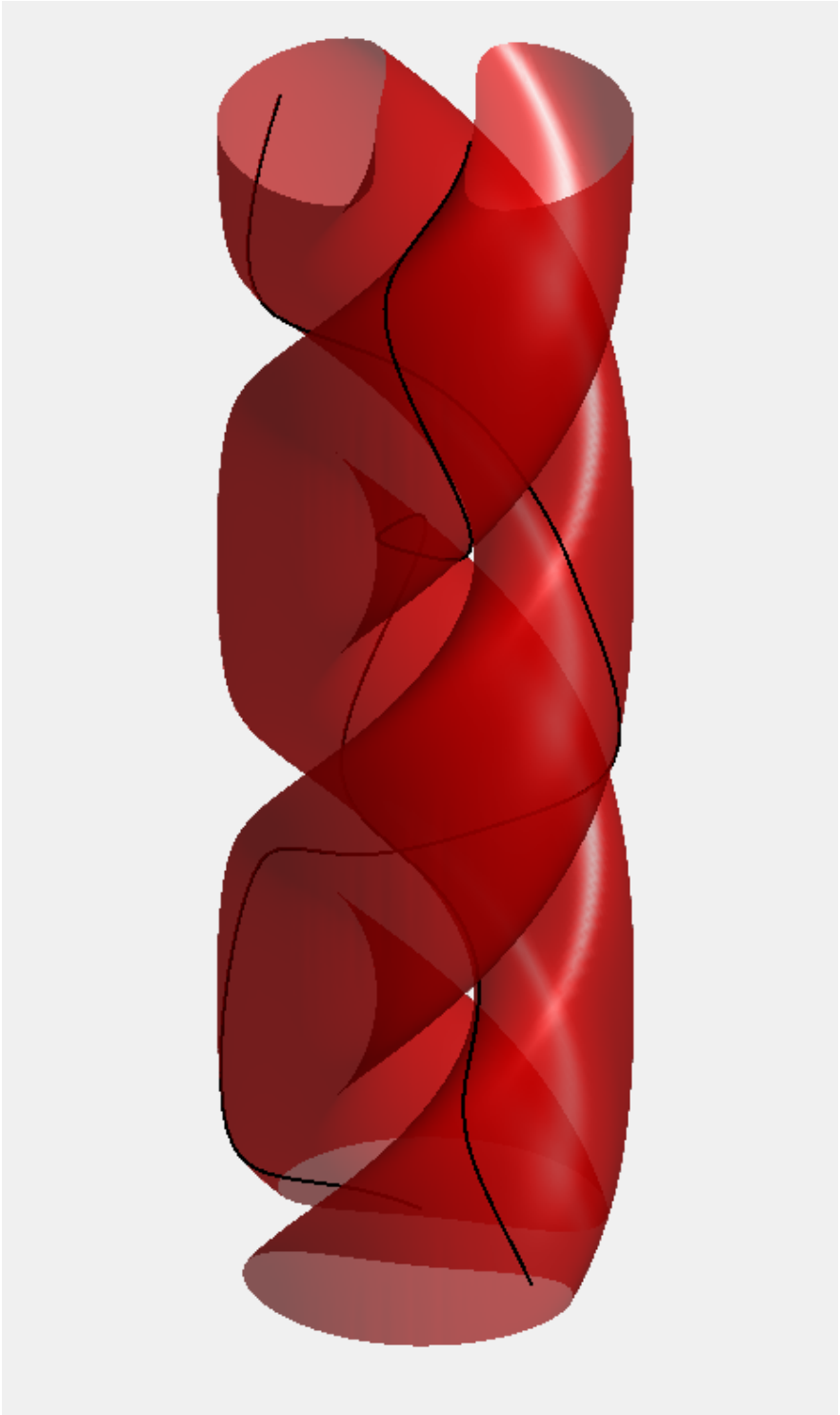

Figure 2.16: Three-dimensional magnetic surfaces $P = \text{const}$ for a sample helically symmetric plasma equilibrium solution belonging to family 2 using (2.48) with $C_1 = 1$, $C_2 = 0$, $\alpha = 3$, $\kappa = 4$, $\gamma = 1$ and $\omega = 1$. Created by a rising and rotating motion of Figure 2.15a. Here the black lines represent the magnetic field lines tangent to this surface.

2.5 Transformation of static equilibrium solutions into dynamic solutions with non-zero velocity

Starting with the transformations discussed in chapter 1 that depend on two arbitrary functions

$$\mathbf{B}_1 = \sqrt{C + F_2^2(\psi)}\mathbf{B}, \quad \mathbf{V}_1 = \frac{F_2(\psi)}{F_1(\psi)\sqrt{\mu}}\mathbf{B}, \tag{2.50a}$$

$$P_1 = CP - \frac{F_2^2(\psi)\mathbf{B}^2}{2\mu}, \tag{2.50b}$$

$$\rho_1 = F_2^2(\psi), \tag{2.50c}$$

the 2nd family of solutions for both axially and helically symmetry found in the previous section will be transformed into new solutions with $\mathbf{V_1} \neq 0$.

2.5.1 Transformation of the second axially-symmetric family of solutions: an example

Starting with the above example for the second family of axially symmetric solutions shown in Figure 2.6, having the magnetic field components and pressure given as

$$\mathbf{B}_{st} = \frac{\psi_r}{r}\mathbf{e}_r + \alpha\frac{\psi}{r}\mathbf{e}_\varphi - \frac{\psi_z}{r}\mathbf{e}_z, \tag{2.51a}$$

$$P = P_0 + \frac{q^2}{2}\psi^2, \tag{2.51b}$$

where ψ is given by (2.30) and using the two arbitrary functions of ψ to be

$$F_1(\psi) = 0.7P^4, \quad F_2(\psi) = P^2, \tag{2.52}$$

and $C = 1$, this transforms the solution into

$$\mathbf{B_1} = \sqrt{1 + P^4}\mathbf{B}_{st}, \quad \mathbf{V_1} = \frac{\mathbf{B}_{st}}{0.7P^2},$$

$$P_1 = P - \frac{P^2\mathbf{B}_{st}^2}{2}, \quad \rho_1 = P^4. \tag{2.53a}$$

The new pressure profile and magnetic energy density can be seen in Figure 2.17a and Figure 2.17b respectively. With the non-zero velocity, a graph of the non-zero kinetic energy density, $\rho_1 V_1^2/2$, can now be seen and is shown in Figure 2.17c.

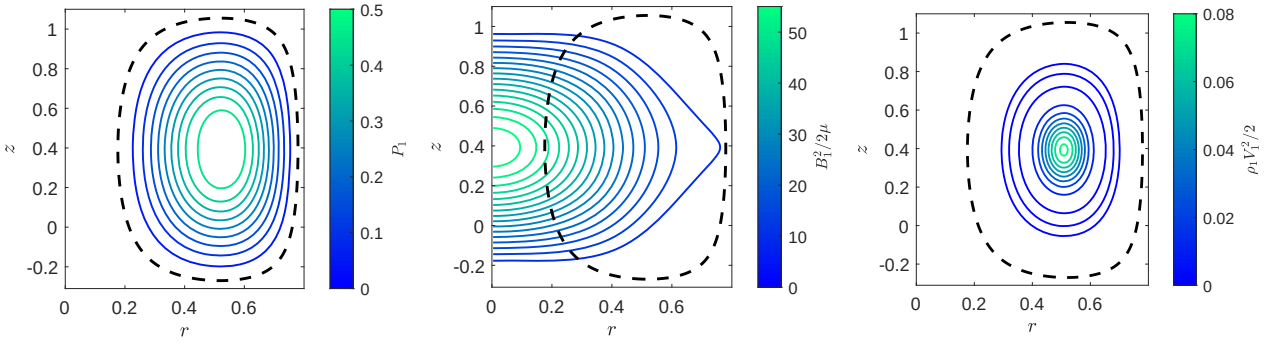

(a) **(b)** **(c)**

Figure 2.17: The new solution transformed from the solution shown in Figure 2.6 with the new solutions given by (2.53) based off of the static equilibrium magnetic field $\mathbf{B}_{st}$ and the static equilibrium pressure P. From left to right, the new pressure profile, P_1, magnetic energy density, $B_1^2/2\mu$ and non-zero kinetic energy density $\rho V_1^2/2$ can be seen.

2.5.2 Transformations of the second helically-symmetric family of solutions: an example

Taking the second family of helically symmetric solutions shown in Figure 2.18, having the magnetic field components and pressure given as

$$\mathbf{B}_{st} = \frac{\psi_\xi}{r}\mathbf{e}_r + \frac{\alpha r\psi + r\psi_r}{r^2+\gamma^2}\mathbf{e}_\varphi + \frac{\gamma\alpha\psi - r\psi_r}{r^2+\gamma^2}\mathbf{e}_z, \tag{2.54a}$$

$$P = P_0 + \frac{\kappa^2}{2}\psi^2, \tag{2.54b}$$

where ψ is given by (2.48) and using the two arbitrary functions of ψ to be

$$F_1(\psi) = 0.035P^2, \quad F_2(\psi) = e^{\frac{\psi^4}{2}}\cos\psi^2. \tag{2.55}$$

and $C = 1$, this transforms the solution into

$$\mathbf{B_1} = \sqrt{1 + e^{\psi^4}\cos^2\psi^2}\,\mathbf{B}_{st}, \quad \mathbf{V_1} = \frac{e^{\frac{\psi^4}{2}}\cos\psi^2}{0.035P^2}\mathbf{B}_{st}, \tag{2.56a}$$

$$P_1 = P - \frac{e^{\psi^4}\cos^2\psi^2}{2}\mathbf{B}_{st}^2, \quad \rho_1 = e^{\psi^4}\cos^2\psi^2. \tag{2.56b}$$

The new pressure profile and magnetic energy density can be seen in Figure 2.18a and Figure 2.18b respectively. With the non-zero velocity, a graph of the non-zero kinetic energy density, $\rho_1 V_1^2/2$, can now be seen and is shown in Figure 2.18c.

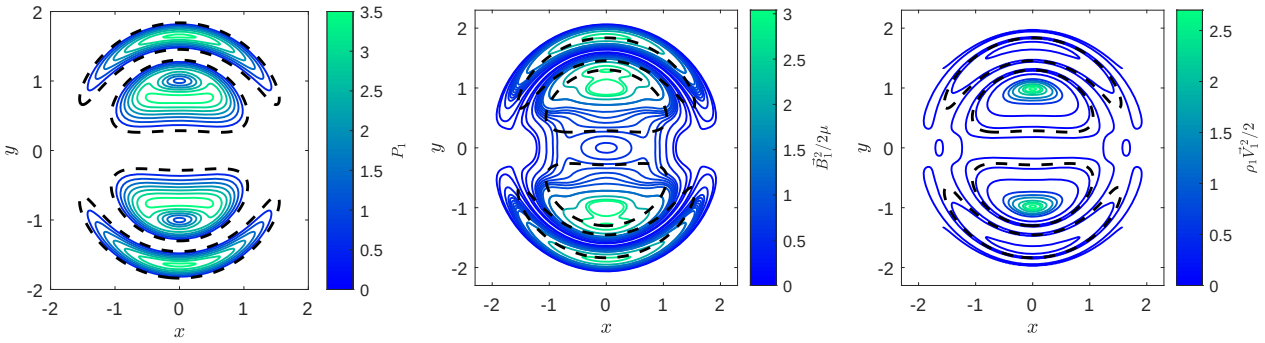

Figure 2.18: The new solution transformed from the solution shown in Figure 2.15 with the new solutions given by (2.56) based off of the static equilibrium magnetic field $\mathbf{B}_{st}$ and the static equilibrium pressure P. From left to right, the new pressure profile, P_1, magnetic energy density, $|\mathbf{B}_1|^2/2\mu$ and non-zero kinetic energy density $\rho|\mathbf{V}_1|^2/2$ can be seen.

3 Spherical vortices in fluid mechanics and MHD

3.1 Introduction

In 1894 Micaiah John Muller Hill published an article describing a sphere moving symmetrically with regards to an axis through a stationary fluid. Using cylinderical coordinates and assuming that the azimuthal velocity component is zero, Hill was able to find a simple solution that describes this fluid flow. This solution and the method that it was computed is available in [30]. A similar modern problem in the MHD framework was put forth in 1987 by A. A. Bobnev in which they considered a spherical vortex moving in an ideally conducting fluid [9]. In this work, several small mistakes were made. Interestingly enough, in 1995 R. Kaiser and D. Lortz again considered the problem of a spherical vortex in MHD equilibrium to model ball lighting [33] essentially re-deriving the solution A. Bobnev found in [9]. In the following chapter, a modern and much simpler derivation of Hill's spherical vortex using the Bragg-Hawthorne equation, (which was first derived in 1898 by William Mitchinson Hicks and only gained popularity after being re-derived in 1950 by William Hawthorne and Stephen Bragg) will be shown to emphasize the usefulness of the Bragg-Hawthorne equation for such problems. By using the moving frame of reference the Euler equations reduce to equilibrium flow which as discussed previously are equivalent to static equilibrium MHD (1.31). Next, the spherical vortex in an ideally conducting fluid is computed similar to methods in both [9] and [33]. Using results from the previous two sections, a new generalized version of Hill's spherical vortex is put forth. After this, a physical solution to the static equilibrium MHD equations (1.31) is computed by looking at a separated solution to the Grad-Shafranov equation in spherical coordinates and lastly, the stability of Hill's spherical vortex is examined by performing an axisymmetric perturbation described in [40]. A similar analysis for the new generalized Hill's spherical vortex is also attempted.

3.2 Hill's spherical vortex: a modern derivation

A sphere of radius R moving through a stationary fluid directed along the z axis can be modelled with the incompressible Euler equations. Starting with the equations of motion for an incompressible fluid

$$\frac{\partial \mathbf{V}}{\partial t} + (\mathbf{V}\cdot\nabla)\mathbf{V} = -\frac{1}{\rho}\operatorname{grad} P, \tag{3.1a}$$

$$\operatorname{div}\mathbf{V} = 0, \tag{3.1b}$$

the well known result that the incompressible Euler equations are invariant under a general Galilean transformations motivates the following change of variables

$$\mathbf{V}(\mathbf{r},t) = \tilde{\mathbf{v}}(\mathbf{r} - Z(t)\mathbf{e}_z) + Z'(t)\mathbf{e}_z, \quad P(\mathbf{r},t) = \tilde{P}(\mathbf{r} - Z(t)\mathbf{e}_z). \tag{3.2}$$

Here $Z(t)$ is an arbitrary function of time and $\tilde{\mathbf{v}}$, $\tilde{P}$ denote fluid parameters measured in the corresponding moving frame of reference.

Assuming that the moving frame of reference is moving at the same speed as the spherical vortex, and the density is constant, after omitting the tilde on the new variables, the Euler equations can be written as

$$\operatorname{curl}\mathbf{v} \times \mathbf{v} = \operatorname{grad} H, \tag{3.3a}$$

$$\operatorname{div}\mathbf{v} = 0, \tag{3.3b}$$

where

$$H = -\left(\frac{P}{\rho} + \frac{1}{2}|\mathbf{v}|^2\right) \tag{3.4}$$

is a modified pressure term. In the rest of this section H will simply be refereed to as the pressure. As one can see, assuming that the motion is axially symmetric it is natural to use cylindrical coordinates and set $\mathbf{v}$ and H independent of ϕ. In doing so, one can reduce (3.3) to the well known Bragg-Hawthorne equation (see Chapter 1 section 6.2 for the derivation)

$$\frac{\partial^2\psi}{\partial r^2} + \frac{\partial^2\psi}{\partial z^2} - \frac{1}{r}\frac{\partial\psi}{\partial r} + F(\psi)F'(\psi) = r^2H'(\psi), \tag{3.5}$$

where

$$\mathbf{v} = \frac{\psi_z}{r}\mathbf{e}_r + \frac{F(\psi)}{r}\mathbf{e}_\phi + \frac{-\psi_r}{r}\mathbf{e}_z, \tag{3.6}$$

and F, H are arbitrary functions of ψ, where ψ is the stream function discussed in Section 6.2. Chapter 1. Following Hill's assumption who considered a two-component axially symmetric flow, the azimuthal component of the velocity is set to zero, giving the condition

$$F(\psi) = 0. \tag{3.7}$$

From this, the vorticity as discussed in chapter one and given by 1.45 becomes

$$\boldsymbol{\omega} = r^2H'(\psi)\mathbf{e}_\phi. \tag{3.8}$$

Note that when the pressure is constant: $H = H_0$, one has $\boldsymbol{\omega} = 0$, which corresponds to an irrotational flow (i.e. potential flow) which was also discussed in Section 6.2. Chapter 1. (3.7) also gives a simplified Bragg-Hawthorne equation

$$\frac{\partial^2\psi}{\partial r^2}+\frac{\partial^2\psi}{\partial z^2}-\frac{1}{r}\frac{\partial\psi}{\partial r}=-r^2H'(\psi), \tag{3.9}$$

with

$$\mathbf{v}=\frac{\psi_z}{r}\mathbf{e}_r+\frac{-\psi_r}{r}\mathbf{e}_z. \tag{3.10}$$

The arbitrary function is chosen as the highest power series expansion in ψ such that the (3.9) becomes separable in spherical coordinates and the asymptotics of the pressure $H(\psi)$ behaves properly. As far as separability of (3.9) goes, $H(\psi)$ cannot be of higher degree then linear in ψ. In regards to the asymptotics, the pressure far away from the sphere must not change and needs to be the ambient pressure H_0. This gives the best choice for $H(\psi)$ to be broken into two pieces that match at the boundary

$$H(\psi)=\begin{cases}H_0-10\delta\psi, & \rho<R\\ H_0. & \rho>R\end{cases} \tag{3.11}$$

Here the coefficient 10δ is only chosen in this way to make the calculation cleaner. The problem is now be decomposed into two pieces: the rotational flow inside of the sphere with pressure linear in ψ, and the irrotational flow outside of the sphere with constant pressure.

1. Rotational flow inside the sphere

$$H(\psi)=H_0-10\delta\psi \tag{3.12a}$$

$$\frac{\partial^2\psi}{\partial r^2}+\frac{\partial^2\psi}{\partial z^2}-\frac{1}{r}\frac{\partial\psi}{\partial r}=10\delta r^2. \tag{3.12b}$$

2. Irrotational flow outside the sphere

$$H(\tilde{\psi})=H_0 \tag{3.13a}$$

$$\frac{\partial^2\tilde{\psi}}{\partial r^2}+\frac{\partial^2\tilde{\psi}}{\partial z^2}-\frac{1}{r}\frac{\partial\tilde{\psi}}{\partial r}=0. \tag{3.13b}$$

Along with these two equations, there is the condition that both pieces must have matching pressure and velocity components at the boundary of the sphere ($r^2+z^2=R^2$). For matching pressure, this implies that for the inside solution, $\psi(r,z)=0$ when $r^2+z^2=R^2$. It turns out that one can effectively seek solutions to (3.12b) and (3.13b) in spherical coordinates, in the separated form $\psi(\rho,\theta)=R(\rho)\Theta(\theta)$. Here standard spherical coordinates are related to cylindrical coordinates by $r=\rho\sin\theta$, $z=\rho\cos\theta$. Converting the above problem into spherical coordinates gives

1. Rotational flow inside the sphere

$$H(\psi)=H_0-10\delta\psi \tag{3.14a}$$

$$\left[\frac{\partial^2}{\partial\rho^2}+\frac{\sin\theta}{\rho^2}\frac{\partial}{\partial\theta}\left(\frac{1}{\sin\theta}\frac{\partial}{\partial\theta}\right)\right]\psi=10\delta\rho^2\sin^2\theta. \tag{3.14b}$$

2. Irrotational flow outside the sphere

$$H(\tilde{\psi}) = H_0 \tag{3.15a}$$

$$\left[\frac{\partial^2}{\partial\rho^2} + \frac{\sin\theta}{\rho^2}\frac{\partial}{\partial\theta}\left(\frac{1}{\sin\theta}\frac{\partial}{\partial\theta}\right)\right]\psi = 0. \tag{3.15b}$$

The velocity components inside and outside are given by

$$\mathbf{v}_{in} = \frac{1}{\rho^2\sin\theta}\frac{\partial\psi}{\partial\theta}\mathbf{e}_\rho - \frac{1}{\rho\sin\theta}\frac{\partial\psi}{\partial\rho}\mathbf{e}_\theta, \tag{3.16}$$

and

$$\mathbf{v}_{out} = \frac{1}{\rho^2\sin\theta}\frac{\partial\tilde{\psi}}{\partial\theta}\mathbf{e}_\rho - \frac{1}{\rho\sin\theta}\frac{\partial\tilde{\psi}}{\partial\rho}\mathbf{e}_\theta. \tag{3.17}$$

respectively. Along with this, the matching conditions and the need for $\psi(\rho,\theta)$ to be regular at $\rho = 0$ give the following four boundary conditions

$$\psi(R,\theta) = 0, \quad |\psi(0,\theta)| < \infty, \quad \left.\frac{\partial\psi}{\partial\theta}\right|_{\rho=R} = \left.\frac{\partial\tilde{\psi}}{\partial\theta}\right|_{\rho=R}, \quad \left.\frac{\partial\psi}{\partial\rho}\right|_{\rho=R} = \left.\frac{\partial\tilde{\psi}}{\partial\rho}\right|_{\rho=R}. \tag{3.18}$$

A general solution for the inhomogeneous inside equation (3.14b) is sought in the form of $\psi(\rho,\theta) = \psi(\rho,\theta)_{gen} + \psi(\rho,\theta)_{part}$ where $\psi(\rho,\theta)_{gen}$ is a general solution to the homogeneous version of (3.14b) given by

$$\left[\frac{\partial^2}{\partial\rho^2} + \frac{\sin\theta}{\rho^2}\frac{\partial}{\partial\theta}\left(\frac{1}{\sin\theta}\frac{\partial}{\partial\theta}\right)\right]\psi = 0. \tag{3.19}$$

and $\psi(\rho,\theta)_{part}$ is a particular solution to (3.14b). A particular solution is found to be

$$\psi(\rho,\theta)_{part} = \delta\rho^4\sin^2\theta. \tag{3.20}$$

The general solution to (3.19) is obtained by a separated solution $\psi(\rho,\theta) = R(\rho)\Theta(\theta)$. Upon substituting the separated form into (3.19) one arrives at the two ODEs

$$\rho^2 R'' - \mathcal{C}R = 0, \tag{3.21}$$

$$\big((-\csc\theta)\Theta'\big)' = \mathcal{C}(\csc\theta)\Theta, \tag{3.22}$$

where $\mathcal{C}$ is a separation constant to be determined. Using the change of variables

$$t = \cos\theta, \quad \Theta(\theta) = T(t), \tag{3.23}$$

the equation (3.22) becomes

$$(1-t^2)T''(t) + \mathcal{C}T(t) = 0. \tag{3.24}$$

This ODE can be related to the associated Legendre ODE with the transformation

$$T(t) = \sqrt{1-t^2}P(t) \tag{3.25}$$

leading to

$$(1-t^2)P''(t) - 2tP'(t) + \left(\mathcal{C} - \frac{1}{1-t^2}\right) P(t) = 0. \tag{3.26}$$

The equation (3.26) is related to the associated Legendre ODE [33].

$$(1-x^2)\tilde{P}''(x) - 2x\tilde{P}'(x) + \left(l(l+1) - \frac{m^2}{1-x^2}\right) \tilde{P}(x) = 0 \tag{3.27}$$

Clearly (3.26) is the same as (3.27) when $m = 1$ and $\mathcal{C} = l(l+1)$. The equation (3.27) has nonsingular solutions on the interval $[-1, 1]$ only when l and m are integer values [3]. For $m = 1$, the associated Legendre polynomials have the form

$$P_l(x) = -\sqrt{1-x^2}\frac{d}{dx}\mathcal{P}_l(x), \tag{3.28}$$

where $\mathcal{P}_l$ refers to the lth order Legendre polynomial. One then arrives at the regular solutions to (3.24)

$$T_l(t) = -(1-t^2)\frac{d}{dt}\mathcal{P}_l. \tag{3.29}$$

which can be written as

$$T_l(t) = (l+1)\mathcal{P}_{l+1}(t) - (l+1)t\mathcal{P}_l(t). \tag{3.30}$$

This gives $\Theta(\theta)$ as

$$\Theta_l(\theta) = (l+1)\mathcal{P}_{l+1}(\cos\theta) - (l+1)\cos\theta\ \mathcal{P}_l(\cos\theta). \tag{3.31}$$

The value $\mathcal{C} = l(l+1)$ can now be substituted into (3.21) giving

$$\rho^2 R''(\rho) - l(l+1)R(\rho) = 0. \tag{3.32}$$

This has the solution

$$R_l(\rho) = a_l\rho^{l+1} + b_l\rho^{-l}. \tag{3.33}$$

As the solution is required to be regular at $\rho = 0$, b_l will be set to zero. A separated solution to the homogeneous PDE (3.19) is therefore

$$\psi_l(\rho, \theta) = a_l\rho^{l+1}\Theta_l(\theta), \tag{3.34}$$

giving the solution for ψ inside of the sphere as

$$\psi(\rho, \theta) = \delta\rho^4\sin^2\theta + \sum_{l=0}^{\infty} a_l\rho^{l+1}\Theta_l(\theta). \tag{3.35}$$

Using the condition that the pressure must match at the boundary which reduces to the condition that $\psi(R, \theta) = 0$ as specified in (3.18) gives

$$\sum_{l=0}^{\infty} a_l R^{l+1}\Theta_l(\theta) = -\delta R^4\sin^2\theta. \tag{3.36}$$

The solutions $\Theta_l(\theta)$ form a complete orthogonal basis as (3.22) is a classical Sturm-Liouville second-order linear ODE with weight $w(\theta) = -\csc\theta$. Using the observation that $\Theta_1(\theta) = -\sin^2\theta$ equation (3.36) can be written as

$$\sum_{l=0}^{\infty} a_l R^{l+1} \Theta_l(\theta) = \delta R^4 \Theta_l(\theta). \tag{3.37}$$

By multiplying the above equation by $-\csc\theta\Theta_l(\theta)$ and integrating from $0 < \theta < \pi$ one arrives at

$$a_l R^{l+1} = \frac{-\int_0^\pi \delta R^4 \csc\theta\Theta_1(\theta)\Theta_l(\theta)d\theta}{-\int_0^\pi \csc\theta(\Theta_l(\theta))^2 d\theta}. \tag{3.38}$$

The right hand side is zero due to the orthogonality of $\Theta_l(\theta)$ for all l except when $l = 1$. In this case one obtains the condition that

$$a_1 = \delta R^2. \tag{3.39}$$

Therefore the solution inside the sphere can be written as

$$\psi(\rho, \theta) = \delta\rho^2 \sin^2\theta(\rho^2 - R^2). \tag{3.40}$$

For outside of the sphere, the solution is the same as the homogeneous solution to 3.14b given by

$$\tilde{\psi}(\rho, \theta) = \sum_{l=0}^{\infty} \left(c_l \rho^{l+1} + \frac{d_1}{\rho} \right) \Theta_l(\theta). \tag{3.41}$$

The forth condition in (3.18) gives the condition that

$$\sum_{l=0}^{\infty} \left(c_l (l+1) R^l - \frac{d_1}{R^2} \right) \Theta_l(\theta) = 3\delta R^3 \sin^2\theta. \tag{3.42}$$

Using the orthogonality of $\Theta_l(\theta)$ as discussed before, $l = 1$. Lastly, the third condition gives

$$\left(c_l R^2 + \frac{d_1}{R} \right) = 0. \tag{3.43}$$

giving $c_1 = -d_1/R^3$. Substituting this back into (3.42) with $l = 1$ one achieves the complete solution

$$\psi(\rho, \theta) = \begin{cases} \delta\rho^2 \sin^2\theta(\rho^2 - R^2), & \rho < R \\ \frac{2}{3}\delta R^2 \sin^2\theta \left(\frac{\rho^3 - R^3}{\rho} \right). & \rho > R \end{cases} \tag{3.44}$$

This can be written in cylindrical coordinates as

$$\psi(r, z) = \begin{cases} \delta \left((r^2 z^2 + r^4) - R^2 r^2 \right), & r^2 + z^2 < R^2 \\ \frac{2}{3}\delta R^2 r^2 \left(1 - \frac{R^3}{(r^2+z^2)^{3/2}} \right). & r^2 + z^2 > R^2 \end{cases}. \tag{3.45}$$

The velocity components can be computed from (3.113) to be

$$v_r = \begin{cases} 2\delta r z, & r^2+z^2 < R^2 \\ \frac{2\delta R^5 r z}{(r^2+z^2)^{5/2}}, & r^2+z^2 > R^2 \end{cases} \tag{3.46}$$

$$v_z = \begin{cases} 2\delta\left(R^2 - r^2 - z^2\right), & r^2+z^2 < R^2 \\ \frac{4}{3}\delta R^2 + \frac{2\delta R^5}{3}\frac{(r^2-2z^2)}{(r^2+z^2)^{5/2}}, & r^2+z^2 > R^2 \end{cases}. \tag{3.47}$$

Moving back into the lab frame with the transformation given by (3.2) one arrives at

$$V_r = \begin{cases} 2\delta r(z - Z(t)), & r^2+(z-Z(t))^2 < R^2 \\ \frac{2\delta R^5 r(z-Z(t))}{(r^2+(z-Z(t))^2)^{5/2}}, & r^2+(z-Z(t))^2 > R^2 \end{cases} \tag{3.48}$$

$$V_z = \begin{cases} Z'(t) + 2\delta\left(R^2 - r^2 - (z-Z(t))^2\right), & r^2+(z-Z(t))^2 < R^2 \\ Z'(t) + \frac{4}{3}\delta R^2 + \frac{2\delta R^5}{3}\frac{(r^2-2(z-Z(t))^2)}{(r^2+(z-Z(t))^2)^{5/2}}. & r^2+(z-Z(t))^2 > R^2 \end{cases} \tag{3.49}$$

The pressure in the stationary frame of reference is given by

$$H(r,z) = \begin{cases} H_0 - 10\delta^2\left(r^2\left((z-Z(t))^2 + r^2 - R^2\right)\right), & r^2+(z-Z(t))^2 < R^2 \\ H_0. & r^2+(z-Z(t))^2 > R^2 \end{cases} \tag{3.50}$$

One additional boundary condition that can be considered is the behaviour of the velocity far away from the spherical vortex. In particular, if the fluid that the sphere is moving through is stationary, it is natural to demand $v_r, v_z \to 0$ as $r^2+z^2 \to \infty$. The first limit for v_r is trivially satified

$$\lim_{r^2+z^2\to\infty} v_r = 0. \tag{3.51}$$

however, for the z component of velocity, v_z one gets

$$\lim_{r^2+z^2\to\infty} v_z = Z'(t) + \frac{4}{3}\delta R^2 = 0. \tag{3.52}$$

This gives the additional condition that $Z'(t) = -\frac{4}{3}\delta R^2$. This implies the interesting result that the group velocity of the moving spherical vortex is constant with a speed that is proportional to the square of the radius. In this case, the solution depending on the freedom of R and δ can be written completely in terms of

$$Z(t) = Z_0 - \frac{4}{3}\delta R^2 t \tag{3.53}$$

as

$$V_r = \begin{cases} 2\delta r(z + \frac{4}{3}\delta R^2 t), & r^2+(z+\frac{4}{3}\delta R^2 t)^2 < R^2 \\ \frac{2\delta R^5 r(z+\frac{4}{3}\delta R^2 t)}{(r^2+(z+\frac{4}{3}\delta R^2 t)^2)^{5/2}}, & r^2+(z+\frac{4}{3}\delta R^2 t)^2 > R^2 \end{cases} \tag{3.54}$$

$$V_z = \begin{cases} -\frac{4}{3}\delta R^2 + 2\delta\left(R^2 - r^2 - (z+\frac{4}{3}\delta R^2 t)^2\right), & r^2+(z+\frac{4}{3}\delta R^2 t)^2 < R^2 \\ -\frac{4}{3}\delta R^2 + \frac{4}{3}\delta R^2 + \frac{2\delta R^5}{3}\frac{(r^2-2(z+\frac{4}{3}\delta R^2 t)^2)}{(r^2+(z+\frac{4}{3}\delta R^2 t)^2)^{5/2}}. & r^2+z+\frac{4}{3}\delta R^2 t)^2 > R^2 \end{cases} \tag{3.55}$$

with the pressure profile in the stationary frame as

$$H(r,z) = \begin{cases} H_0 + 10\delta^2 \left(r^2 \left((z + \frac{4}{3}\delta R^2 t)^2 + r^2 - R^2 \right) \right), & r^2 + (z + \frac{4}{3}\delta R^2 t)^2 < R^2 \\ H_0. & r^2 + (z + \frac{4}{3}\delta R^2 t)^2 > R^2 \end{cases} \tag{3.56}$$

Level curves of $H(r,z)$ can be seen in Figure 3.1.

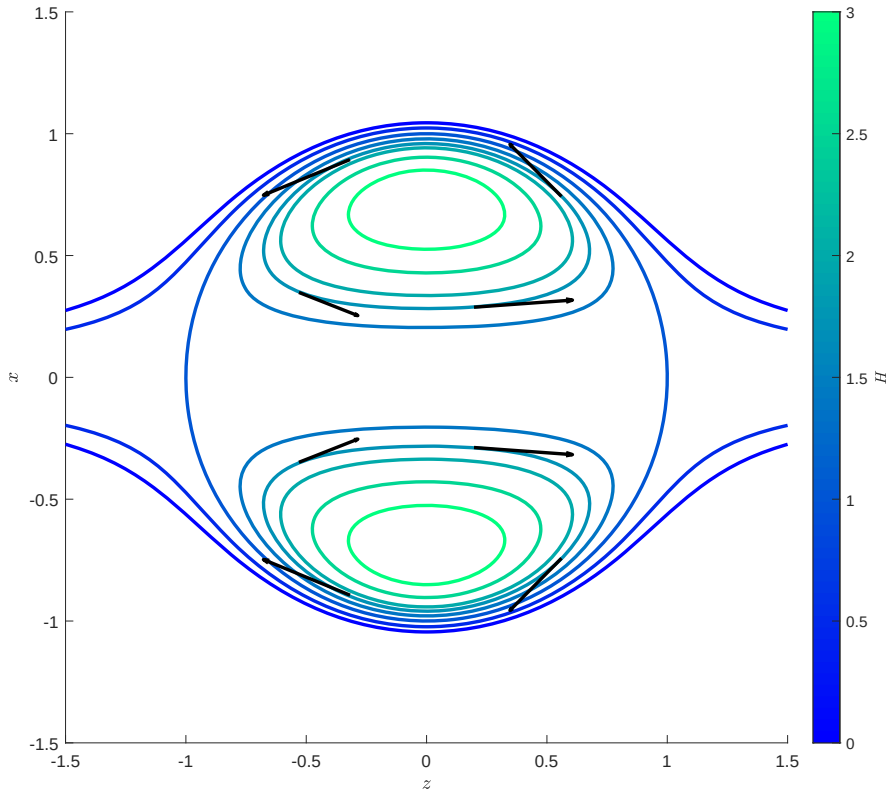

Figure 3.1: A cross-section of surfaces $H(\psi) = \text{const}$ in the lab frame given by (3.56). Here $R = 1$, $H_0 = 1$, $\delta = 1$ and $t = 0$. The black arrows correspond to the velocity vectors on a given surface. By the first equation of (3.3), both $\mathbf{v}$ and $\operatorname{curl} \mathbf{v}$ are tangent to this surface.

3.3 A stationary spherical MHD vortex

A similar problem to Hill's spherical vortex is the concept of a spherical vortex moving through an ideally conducting fluid. With this problem, negligibly small fluid motion ($\mathbf{V} = 0$) is assumed which reduces the dynamic MHD system (1.27) to the static equilibrium MHD equations

$$\operatorname{curl} \mathbf{B} \times \mathbf{B} = \mu \operatorname{grad} P, \tag{3.57a}$$

$$\operatorname{div} \mathbf{B} = 0. \tag{3.57b}$$

Here, the main differences between Hill's spherical vortex and this stationary conducting spherical vortex is: the search for $\mathbf{v}$ inside and outside the sphere is replaced with the search for $\mathbf{B}$, and the azimuthal component of this magnetic field is *not* assumed to be zero. Two assumptions of this conducting spherical vortex are: the pressure goes to a constant value taken to be zero at the boundary of the sphere (similar to Hill's spherical vortex), and every magnetic field component goes to zero at the boundary. The last condition here regarding the magnetic field is chosen in this way because the asymptotic behaviour of the magnetic field must decay at least as quickly as a dipole moment, but it was shown in [33], that the only solution outside of the sphere consistent with the inside pressure and magnetic field that has the proper asymptotic behaviour is when $\mathbf{B} = 0$.

The spherical vortex is assumed to have inherent axial symmetry which allows the reduction of (3.57) to the Grad-Shafranov equation

$$\frac{\partial^2 \psi}{\partial r^2} + \frac{\partial^2 \psi}{\partial z^2} - \frac{1}{r}\frac{\partial \psi}{\partial r} + I(\psi)I'(\psi) = -r^2 P'(\psi). \tag{3.58}$$

where the magnetic field components are given by

$$\mathbf{B} = \frac{\psi_z}{r}\mathbf{e}_r + \frac{I(\psi)}{r}\mathbf{e}_\phi - \frac{\psi_r}{r}\mathbf{e}_z. \tag{3.59}$$

Inside of the sphere, the pressure $P(\psi)$ and the arbitrary function related to the toroidal magnetic field $I(\psi)$ are taken to be linear (as any higher power series expansion of $P(\psi)$ and $I(\psi)$ makes (3.58) not separable in spherical coordinates). Therefore, these arbitrary functions are written as

$$P(\psi) = P_0 - \gamma\psi, \quad I(\psi) = \lambda\psi. \tag{3.60}$$

The Grad-Shafranov equation now becomes a second order linear homogeneous PDE. This equation is now converted to spherical coordinates

$$\left[\frac{\partial^2}{\partial \rho^2} + \frac{\sin\theta}{\rho^2}\frac{\partial}{\partial \theta}\left(\frac{1}{\sin\theta}\frac{\partial}{\partial \theta}\right) + \lambda^2\right]\psi = \gamma\rho^2\sin^2\theta, \tag{3.61}$$

where the magnetic field is given by

$$\mathbf{B} = \frac{1}{\rho^2\sin\theta}\frac{\partial \psi}{\partial \theta}\mathbf{e}_\rho + \frac{I(\psi)}{\rho\sin\theta}\mathbf{e}_\phi - \frac{1}{\rho\sin\theta}\frac{\partial \psi}{\partial \rho}\mathbf{e}_\theta. \tag{3.62}$$

Following a similar method to the previous section, $\psi(\rho,\theta) = \psi(\rho,\theta)_{gen} + \psi(\rho,\theta)_{part}$ where $\psi(\rho,\theta)_{gen}$ is a general solution to the homogeneous version of (3.61) given by

$$\left[\frac{\partial^2}{\partial \rho^2} + \frac{\sin\theta}{\rho^2}\frac{\partial}{\partial \theta}\left(\frac{1}{\sin\theta}\frac{\partial}{\partial \theta}\right) + \lambda^2\right]\psi = 0, \tag{3.63}$$

A particular solution to (3.61) is found to be

$$\psi(\rho,\theta) = \frac{\delta}{\lambda^2}\rho^2\sin^2\theta. \tag{3.64}$$

The general solution to (3.63) is obtained by a separated solution $\psi(\rho,\theta) = R(\rho)\Theta(\theta)$. Upon substituting the separated form into (3.63) one arrives at the two ODEs

$$\rho^2 R''(\rho) - (c+\lambda^2)R(\rho) = 0 \tag{3.65}$$

$$\big((-\csc\theta)\Theta'\big)' = \mathcal{C}(\csc\theta)\Theta. \tag{3.66}$$

One can notice that (3.66) is the exact same as in the previous section given by (3.22). Therefore, due to the $\sin^2\theta$ dependence in (3.64) and the orthogonality of $\Theta_l(\theta)$ given by (3.31), one can conclude in a similar fashion to the previous section that the only value of l which satisfies the pressure P going to the constant ambient pressure P0 on the boundary is $l = 1$. This gives the following separated anzats to use

$$\psi(\rho,\theta) = G(\rho)\rho^2\sin^2\theta. \tag{3.67}$$

Upon substituting the above into equation (3.61), the second order linear ODE is obtained

$$G''(\rho) + \frac{4}{\rho}G'(\rho) + G(\rho)\lambda^2 = \gamma. \tag{3.68}$$

This third order equation, (3.68), along with the following three physical conditions gives a well posed eigenvalue problem [9].

1. To achieve finite energy inside the sphere $\lim_{\rho\to 0}|G(\rho)| < \infty$.
2. The magnetic field components given by (3.62) must vanish at the boundary for the proper asymptotic behaviour as discussed in [9, 33], $G'(R) = G(R) = 0$.
3. The pressure must go to the constant ambient pressure P_0 at the boundary, $G(R) = 0$.

A general solution to (3.68) can be found to be

$$G(\rho) = C_1\frac{\rho\lambda\sin(\rho\lambda)+\cos(\rho\lambda)}{\rho^3} + C_2\frac{\rho\lambda\cos(\rho\lambda)-\sin(\rho\lambda)}{\rho^3} + \frac{\gamma}{\lambda^2}. \tag{3.69}$$

From the first condition above, $C_1 = 0$. The second condition gives a countable number of normalized eigenvalues $\lambda_n = \lambda R$ corresponding to the nth root of the following transcendental equation

$$x^2\tan x - 3\tan x + 3x = 0. \tag{3.70}$$

Lastly, the third condition gives a value for γ depending on the value of λ_n,

$$\gamma_n = -C_2\lambda_n^2\frac{\lambda_n\cos\lambda_n - \sin\lambda_n}{R^5}. \tag{3.71}$$

This gives the flux function inside of the sphere as

$$\psi(\rho,\theta) = \left(C_2\frac{\frac{\rho}{R}\lambda_n\cos(\frac{\rho}{R}\lambda_n) - \sin(\frac{\rho}{R}\lambda_n)}{\rho} + \frac{\rho^2R^2\gamma_n}{\lambda_n^2}\right)\sin^2\theta. \tag{3.72}$$

which can be written in terms of a first order spherical Bessel function of the first kind, j_1 as

$$\psi(\rho,\theta) = \left(\tilde{C}_2 \frac{\rho}{R}\lambda_n j_1\left(\frac{\rho}{R}\lambda_n\right) + \frac{\rho^2 R^2 \gamma_n}{\lambda_n^2}\right)\sin^2\theta. \tag{3.73}$$

Outside of the sphere $\rho > R$ all of the magnetic field components are zero and the pressure is equal to the ambient pressure P_0. An example of this solution for $n = 1$ has its pressure shown in Figure 3.2.

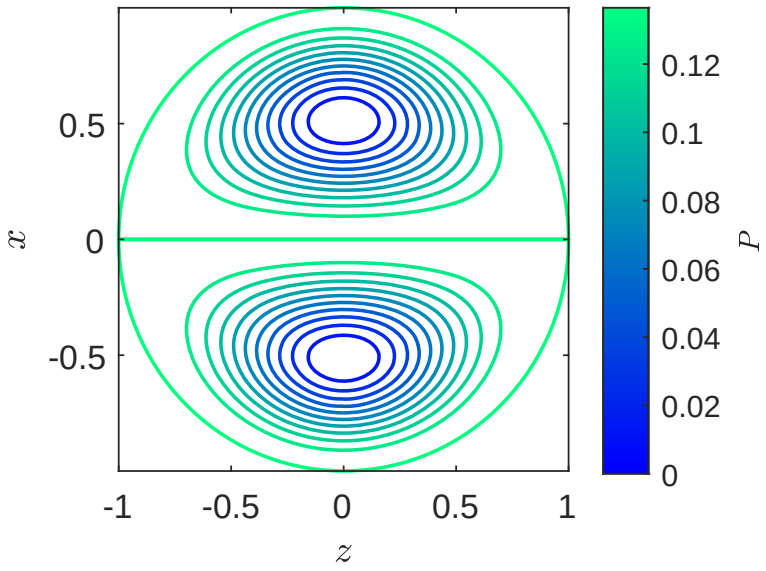

Figure 3.2: Pressure profile of static spherical vortex in ideally conducting fluid given by $P(\psi_n) = P_0 - \gamma_n\psi_n$ where ψ_n is given by (3.72) for $R = 1$, $n = 1$ and $C_2 = 1$. **B** is not shown on this plot as the non-zero ϕ component would make it point out of, or into the page.

A few other solutions are shown for higher values of n. In Figure 3.3 pressure profiles $P(\psi_n) = P_0 - \gamma_n\psi_n$ for ψ_n given by (3.72) with $n = 2$ and $n = 3$ can be seen.

In Figure 3.4 $n = 4$ and $n = 5$.

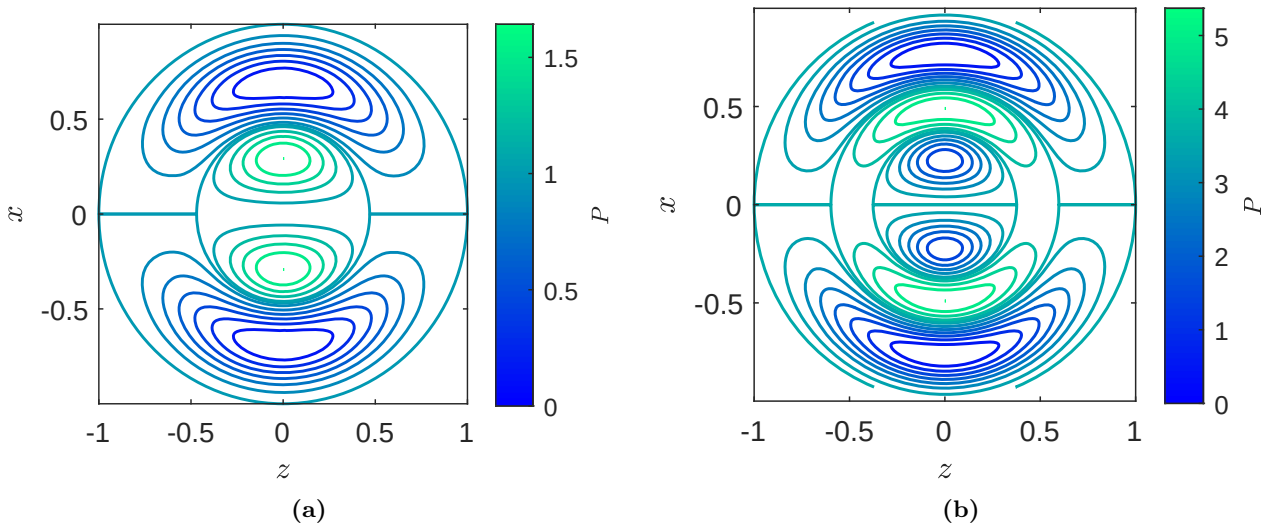

Figure 3.3: Pressure profile of static spherical vortex in ideally conducting fluid given by $P(\psi_n) = P_0 - \gamma_n \psi_n$ where ψ_n is given by (3.72) for $C_2 = 1$, $R = 1$, $n = 2$ on the left, and $n = 3$ on the right.

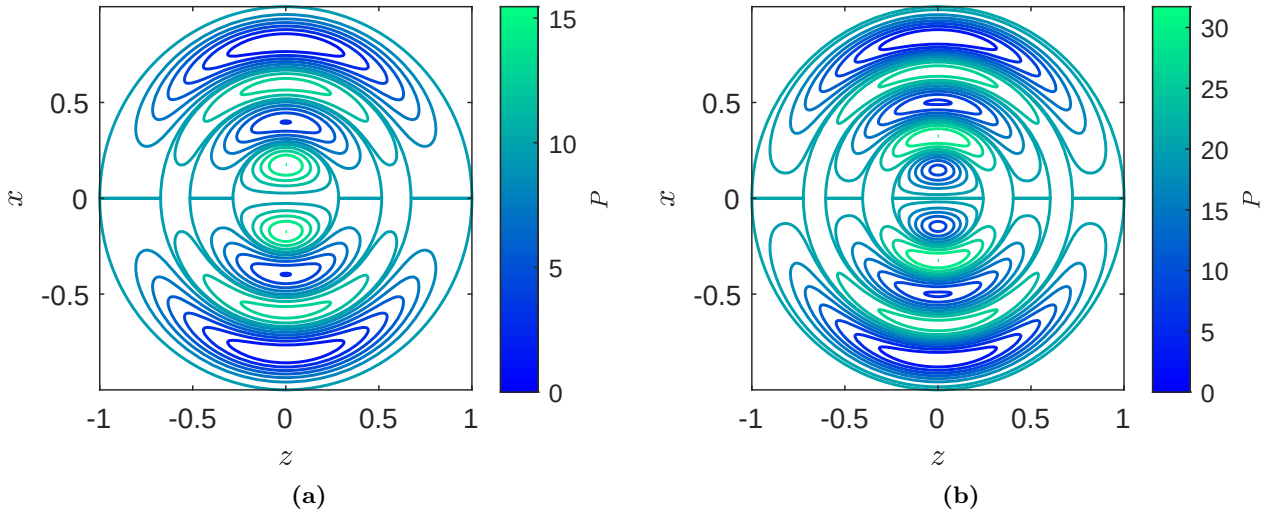

Figure 3.4: Pressure profile of static spherical vortex in ideally conducting fluid given by $P(\psi_n) = P_0 - \gamma_n \psi_n$ where ψ_n is given by (3.72) for $C_2 = 1$, $R = 1$, $n = 4$ on the left, and $n = 5$ on the right.

3.4 A generalized version of Hill's spherical vortex

In the last section, as the magnetic field outside of the spherical vortex needed to vanish in order to satisfy asymptotic behaviour that decays at least as fast as a dipole moment [33], and as the velocity asymptotics of Hill's spherical vortex outside of the sphere have good behaviour from a fluid dynamics standpoint, a generalized spherical vortex with a non-zero V^ϕ can be considered in a very similar way to the previous section.

Similar to the first section of chapter 3, using a moving frame of reference, assuming axial invariance, the Euler equations can reduce to the Bragg-Hawthorne equation (1.42). Starting from said equation in spherical coordinates

$$\left[\frac{\partial^2}{\partial\rho^2}+\frac{\sin\theta}{\rho^2}\frac{\partial}{\partial\theta}\left(\frac{1}{\sin\theta}\frac{\partial}{\partial\theta}\right)+F(\psi)F'(\psi)\right]\psi=-H'(\psi)\rho^2\sin^2\theta, \tag{3.74}$$

the arbitrary functions are again chosen as the highest power series expansion in ψ such that the (3.74) becomes separable and the asymptotics of the pressure $H(\psi)$ and the toroidal velocity component function $F(\psi)$ behave properly. As far as seperability of (3.74) goes, both functions cannot be of higher degree then linear in ψ. In regards to the asymptotics, the pressure far away from the sphere is chosen to change and thus needs to be the ambient pressure H_0, similarly, $F(\psi)$ must also not change far away from the sphere, however, $F(\psi)=F_0$ where $F_0=\text{const}$ is not allowed as it corresponds to a singular V^ϕ. This gives the best option for the free functions as

$$H(\psi)=\begin{cases}H_0-\gamma\psi, & \rho<R\\ H_0, & \rho>R\end{cases} \tag{3.75}$$

$$F(\psi)=\begin{cases}\lambda\psi, & \rho<R\\ 0. & \rho>R\end{cases} \tag{3.76}$$

This allows one to decompose the spherical Grad-Shafranov equation into two problems like before, one inside and one outside of the sphere, namely:

1. Rotational flow inside the sphere $\rho<R$

$$H(\psi)=H_0-\gamma\psi, \tag{3.77a}$$

$$\left[\frac{\partial^2}{\partial\rho^2}+\frac{\sin\theta}{\rho^2}\frac{\partial}{\partial\theta}\left(\frac{1}{\sin\theta}\frac{\partial}{\partial\theta}\right)+\lambda^2\right]\psi=\gamma\rho^2\sin^2\theta. \tag{3.77b}$$

2. Irrotational, force-free flow outside the sphere $\rho>R$

$$H(\tilde{\psi})=H_0, \tag{3.78a}$$

$$\left[\frac{\partial^2}{\partial\rho^2}+\frac{\sin\theta}{\rho^2}\frac{\partial}{\partial\theta}\left(\frac{1}{\sin\theta}\frac{\partial}{\partial\theta}\right)\right]\psi=0. \tag{3.78b}$$

The velocity components inside and outside are given by

$$\mathbf{v}_{in}=\frac{1}{\rho^2\sin\theta}\frac{\partial\psi}{\partial\theta}\mathbf{e}_\rho+\frac{F(\psi)}{\rho\sin\theta}\mathbf{e}_\phi-\frac{1}{\rho\sin\theta}\frac{\partial\psi}{\partial\rho}\mathbf{e}_\theta, \tag{3.79}$$

and

$$\mathbf{v}_{out}=\frac{1}{\rho^2\sin\theta}\frac{\partial\tilde{\psi}}{\partial\theta}\mathbf{e}_\rho-\frac{1}{\rho\sin\theta}\frac{\partial\tilde{\psi}}{\partial\rho}\mathbf{e}_\theta. \tag{3.80}$$

respectively. Along with this, the matching pressure at the boundary, the need for $\psi(\rho,\theta)$ to be regular at $\rho=0$ and the matching velocity at the boundary give in order the following four boundary conditions identical to the first section of Chapter 1

$$\psi(R,\theta)=0,\quad |\psi(0,\theta)|<\infty,\quad \left.\frac{\partial\psi}{\partial\theta}\right|_{\rho=R}=\left.\frac{\partial\tilde{\psi}}{\partial\theta}\right|_{\rho=R},\quad \left.\frac{\partial\psi}{\partial\rho}\right|_{\rho=R}=\left.\frac{\partial\tilde{\psi}}{\partial\rho}\right|_{\rho=R}. \tag{3.81}$$

From the last Section, a solution inside the sphere that is bounded at the origin is found to be

$$\psi(\rho,\theta)=\left(C\frac{\rho\lambda\cos(\rho\lambda)-\sin(\rho\lambda)}{\rho}+\frac{\gamma}{\lambda^2}\rho^2\right)\sin^2\theta, \tag{3.82}$$

and from the first section, the solution outside of the sphere is given by

$$\tilde{\psi}(\rho,\theta)=\rho^2\sin^2\theta\left(A+\frac{B}{\rho^3}\right). \tag{3.83}$$

After applying the matching pressure boundary condition given by the first equation in (3.81) one obtains the transcendental equation between λ and γ

$$C\lambda^2R\cos(R\lambda)-C\lambda\sin(R\lambda)+R^3\gamma=0. \tag{3.84}$$

Using the third boundary condition in (3.81) one obtains

$$A=-\frac{B}{R^3} \tag{3.85}$$

giving the outside solution as

$$\tilde{\psi}(\rho,\theta)=B\rho^2\sin^2\theta\left(\frac{1}{\rho^3}-\frac{1}{R^3}\right). \tag{3.86}$$

Lastly, the final boundary condition in (3.81) allows one to solve for B in terms of the other constants, giving

$$B=\frac{CR\lambda^3\cos(R\lambda)+C\lambda^4R^2\sin(R\lambda)-C\lambda^2\sin(R\lambda)-2\gamma R^3}{3\lambda^2}. \tag{3.87}$$

The three conditions on the constants given by (3.84), (3.85) and (3.87) gives $\psi(\rho,\theta)$ in the whole space as

$$\psi(\rho,\theta)=\begin{cases}\left(C\frac{\rho\lambda\cos(\rho\lambda)-\sin(\rho\lambda)}{\rho}+\frac{\gamma}{\lambda^2}\rho^2\right)\sin^2\theta, & \rho<R\\ \frac{CR\lambda^3\cos(R\lambda)+C\lambda^4R^2\sin(R\lambda)-C\lambda^2\sin(R\lambda)-2\gamma R^3}{3\lambda^2}\rho^2\sin^2\theta\left(\frac{1}{R^3}-\frac{1}{\rho^3}\right). & \rho>R\end{cases}. \tag{3.88}$$

This solution (3.88) of the spherical Grad-Shafranov equations (3.77) and (3.78) is a more general version of Hill's spherical vortex as:

- The ϕ component of the velocity is non-zero inside of the sphere. Whereas Hill's original vortex solution had $V^\phi=0$.
- There is the choice of freedom for three constants, C, (λ or γ) and R, whereas Hill's original solution only has a choice of freedom for R and one constant δ.

The asymptotics of the velocity field outside of the sphere behave in a suitable manner as this is the same outside solution of Hill's spherical vortex given in cylindrical coordinates by (3.46) and (3.47) which has correct asymptotics as discussed in [30]. One interesting remark is that if the outside magnetic field must vanish which corresponds in this case to the coefficient of the outside solution given in 3.88 as B, then this problem reduces to the problem in the previous section and the equations (2.53a) and (2.56b) reduce to the transcendental equations given by (3.70) and (3.71) as they should. This result is briefly discussed in [33] as they require this condition for the proper asymptotics of the magnetic field.

3.5 Generalized spherical separation of variables

In Section 3 of this Chapter, a separated solution in spherical coordinates to the Grad-Shafranov equation 3.89 was obtained to satisfy boundary conditions that correspond to a spherical vortex moving through a stationary fluid. During this, the behaviour of $\Theta_l(\theta)$ given by (3.31) was restricted to $l=1$ to satisfy the boundary conditions. In this section, a fully separated solution is considered in its own right.

Using the first part of Section 3 up until 3.66, the linear Grad-Shafranov equation in spherical coordinates

$$\left[\frac{\partial^2}{\partial\rho^2}+\frac{\sin\theta}{\rho^2}\frac{\partial}{\partial\theta}\left(\frac{1}{\sin\theta}\frac{\partial}{\partial\theta}\right)+\lambda^2\right]\psi=\gamma\rho^2\sin^2\theta. \tag{3.89}$$

which from (1.40) corresponds to the free functions from Section 3 given by $I(\psi)=\lambda\psi$ and $P(\psi)=P_0-\gamma\psi$. A solution in the form of $\psi(\rho,\theta)=\psi(\rho,\theta)_{gen}+\psi(\rho,\theta)_{part}$ is sought with $\psi(\rho,\theta)_{part}=\frac{\gamma\rho^2\sin^2\theta}{\lambda^2}$. A separated solution for the homogenous version of (3.89) is sought in the form $\psi(\rho,\theta)=R(\rho)\Theta(\theta)$.

The homogeneous version of equation (3.89) then reduces to the two ODEs

$$\rho^2R''(\rho)-(\mathcal{C}+\lambda^2)R(\rho)=0, \tag{3.90}$$

$$\Theta''(\theta) - \frac{\cos\theta}{\sin\theta}\Theta'(\theta) + c\Theta(\theta) = 0, \tag{3.91}$$

where $\mathcal{C}$ is a separation constant to be determined.

From Section 1 of this chapter, the separation constant is found to be $\mathcal{C} = l(l+1)$ for $l \in \mathbb{N}$ with a solution to (3.91) given by

$$\Theta_l(\theta) = (l+1)\mathcal{P}_{l+1}(\cos\theta) - (l+1)\cos\theta\ \mathcal{P}_l(\cos\theta). \tag{3.92}$$

The value $\mathcal{C} = l(l+1)$ can now be substituted into (3.90) giving

$$\rho^2 R''(\rho) - (l(l+1) + \lambda^2)R(\rho) = 0. \tag{3.93}$$

This has a solution in terms of the Bessel function of the first kind

$$R_l(\rho) = \sqrt{\rho}\mathcal{J}\left(\frac{2l+1}{2}, \rho\lambda\right). \tag{3.94}$$

So a separated solution to the homogenous version of (3.89) is given by

$$\psi_l(\rho,\theta) = \sqrt{\rho}\mathcal{J}\left(\frac{2l+1}{2}, \rho\lambda\right)\Big((l+1)\mathcal{P}_{l+1}(\cos\theta) - (l+1)\cos\theta\mathcal{P}_l(\cos\theta)\Big). \tag{3.95}$$

As equation (3.89) is linear, any linear combination of the separated solution (3.95) with the addition of the particular solution will also be a solution. This can be written in a general way as

$$\Psi(\rho,\theta) = \frac{\gamma\rho^2\sin^2\theta}{\lambda^2} + \sum_{l=0}^{n} a_l\sqrt{\rho}\mathcal{J}\left(\frac{2l+1}{2}, \rho\lambda\right)\Theta_l(\theta). \tag{3.96}$$

Where $\Theta_l(\theta)$ is given by (3.92). Clearly this solution is no longer related to the spherical vortex but is an MHD equilibria solution which can be considered in its own right. A pressure profile $P = P_0 - \gamma\psi$ with ψ given by (3.96) can be seen in Figure 3.5.

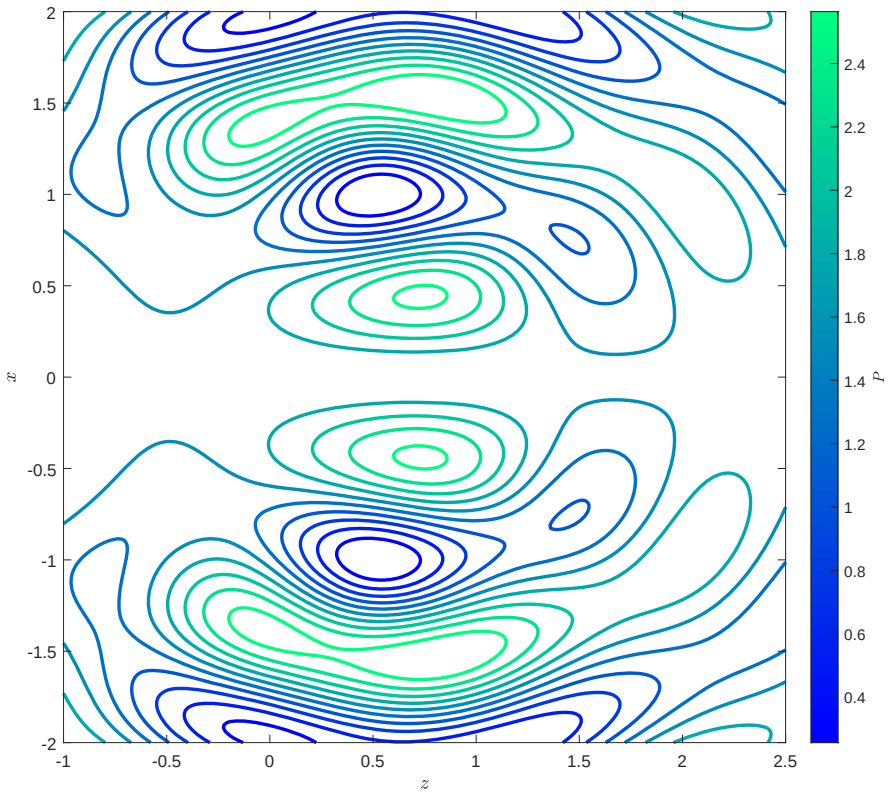

Figure 3.5: A cross-section of magnetic surfaces where the magnetic surfaces are shown by $P(\psi) =$ const for $P = P_0 - \gamma\psi$ where ψ is given by (3.96). Here $\gamma = 1$, $\lambda = 1$, $n = 5$, $a_l = 1$, $l = 1, 2, 3, 4, 5$. Any toroidal surface can be considered a truncated solution with the outer surface described by a current sheet.

3.6 Stability considerations for the spherical vortex

In this section, stability of the spherical vortices solutions described in the previous chapters will be analyzed. These include Hill's vortex solutions from Section 1 given by (3.44), the MHD spherical vortex solution given in Section 2 given by (3.72) and the generalized Hill's vortex from Section 3 given by (3.88). In the first part, an axially-symmetric perturbation of Hill's spherical vortex on the sphere following a method described in [40] is performed with the goal of observing modes that grow exponentially in time to conclude the instability of the solution. In the next sections, a similar perturbation is attempted but is shown to not be possible. A generalized perturbation is performed with the goal of observing modes that grow exponentially in time.

3.6.1 Axisymmetric perturbation of Hill's vortex

The solution of Hill's spherical vortex at the surface of the sphere $\rho = R$ is considered. Using the dynamic equation for ψ found in Hill's paper [30]

$$\left(\frac{\partial}{\partial t}+\frac{1}{r}\frac{\partial\psi}{\partial z}\frac{\partial}{\partial r}-\frac{1}{r}\frac{\partial\psi}{\partial r}\frac{\partial}{\partial z}\right)\left[\frac{1}{r^2}\left(\frac{\partial^2\psi}{\partial z^2}+\frac{\partial^2\psi}{\partial r^2}-\frac{1}{r}\frac{\partial\psi}{\partial r}\right)\right]=0. \tag{3.97}$$

The inside solution given by (3.44) is perturbed using

$$\rho\mapsto\rho(1+\epsilon h(\theta,t)) \tag{3.98}$$

giving

$$\psi(\rho,\theta)=\delta\rho^2(1+\epsilon h(\theta,t))^2\sin^2\theta(\rho^2(1+\epsilon h(\theta,t))^2-R^2). \tag{3.99}$$

This perturbed solution is now substituted into the spherical version of the dynamic ψ equation (3.97). After this, the substitution ($\rho=R$) is made and then discarding terms beyond the first order of ϵ the following third order PDE for $h(\theta,t)$ is obtained

$$2R\delta\sin\theta\frac{\partial^3h}{\partial\theta^3}+\frac{\partial^3h}{\partial t\partial\theta^2}+6R\delta\cos\theta\frac{\partial^2h}{\partial\theta^2}+3\frac{\cos\theta}{\sin\theta}\frac{\partial^2h}{\partial t\partial\theta}-\frac{40R\delta}{\sin\theta}\left(\cos^2\theta-\frac{17}{20}\right)\frac{\partial h}{\partial\theta}+20\frac{\partial h}{\partial t}=0. \tag{3.100}$$

This linear homogeneous equation is separable: one can seek its solutions as $h(\theta,t)=\Theta(\theta)T(t)$ where $\Theta(\theta)$ and $T(t)$ satisfy

$$\frac{d^3\Theta}{d\theta^3}=-3\left(\frac{\cos\theta}{\sin\theta}+\frac{\lambda}{6R\delta\sin\theta}\right)\frac{d^2\Theta}{d\theta^2}+\left(20\frac{\cos^2\theta}{\sin^2\theta}-3\frac{\cos\theta}{2R\delta\sin^2\theta}\lambda-\frac{17}{\sin^2\theta}\right)\frac{d\Theta}{d\theta}-10\frac{\lambda}{R\delta\sin\theta}\Theta, \tag{3.101}$$

$$\frac{dT}{dt}=\lambda T. \tag{3.102}$$

The T equation above has the exponential solution $T(t)=Ae^{\lambda t}$. The Θ equation (3.101) can be converted into a simpler equation with the transformation $z=\cos\theta$ with $\Theta(\theta)=Z(z)$. This gives

$$(1-z^2)\frac{d^3Z}{dz^3}-(2K_2+6z)\frac{d^2Z}{dz^2}+8\left(2+\frac{K_2z}{1-z^2}\right)\frac{dZ}{dz}-\frac{40K_2}{1-z^2}Z=0. \tag{3.103}$$

Solutions to (3.103) can be expressed as a linear combination of the following functions written in terms of the hypergeometric functions

$$Z_1=\mathcal{H}\left(\left[\frac{3}{4}+\frac{\sqrt{89}}{4},\frac{3}{4}-\frac{\sqrt{89}}{4}\right],\frac{1}{2},z^2\right), \tag{3.104a}$$

$$Z_2=z\mathcal{H}\left(\left[\frac{5}{4}+\frac{\sqrt{89}}{4},\frac{5}{4}-\frac{\sqrt{89}}{4}\right],\frac{3}{2},z^2\right), \tag{3.104b}$$

$$Z_3=-Z_1\int_{z_0}^{z}z(z+1)^{1+\frac{\lambda}{4R\delta}}(z-1)^{1-\frac{\lambda}{4R\delta}}Z_2dz+Z_2\int_{z_0}^{z}(z+1)^{1+\frac{\lambda}{4R\delta}}(z-1)^{1-\frac{\lambda}{4R\delta}}Z_1dz. \tag{3.104c}$$

Here z_0 is any constant such that $z_0<z$. One should notice that both the first and second solution of (3.104) do not depend on the separation constant λ. This is because (3.103) can be written as

$$\mathcal{L}=\left(\frac{d}{dz}-\frac{2K_2}{1-z^2}\right)\mathcal{G}, \tag{3.105}$$

where

$$\mathcal{G} \equiv \left(1-z^2\right)\frac{d^2Z}{dz^2} - 4z\frac{dZ}{dz} + 20Z = 0. \tag{3.106}$$

Here (3.106) has the general solution

$$Z = C_1 Z_1 + C_2 Z_2 \tag{3.107}$$

where Z_1 and Z_2 are given in (3.104).

As λ does not appear in Z_1 and Z_2, there will exist $h(\theta,t)$ which grows exponentially in time as λ can by positive. However, one must check and make sure that these $h(\theta,t)$ that grow in time correspond to regular surfaces. One such $h(\theta,t)$ that gives regular surfaces utilizes Z_1 given above by 3.104a. This gives $h(\theta,t)$ as

$$h(\theta,t) = Ae^{\lambda t}\mathcal{H}\left(\left[\frac{3}{4}+\frac{\sqrt{89}}{4},\frac{3}{4}-\frac{\sqrt{89}}{4}\right],\frac{1}{2},\cos^2\theta\right) \tag{3.108}$$

This is now substituted into (3.99). After expanding out, and converting back to cylindrical coordinates, one arrives at

$$\psi(r,z,t) = -2\delta\left(Ae^{\lambda t}\epsilon^2(R^2-2r^2-2z^2)\mathcal{H}\left(\left[\frac{3}{4}+\frac{\sqrt{89}}{4},\frac{3}{4}-\frac{\sqrt{89}}{4}\right],\frac{1}{2},\frac{r^2}{r^2+z^2}\right)+\frac{R^2-r^2-z^2}{2}\right). \tag{3.109}$$

When $\psi = 0$ this corresponds to the boundary of the sphere. Several plots of the evolution of this surface are shown in 3.6.

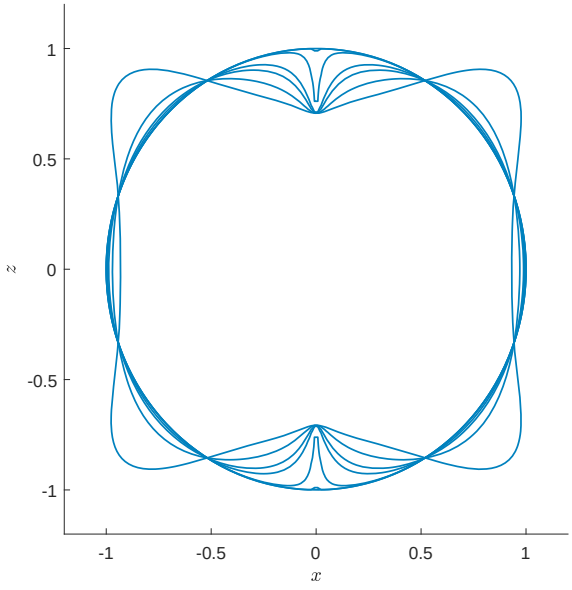

Figure 3.6: The evolution of the perturbation given by 3.109 is shown for $\epsilon = 0.0001$, $\delta = 1$, $R = 1$, $A = 1$, $\lambda = 1$, at several different times $0 < t < 16$. These surfaces are regular as shown in Appendix C.

Despite the irregular look of this surface at some of the points in time, the implicit derivative dz/dr of (3.109) when $\psi(r,z,t)=0$ can be shown to be zero at the irregular looking points $r=0$. This is found in Appendix C.

The above analysis leads to the following conclusion that Hill's spherical vortex is in general not linearly stable with respect to magnetic surface perturbations described by (3.99). Stability analysis of Hill's vortex has been previously considered numerically in ref [40], however, no details including mathematical formulas, numerical method used, and initial/boundary conditions were presented; we were not able to reproduce the results of [40].

3.6.2 An axisymmetric perturbation of generalized Hill's spherical vortex and MHD vortex

The goal here is to use a similar axisymmetric perturbation method as above following the method in [40] to study the stability of the generalized hill's spherical vortex solution (3.88) and the MHD spherical vortex in an ideally conducting fluid solution (3.72). The dynamic equation for ψ (3.97) taken from [30] in which $V^\phi=0$ was used to study the time evolution of ψ with the perturbation given by equation (3.98). Therefore for a similar analysis of the two other solutions, a dynamic equation for ψ needs to be derived from the time dependent, axially symmetric Euler equations with $V^\phi=I(\psi)/r$ (which is the form of V^ϕ in both (3.72) and (3.88)).

Deriving axially symmetric dynamic ψ equation with non-zero V^ϕ

Starting with the dynamic Euler Equations (1.15) in cylindrical coordinates with axial invariance one arrives at the system

$$V^r_t + rV^z(V^r_z - V^z_r) - V^\phi(rV^\phi)_r = rH_r, \tag{3.110a}$$

$$V^\phi_t + V^z(rV^\phi)_z + V^r(rV^\phi)_r = 0, \tag{3.110b}$$

$$V^z_t + V^r(V^z_r - V^r_z) - V^\phi V^\phi_z = H_z, \tag{3.110c}$$

$$(rV^z)_z + (rV^r)_r = 0, \tag{3.110d}$$

where superscripts denote the vector component and subscripts denote the partial differentiation. The last equation, by the Poincaré lemma, implies the local existence of a potential such that

$$V^r = \frac{\psi_z}{r}, \quad V^z = -\frac{\psi_r}{r}. \tag{3.111}$$

Upon substituting the above vector components and the form of ϕ component of the velocity to be $V^\phi = I(\psi)/r$, (as taken from both the MHD spherical vortex solution and generalized hill solution) into (3.110b) one obtains

$$I'(\psi)\frac{\partial \psi}{\partial t} = 0. \tag{3.112}$$

This implies that for $V^\phi = I(\psi)/r$, either

1. $\psi(r, z, t)$ is time independent, in which case (3.110) can reduce to the Grad-Shafranov (Bragg Hawthorn) equation (1.40) or (1.42).

2. $I(\psi)$ is constant with respect to ψ. For the case when $I(\psi) = 0$, 3.97 can be obtained.

Therefore, either ψ is time independent or $V^\phi = I(\psi)/r$ is not the correct form of V^ϕ concluding that no dynamic ψ equation with $V^\phi = I(\psi)/r$ can exist. If V^ϕ is an arbitrary function of r, z and t, with the use of Poisson Brackets, dynamic equations for ψ were derived in [10]. However, these are of no use for studying the case when $V^\phi = I(\psi)/r$. Therefore, the time evolution of ψ using a single equation is not possible and more general type of perturbation analysis needs to be considered.

3.6.3 A general linear perturbation for generalized Hill's spherical Vortex

In this section, finding solutions to the general linear perturbations was not successful, however the following methodology is still presented to show how one can derive the perturbed linear systems.

In order to study the stability of the solution given by (3.88) a linear perturbation on the dependent variables will be considered. As the r and z components of $\mathbf{V}$ are related by the stream function ψ by

$$\mathbf{v} = \frac{\psi_z}{r}\mathbf{e}_r + \frac{-\psi_r}{r}\mathbf{e}_z, \tag{3.113}$$

and the other dependent variables being the pressure H and the ϕ component of the magnetic field V^ϕ, instead of the usual four dependent variables, there are only three. These three quantities are perturbed as follows

$$\psi(r, z, t) = \psi_0(r, z) + \epsilon\psi_1(r, z, t), \tag{3.114a}$$

$$F(r, z, t) = F_0(\psi_0) + \epsilon F_1(r, z, t), \tag{3.114b}$$

$$H(r, z, t) = H_0(\psi_0) + \epsilon H_1(r, z, t). \tag{3.114c}$$

where ψ_0 is the static solution given by (3.88), $F_0(\psi_0) = \lambda\psi_0$ and $H_0(\psi_0) = H_0 - \gamma\psi_0$. Substituting these into the axially invariant Euler equations and discarding terms of ϵ^2 and higher one obtains a closed linear system for the three unknown functions $\psi_1(r,z,t)$, $F_1(r,z,t)$, $H_1(r,z,t)$. The goal now is to see if any solutions to this linear system have time dependence that grows unbounded. The system, though linear is still very large and complex (so much so that it is not even written here), and no meaningful nontrivial solutions were able to be found to this variable coefficient linear system.

3.6.4 General perturbation for an MHD spherical vortex

Similarly to above, one can considered the perturbation of the MHD spherical vortex with the solution given by (3.72). The main difference from the previous section being that the magnetic field components are perturbed as well as the velocity field components. The static equilibrium MHD equations, $\operatorname{div}\mathbf{B} = 0$ gives the condition that $B^r = psi_z/r$ and $B^z = -\psi_r/r$. Also from $\operatorname{div}\mathbf{V} = 0$ gives the condition that $V^r = \xi_z/r$ and $V^z = -\xi_r/r$ This gives 5 dependent variables $\psi(r,z,t)$, $\xi(r,z,t)$, $I(r,z,t)$, $F(r,z,t)$ and $P(r,z,t)$, instead of the usual 6. These quanities are perturbed and written as

$$\psi(r,z,t) = \psi_0(r,z) + \epsilon\psi_1(r,z,t), \tag{3.115a}$$

$$I(r,z,t) = I_0(\psi_0) + \epsilon I_1(r,z,t), \tag{3.115b}$$

$$P(r,z,t) = P_0(\psi_0) + \epsilon P_1(r,z,t). \tag{3.115c}$$

$$\xi(r,z,t) = 0 + \epsilon\xi_1(r,z,t), \tag{3.115d}$$

$$F(r,z,t) = 0 + \epsilon F_1(r,z,t), \tag{3.115e}$$

where ψ_0 is given by 3.72. Here $B^\phi = I(r,z,t)/r$ and $V^\phi = F(r,z,t)/r$. Substituting these into the axially MHD equations gives an overdetermined system of 6 equations for the 5 unknown $\psi_1(r,z,t)$, $I_1(r,z,t)$, $P_1(r,z,t)$, $\xi_1(r,z,t)$ $F_1(r,z,t)$, and $H_1(r,z,t)$. Similar to above, no solutions were able to be found to this variable coefficient linear system.

4 Conclusion

From studying astrophysical phenomena to working with industrial applications, plasma descriptions are vital for modelling plasmas in various physical contexts that arise. In the first chapter, several mathematical descriptions of plasma were discussed with the focus being on the idealized MHD system of equations which gives a great first approach to many problems in plasma physics. The MHD system of equations is still a very rich mathematical model with many different instabilities and waves. In the adiabatic MHD system (1.16) and (1.17), different types of waves which can arise were computed by looking at the harmonics of the linearized system. The dispersion relations yield three different types of linear waves including the transverse shear-Alfveń waves, the longitudinal fast magnetosonic waves and the longitudinal slow magnetosonic waves. The main focus of this work is the incompressible MHD model (1.27) along with several reductions including the Euler fluid equations (1.15) for ($\mathbf{B} = 0$), the time independent MHD system (1.28), and the static equilibrium MHD model (1.31) for ($\mathbf{V} = 0$). Along with these, a brief discussion about the field line topology was presented with the main result being that bounded magnetic surfaces, to which $\mathbf{B}$ and $\mathbf{J} \sim \operatorname{curl} \mathbf{B}$ are tangent, are homeomorphic to tori [20, 35]. After this, several important solutions to the incompressible MHD model (1.27) were discussed. This included the ABC flow given by (1.32) as a solution to both the time independent Euler equations (1.15), as well as the static equilibrium MHD equations (1.31) as these two systems of equations are analogous. A further common approach to simplify static equilibrium MHD equations (1.31) includes the concept of symmetry reductions which, for each symmetry, reduce the number of spatial variables by one. Some important symmetry reduction solutions include models of axially symmetric jets and solar prominences found in [11] and helically symmetric jets found in [12]. In the axial and helical symmetries, the static MHD equations reduce to the single Grad-Shafranov equation (1.40) and the JFKO equation respectively (1.48). New solutions for both axial and helical reductions of the static equilibrium MHD equations (1.31) make up most of the work found in Chapter 2. Lastly, the Bogoyavlenskij transformations given by (1.52) are presented with the focus being on converting solutions to the static equilibrium MHD equations (1.31) into dynamic solutions to (1.28) with $\mathbf{V} \neq 0$ and used in .

In Chapter 2 the main focus was to derive new solutions to the time independent MHD equations (1.28) by first finding new solutions to the static equilibrium MHD equations (1.31) and then with the use of the Bogoyavlenskij transformations (1.52), arrive at new dynamic solutions to (1.28). First off, the physical restrictions on solutions were discussed for both truncated solutions (solutions only valid inside some bounded plasma domain) and global solutions (solutions which are valid in the entire space). These restrictions included regularity of the dependent variables, proper pressure behaviour and finite total energy. For a

truncated solution, the boundary condition at the border of the plasma domain $\partial\mathcal{U}$ was derived with the use of the surface current density $\mathbf{K}_{encl}$. This boundary condition is given by (2.8). Starting with the axial reduction of the static equilibrium equations (1.31), in which case they reduce into the single PDE known as the Grad-Shafranov equation (1.40), there are choices of the arbitrary function in (1.40) such that it becomes a linear homogeneous PDE. Choosing the highest power series expansion for both $P(\psi)$ and $I(\psi)$ such that (1.40) becomes linear homogeneous, separated solutions can be sought. This corresponds to a linear function of ψ for $I(\psi)$ and a quadratic function of ψ for $P(\psi)$. Depending on the sign of the coefficient in the ψ^2 term for the pressure $P(\psi)$, two separate families of solutions arise. The first family corresponds to the ψ^2 coefficient in the pressure being negative. In this case, a general separated solution given by (2.20) can be found in terms of Whittaker functions in the radial variable, and regular trigonometric functions in the z variable. For this solution, a proposition is proved that states the solution (2.20) is global if and only if the first parameter in the Whittaker functions take on an integer value. In this case, a linear combination of these global solutions given by (2.23) is the same solution as Bogoyavlenskij's axially symmetric astrophysical jets given by (1.46) and derived in [11]. Therefore, this new solution (2.20) is a generalization of (1.46). For this first family of solutions, an example of a truncated solution in which the first parameter of the Whittaker functions is not an integer is shown in Figure 2.1 along with a linear combination of global solutions that need not be truncated in Figure 2.3. The second family of solutions where the ψ^2 coefficient in the pressure term is positive has a separated form in terms of Coulomb wave functions in the radial variable and trigonometric functions in the z variable. This solution is shown in (2.30). Due to the oscillating nature of the Coulomb wave functions, all physical solutions of this type are truncated. One truncated example is shown in Figure (2.6) along with a 3D image of the magnetic surfaces seen in Figure 2.8. Next, the helical reduction of the static equilibrium equations (1.31) gives the JFKO equation (1.48) and similar to the axial case, for the right choices of $P(\psi)$ and $I(\psi)$ this equation becomes linear homogeneous. As before, $I(\psi)$ is chosen to be linear, and $P(\psi)$ is chosen to be quadratic. Again, for the sign of the coefficient in the ψ^2 term for the pressure $P(\psi)$ one achieves two separate families of solutions. The first family of solutions which corresponds to the coefficient in the ψ^2 term for the pressure $P(\psi)$ being negative is expressed as a separated solution in terms of the confluent Heun function multiplied by a power function and Gaussian in the radial variable, along with trigonometric functions in the ξ variable. This radial dependence is similar to the Whittaker functions from the axial reduction. In the special case where the confluent Heun function produces polynomials, the separated solution given by (2.42) is a global solution which has the same form as the helical jet solution (1.50) discussed in [12]. Thus this new solution is a generalization of (1.50). A necessary condition for such polynomials is given by $c = -a(n+(b/2))$ where n is a non-negative integer and a, b and c are given by (2.39). A truncated solution for which $c \neq -a(n + (b/2))$ is shown in Figure 2.10 along with a linear combination of these solutions in Figure 2.11. One of the global solutions given by (1.50) expressed by Bogoyavlenskij in [12] which corresponds to the confluent Heun function producing polynomials are shown in Figure 2.12 along with a 3D image of the magnetic surfaces shown in Figure 2.13. The second family of solutions which

corresponds to the coefficient of the ψ^2 term in the pressure $P(\psi)$ being positive gives a separated solution given by (2.48) in terms of the confluent Heun function with imaginary parameters multiplied by a power function and an imaginary Gaussian in the radial variable and the trigonometric functions in the ξ variable. The radial dependence behaves similarly to the Coulomb wave functions in the axial reduction as it oscillates and must be truncated in order to be a physical solution. One of these solutions is shown in Figure (2.15) along with a 3D image of the magnetic surfaces in Figure 2.16 where the magnetic field lines can be seen curling up these twisted cylinders. In the last section, with the use of the Bogoyavlenskij transformations (1.52) an example of an axial solution and helical solution to the time independent MHD equations (1.28) is shown in Figure 2.17 and Figure 2.18 respectively.

In Chapter 3 the overall goal was to rederive Hill's spherical vortex discussed in [30] as well as to use a related MHD spherical vortex [9, 33] in order to develop a more general spherical vortex in fluid dynamics. In the first section, a modern derivation of Hill's spherical vortex with the use of the Grad-Shafranov (Bragg-Hawthorne) equation (1.42) and Galilean invariance was presented. This was accomplished by using a moving frame of reference and converting the Euler equations (3.1) into the time independent Euler equations (3.3). As mentioned previously, the time independent Euler equations are analogous to the static equilibrium MHD equations (1.31) and for an axially symmetric flow, can be reduced to the Grad-Shafranov (Bragg-Hawthorne) equation (1.42). Following Hill's simplification of setting $V^\phi = 0$ with the choice of the arbitary pressure function $H(\psi)$ chosen such to be the highest power series expansion of $H(\psi)$ such that the simplified Grad-Shafranov equation (3.9) is separable in spherical coordinates. With this, $H(\psi)$ is chosen to be at most linear in ψ. Far away from the sphere, it is assumed that the pressure goes to the ambient pressure H_0. Therefore, the pressure is decomposed into the piece-wise function (3.11) and thus decomposes the Bragg-Hawthrone equation into the following two pieces in spherical coordinates (3.14) and)3.15. These equations, along with the condition that the solutions must be regular at the origin, have matching pressure and velocity at the boundary gives a well posed problem. The solution $\psi(\rho, \theta)$ is computed to be (3.44). The level curves of the pressure $H(\psi)$ which coincide with the surfaces that $\mathbf{V}$ and $\boldsymbol{\omega} \sim \operatorname{curl} \mathbf{V}$ are tangent to can be seen in Figure 3.1. In the next section, a similar problem regarding an MHD spherical vortex which was first discussed in [9] is derived using the Grad-Shafranov equation (1.40) with the assumptions that the pressure must go to a constant value at the boundary of the sphere, $B^\phi \neq 0$ inside the sphere and every magnetic field components vanishes at the boundary. Again, $I(\psi)$ and $P(\psi)$ are chosen such to be the highest power series expansion such that the Grad-Shafranov equation becomes separable in spherical coordinates. In this case both functions are chosen to be linear in ψ. With equation (3.68) and the boundary conditions given by 3.3, a well posed eigenvalue problem is given with the solution given by (3.72) along with the transcendental equations (3.70) and (3.71) that give conditions on the values of λ and γ for $I(\psi)$ and $P(\psi)$ from (3.60). Different solutions are shown for different choices of the eigenvalues λ_n in Figure 3.2, Figure 3.3a and 3.3b. In the next section, using the first two sections from this chapter, a new general spherical vortex solution is presented. This solution is more general as it does not assume V^ϕ to be zero. Again the arbitrary functions

$F(\psi)$ and $H(\psi)$ are chosen as the highest power series expansion such that the Grad-Shafranov equation is still separable in spherical coordinates. In this case, both functions are chosen to be linear inside the sphere and outside the sphere the pressure is taken to be constant $H(\psi) = H_0$ and $F(\psi)$ is chosen to go to zero as it did in the related MHD problem from Section 3 in this Chapter. This again decomposes the problem into two pieces with the condition that the pressure and velocity components must match at the boundary. The solution to this problem is given by equation (3.88) along with the transcendental equation (3.84) relating λ and γ along with (3.87) which determine the coefficient of the outside solution. In the case where this outside solution must be zero, we recover the transcendental equations (3.70) and (3.71) from Section 3 as we should. Next, a related spherical solution to the static MHD equilibrium equations (1.31) is presented as a general linear combination after substituting the pressure as $P(\psi) = P_0 - \gamma\psi$ and function related to the toroidal magnetic field as $I(\psi) = \gamma\psi$ and searching for a spherically separable solution similar to the previous sections. The solution is given by (3.96) and the pressure profile of this solution is shown in Figure 3.5. As the Bessel function in (3.96) continue to oscillate, this is not a global solution and must be truncated to be considered physical. Lastly, the stability of Hill's spherical vortex is analyzed using a perturbation mentioned in [6]. An example of one evolution of the perturbation as time increases is shown in Figure 3.6. This gives the conclusion that Hill's spherical vortex is unstable which is a well known result [40, 22]. The stability of the MHD spherical vortex solution 3.72, and the generalized Hill's vortex solution 3.88 was attempted to be analyzed similarly, however as shown in Section 3.6.2 this was not possible with the use of a dynamic equation for ψ similar to 3.97 as one was not able to be derived in the ansatz $V^\phi = I(\psi)/r$ for the azimuthal velocity component. A more general linear perturbation was considered in Section 3.6.3 and 3.6.4 but no solutions were found.

Some open problems related to this work include the following ones.

1. What other coordinate systems lead to separable solutions for the Grad-Shafranov equation (1.40) and JFKO equation (1.48) for appropriate choices of $P(\psi)$ and $I(\psi)$?

2. What are the necessary conditions for the confluent Heun polynomials in the first family of helical solutions (2.42) to give rise to global solutions analogous to Bogoyavlenskij's astrophysical helical jets (1.50) and are these the only global solutions that exist for (2.42)?

3. Is the MHD spherical vortex solution (3.72) and the generalized Hill's spherical vortex solution (3.88) stable?

Bibliography

[1] Hannes Alfvén. Existence of electromagnetic-hydrodynamic waves. *Nature*, 150(3805):405–406, 1942.

[2] K Appert, GA Collins, T Hellsten, J Vaclavik, and L Villard. Theory of MHD waves. *Plasma Physics and Controlled Fusion*, 28(1A):133, 1986.

[3] George B Arfken and Hans J Weber. *Mathematical Methods for Physicists*. American Association of Physics Teachers, 1999.

[4] C K Batchelor and GK Batchelor. *An Introduction to Fluid Dynamics*. Cambridge University Press, 2000.

[5] AD Beklemishev. Helical plasma thruster. *Physics of Plasmas*, 22(10):103506, 2015.

[6] Dieter Biskamp. *Nonlinear Magnetohydrodynamics*, volume 1. Cambridge University Press, 1997.

[7] David E Blair. *Inversion Theory and Conformal Mapping*, volume 9. American Mathematical Society, 2000.

[8] RD Blandford and DG Payne. Hydromagnetic flows from accretion discs and the production of radio jets. *Monthly Notices of the Royal Astronomical Society*, 199(4):883–903, 1982.

[9] A. A. Bobnev. A spherical vortex in an ideal and in an ideally conducting fluid. *Magnitnaya Gidrodinamika*, 24(4):10 – 19, 1987.

[10] Oleg Bogoyavlenskij. Restricted lie point symmetries and reductions for ideal magnetohydrodynamics equilibria. *Journal of Engineering Mathematics*, 66(1):141–152, 2010.

[11] Oleg I Bogoyavlenskij. Astrophysical jets as exact plasma equilibria. *Physical Review Letters*, 84(9):1914, 2000.

[12] Oleg I Bogoyavlenskij. Helically symmetric astrophysical jets. *Physical Review E*, 62(6):8616, 2000.

[13] Oleg I Bogoyavlenskij. Infinite symmetries of the ideal mhd equilibrium equations. *Physics Letters A*, 291(4-5):256–264, 2001.

[14] Oleg I Bogoyavlenskij. Symmetry transforms for ideal magnetohydrodynamics equilibria. *Physical Review E*, 66(5):056410, 2002.

[15] Michael Bonitz, Alexei Filinov, Jens Böning, and James W Dufty. Introduction to quantum plasmas. In *Introduction to Complex Plasmas*, pages 41–77. Springer, 2010.

[16] Alain J Brizard and Taik Soo Hahm. Foundations of nonlinear gyrokinetic theory. *Reviews of Modern Physics*, 79(2):421, 2007.

[17] Kwing Lam Chan and RN Henriksen. On the supersonic dynamics of magnetized jets of thermal gas in radio galaxies. *The Astrophysical Journal*, 241:534–551, 1980.

[18] Francis F Chen. *Introduction to Plasma Physics*. Springer Science & Business Media, 2012.

[19] Francis F Chen et al. *Introduction to Plasma Physics and Controlled Fusion*, volume 1. Springer, 1984.

[20] Alexei F Cheviakov. *Symmetries and Exact Solutions of Plasma Equilibrium Equations*. Queen's University, 2004.

[21] R Chodura. A hybrid fluid-particle model of ion heating in high-mach-number shock waves. *Nuclear Fusion*, 15(1):55, 1975.

[22] Kyudong Choi. Stability of Hill's spherical vortex. *arXiv preprint arXiv:2011.06808*, 2020.

[23] Dominik Dierkes, Alexei Cheviakov, and Martin Oberlack. New similarity reductions and exact solutions for helically symmetric viscous flows. *Physics of Fluids*, 32(5):053604, 2020.

[24] Dominik Dierkes and Martin Oberlack. Euler and Navier–Stokes equations in a new time-dependent helically symmetric system: derivation of the fundamental system and new conservation laws. *Journal of Fluid Mechanics*, 818:344–365, 2017.

[25] *NIST Digital Library of Mathematical Functions*. http://dlmf.nist.gov/, Release 1.0.26 of 2020-03-15. F. W. J. Olver, A. B. Olde Daalhuis, D. W. Lozier, B. I. Schneider, R. F. Boisvert, C. W. Clark, B. R. Miller, B. V. Saunders, H. S. Cohl, and M. A. McClain, eds.

[26] Attilio Ferrari. Modeling extragalactic jets. *Annual Review of Astronomy and Astrophysics*, 36(1):539–598, 1998.

[27] Richard Fitzpatrick. *Plasma Physics: An Introduction*. CRC Press, 2014.

[28] David Gaspard. Connection formulas between coulomb wave functions. *Journal of Mathematical Physics*, 59(11):112104, 2018.

[29] Dirk Hegemann and Sandra Gaiser. Plasma surface engineering for manmade soft materials: A review. *Journal of Physics D: Applied Physics*, 2021.

[30] Micaiah John Muller Hill. VI. on a spherical vortex. *Philosophical Transactions of the Royal Society of London.(A.)*, (185):213–245, 1894.

[31] Gregory G Howes, Steven C Cowley, William Dorland, Gregory W Hammett, Eliot Quataert, and Alexander A Schekochihin. Astrophysical gyrokinetics: basic equations and linear theory. *The Astrophysical Journal*, 651(1):590, 2006.

[32] Gregory G Howes, Jason M TenBarge, William Dorland, Eliot Quataert, Alexander A Schekochihin, Ryusuke Numata, and Tomoya Tatsuno. Gyrokinetic simulations of solar wind turbulence from ion to electron scales. *Physical Review Letters*, 107(3):035004, 2011.

[33] R Kaiser and D Lortz. Ball lightning as an example of a magnetohydrodynamic equilibrium. *Physical Review E*, 52(3):3034, 1995.

[34] Olga Kelbin, Alexei F Cheviakov, and Martin Oberlack. New conservation laws of helically symmetric, plane and rotationally symmetric viscous and inviscid flows. *Journal of Fluid Mechanics*, 721:340–366, 2013.

[35] Martin David Kruskal and RM Kulsrud. Equilibrium of a magnetically confined plasma in a toroid. *The Physics of Fluids*, 1(4):265–274, 1958.

[36] Giovanni Manfredi. How to model quantum plasmas. *Fields Institute Communications*, 46:263–287, 2005.

[37] EK Maschke. Exact solutions of the mhd equilibrium equation for a toroidal plasma. *Plasma Physics*, 15(6):535, 1973.

[38] Kenro Miyamoto. *Plasma Physics and Controlled Nuclear Fusion*, volume 38. Springer Science & Business Media, 2005.

[39] Dwight Roy Nicholson and Dwight R Nicholson. *Introduction to Plasma Theory*, volume 582. Wiley New York, 1983.

[40] C Pozrikidis. The Nonlinear Instability of Hill's Vortex. *Journal of Fluid Mechanics*, 168:337–367, 1986.

[41] André Ronveaux and Felix M Arscott. *Heun's Differential Equations*. Oxford University Press, 1995.

[42] Nasser Saad. On the solvability of confluent heun equation and associated orthogonal polynomials. *arXiv preprint arXiv:1509.00090*, 2015.

[43] Megh Nad Saha. Ionization in the solar chromosphere. *The London, Edinburgh, and Dublin Philosophical Magazine and Journal of Science*, 40(238):472–488, 1920.

[44] Padma K Shukla and Bengt Eliasson. Nonlinear aspects of quantum plasma physics. *Physics-Uspekhi*, 53(1):51, 2010.

[45] VM Sorokin and GV Fedorovich. The physics of slow mhd waves in the ionospheric plasma. *Moscow Energoizdat*, 1982.

[46] Donald Gary Swanson. *Plasma Waves*. CRC Press, 2003.

[47] Vladimir A Vladimirov and HK Moffatt. On general transformations and variational principles for the magnetohydrodynamics of ideal fluids. Part 1. Fundamental principles. *Journal of Fluid Mechanics*, 283:125–139, 1995.

[48] Frank W Warner. *Foundations of Differentiable Manifolds and Lie Groups*, volume 94. Springer Science & Business Media, 1983.

[49] Dan Winske, Lin Yin, Nick Omidi, Homa Karimabadi, and Kevin Quest. Hybrid simulation codes: Past, present and future—a tutorial. *Space Plasma Simulation*, pages 136–165, 2003.

[50] Xiao-Hua Zhao, Keng-Huat Kwek, JI-Bin Li, and Ke-Lei Huang. Chaotic and resonant streamlines in the abc flow. *SIAM Journal on Applied Mathematics*, 53(1):71–77, 1993.

Appendix A

Proof of Proposition 1

Proposition 2. *For a pressure type of the form given by (2.14), the separated solution (2.20) is a global solution if and only if* $\delta \in \mathbb{N}$.

If $\delta \notin \mathbb{N}$, *equation (2.20) must be truncated to be a physical solution.*

Assuming $\delta \notin \mathbb{N}$. The general $R(r)$ solution given by (2.18) with $C_1 = 1$ and $C_2 = 0$, for a large argument, $r \to \infty$ can be approximated by [25] as

$$W_M(\delta, 1/2, qr^2) \approx \frac{\Gamma(2)}{\Gamma(1-\delta)} e^{\frac{qr^2}{2}} (qr^2)^{-\delta}. \tag{A.1}$$

Next, the limit of this at ∞ is considered, which is related to the well known limit $\lim_{x\to\infty} \frac{e^x}{x^k}$ which is known to diverge to ∞, giving

$$\lim_{r\to\infty} W_M(\delta, 1/2, qr^2) \to \infty.$$

Therefore, the axial magnetic field component which behaves like $W_M(\delta, 1/2, qr^2)/r$ in the r variable will also diverge at infinity,

$$\lim_{r\to\infty} B^\phi \to \infty.$$

For $C_1 = 0, C_2 = 1$, and small r, the approximation of $W_W(\delta, 1/2, qr^2)$ given by [25] can written as

$$W_W\left(\kappa, \frac{1}{2}, qr^2\right) \approx \frac{1}{\Gamma(1-\delta)},$$

which is simply a non-zero constant term which are well defined as the argument of the Gamma function will never be negative integers. Therefore, the value of $B^\phi(r, z)$ which behaves like $W_W(\delta, 1/2, qr^2)/r$ in the r variable will diverge at the origin, namely

$$\lim_{r\to 0} B^\phi \to \infty.$$

Clearly any linear combination of $W_M(\delta, 1/2, qr^2)$ and $W_W(\delta, 1/2, qr^2)$ will not have finite B^ϕ for $0 \le r < \infty$, so this solution cannot be physical without a domain size restriction in the radial direction.

If $\delta \in \mathbb{N}$, *the solution (2.20) is valid for a plasma domain unbounded in the radial direction.*

Assuming $\delta \in \mathbb{N}$, then $W_M(\delta, 1/2, qr^2)$ and $W_W(\delta, 1/2, qr^2)$ in (2.18) become linearly dependent and behave like

$$W_M(\delta, 1/2, qr^2) \propto W_W(\delta, 1/2, qr^2) \propto r^2 e^{(-\frac{qr^2}{2})} L_{\delta-1}(qr^2), \tag{A.2}$$

where $L_{\delta-1}$ are the $\delta - 1$ order Laguerre polynomials. Using (2.10), clearly the B^ϕ and B^r which behave like $re^{(-\frac{qr^2}{2})} L_{\delta-1}(qr^2)$ in the r variable, are smooth, finite in the interval $0 \le r < \infty$ and go to zero for $r \to \infty$ as this is simply the product of a polynomial and Gaussian, using the well-known result that $\lim_{r\to\infty} P(r)e^{-r^2} = 0$, where $P(r)$ is any polynomial in r. Therefore finite magnetic energy will be the case with these components. For the last component, B^z, from (2.10), the first derivative in r must be checked,

$$\frac{d}{dr}\left(r^2 e^{(-\frac{qr^2}{2})} L_{\delta-1}(qr^2)\right) = -re^{(-\frac{qr^2}{2})}\left(2\delta L_{\delta-1}(qr^2) + (qr^2 - 2\delta - 2))L_\delta(qr^2)\right) \tag{A.3}$$

Clearly then B^z which behaves like $-e^{(-\frac{qr^2}{2})}\left(2\delta L_{\delta-1}(qr^2)+(qr^2-2\delta-2))L_\delta(qr^2)\right)$ in the r variable is also smooth, finite in the interval $0 \leq r < \infty$ and goes to zero for $r \to \infty$ again since this is the product of a Gaussian and polynomial. Therefore the quantity

$$\int_{\mathcal{U}} |\mathbf{B}(\mathbf{x})|^2 \, d^3x \tag{A.4}$$

will be finite. Also, the pressure $P(\psi) = P_0 - 1/2q^2\psi^2/\mu \to P_0$ for $r \to \infty$ since $\psi = R(r)Z(z) \to 0$ for $r \to \infty$. Therefore all required physical constraints given in Section 1 of Chapter 2 are satisfied. □

Appendix B

The computation of Coulomb wave functions

Numerical calculations for the Coulomb wave functions with available power series have a very small radius of convergence of $|z| < \frac{1}{2}$ which make its uses quite limited. In most cases, it is much more practical to go through the way described below which is discussed further in [28].

These Coulomb wave functions can be calculated by introducing other types of wavefunctions defined as the incoming and outgoing waves denoted by $H^{\pm}_{\eta L}(x)$ where the normalization coefficients are given below and the confluent hypergeometric function of the second kind is denoted by $U(a, b, x)$.

$$H^{\pm}_{\delta L}(x) = D^{\pm}_{\delta L} x^{L+1} e^{\pm ix} U(L + 1 \pm i\delta, 2L + 2, \mp 2ix), \tag{B.1a}$$

where

$$D^{\pm}_{\delta L} = (\mp 2i)^{2L+1} \frac{\Gamma(L + 1 \pm i\delta)}{C_{\eta L}\Gamma(2L + 2)} \tag{B.1b}$$

and

$$C_{\delta L} = \frac{2^L \sqrt{\Gamma(L + 1 + i\delta)\Gamma(L + 1 - i\delta)}}{\Gamma(2L + 2)e^{\delta\pi/2}}. \tag{B.1c}$$

The Coulomb wave functions can then be computed as follows:

$$\mathcal{C}_F(L, \delta, x) = \frac{H^{+}_{\delta L}(x) - H^{-}_{\delta L}(x)}{2i}, \tag{B.2}$$

$$\mathcal{C}_G(L, \delta, x) = \frac{H^{+}_{\delta L}(x) + H^{-}_{\delta L}(x)}{2}. \tag{B.3}$$

Appendix C

The regularity of the unstable perturbation of Hill's spherical vortex

Starting with the perturbed solution $\psi(r,z,t)$,

$$\psi(r,z,t) = -2\delta\left(Ae^{\lambda t}\epsilon^2(R^2-2r^2-2z^2)\mathcal{H}\left(\left[\frac{3}{4}+\frac{\sqrt{89}}{4},\frac{3}{4}-\frac{\sqrt{89}}{4}\right],\frac{1}{2},\frac{r^2}{r^2+z^2}\theta\right)+\frac{R^2-r^2-z^2}{2}\right), \tag{C.1}$$

the level curve $\psi(r,z,t)=0$ which corresponds to the boundary of the spherical vortex is shown at different points in time as seen in Figure 3.6. It appears, as is motivated in the Figure that the surfaces may not be regular. With the use of a symbolic software package, the value of $\frac{\partial z}{\partial r}\big|_{r=0}$ is computed for the above equation (C.1). It was found that

$$\frac{\partial z}{\partial r}\big|_{r=0} = 0. \tag{C.2}$$

This implies that the perturbed magnetic surface $psi(r,z,t)=0$ remains smooth where it intersects the z-axis for all $t>0$. This computation was done in `Maple` symbolic package; the code is given below.

```
################## The perturbed equation of psi given by ######################
psi_pert := -2*(epsilon^2*(R^2 - 2*r^2 - 2*z^2)*hypergeom([3/4 + sqrt(89)/4,
3/4 - sqrt(89)/4], [1/2], z^2/(r^2 + z^2)) + R^2/2 - r^2/2 - z^2/2)*r^2*delta:
################## Solving implicetly for z ############################
solve({psi_pert = 0},z):
################## copying the above equation for z ################
z := RootOf(2*hypergeom([3/4 + sqrt(89)/4, 3/4 - sqrt(89)/4], [1/2], _Z^2/(_Z^2 + r^2))
*R^2*epsilon^2 - 4*hypergeom([3/4 + sqrt(89)/4, 3/4 - sqrt(89)/4], [1/2], _Z^2/(_Z^2 + r^2))
*_Z^2*epsilon^2 - 4*hypergeom([3/4 + sqrt(89)/4, 3/4 - sqrt(89)/4], [1/2], _Z^2/(_Z^2 + r^2))
*epsilon^2*r^2 + R^2 - _Z^2 - r^2):
################## computing the derivative implicitly ###############
z_r := diff(z,r):
################## computing the limit as r -> 0 ######################
limit(z_r,r=0)
0
```